Universidade de Lisboa

Faculdade de Ciências

Departamento de Química e Bioquímica

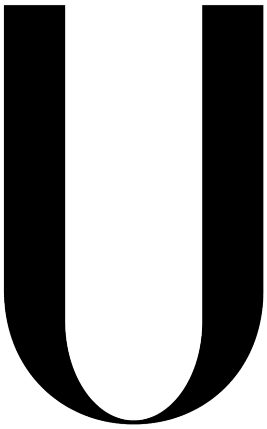

LISBOA

UNIVERSIDADE
DE LISBOA

Constant-pH MD simulations of higher complexity lipid bilayer models: PA/PC binary mixtures

Hugo Alexandre Feiteira dos Santos

Dissertação

Mestrado em Bioquímica

(Bioquímica)

2013

Universidade de Lisboa

Faculdade de Ciências

Departamento de Química e Bioquímica

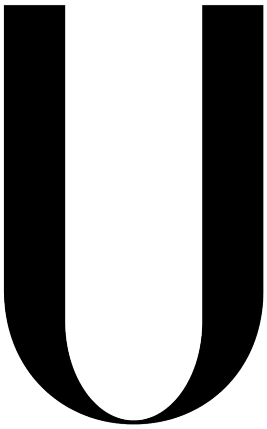

LISBOA

UNIVERSIDADE
DE LISBOA

Constant-pH MD simulations of higher complexity lipid bilayer models: PA/PC binary mixtures

Hugo Alexandre Feiteira dos Santos

Dissertação

Mestrado em Bioquímica

(Bioquímica)

Orientador: Doutor Miguel Ângelo dos Santos Machuqueiro

2013

Summary

Biological membranes fulfill a central role on a vast array of molecular processes, most of them crucial for cell viability. These entitities may contain up to 30% ionizable lipids, which results in pH having a major impact on the structure and dynamics of membranes.

In certain organelles, phosphatidic acid (PA) is the major anionic lipid. Being a phosphomonoester, PA has three different charge states (PA^0, PA^{-1} and PA^{-2}) that are interchanging at physiological pH. After obtaining a titration curve for a 25% PA/PC binary mixture, we computed the $pK_{a1} \sim 2.5$ and $pK_{a2} \sim 7.0$, which illustrate that, at physiological conditions, this lipid can act as a "pH biosensor" by effectively changing its charge upon small intracellular pH variations.

We observed that (de)protonation induces drastic changes in the membrane conformation with adjustment of its lateral packing. In fact, it has been shown that an isothermal phase transition is possible, when triggered electrostatically. According to Garidel *et al*, a bilayer composed of a binary mixture similar to the one simulated is expected to present a gel phase coexisting with a liquid-crystalline phase at pH 4. At around physiological and higher pH values, the bilayer should be in its pure fluid phase (L_α). Our results are in very good agreement with the ones reported.

In addition to pH, also the ionic strength can have a strong effect on charged lipid bilayers. Nevertheless, the problem regarding the number of counter-ions solvating membranes is usually overlooked. Here, we present a new approach to estimate the amount of counter-ions that should be added in a typical MD simulation. This methodology was validated with experimental data from DMPA/ DMPC phase transition, and compared with other commonly used approaches based on different treatments of the long-range electrostatics (GRF and PME).

Keywords: Phosphatidic acid, pH, Protonation, Ions, Ionic Strength, Constant-pH molecular dynamics, Electrostatic interactions, Phase transitions

Sumário

As membranas biológicas são estruturas ubíquas altamente flexíveis cuja formação é, do ponto de vista termodinâmico, espontânea. Estas estão envolvidas em inúmeros processos moleculares essenciais para a célula desde o tráfego e sinalização intracelulares até ao equilíbrio vida–morte da própria célula. Fundamentalmente, estas entidades macromoleculares são características de todos os seres vivos, sendo uma das principais distinções entre estes e os seres inanimados. Em suma, a existência de membranas biológicas é crucial para a manutenção da Vida, tal como a conhecemos.

As bicamadas fosfolipídicas constituem o elemento estrutural primário das membranas biológicas, sendo que os principais componentes estruturais das bicamadas lipídicas são os lípidos, designadamente, os fosfolípidos. Durante vários anos os componentes lipídicos das membranas biológicas foram considerados simplesmente como elementos estruturais ("espectadores passivos" do ponto de vista funcional) sendo que a própria funcionalidade da membrana se centrava fundamentalmente em torno do seu papel estrutural e de suporte. Mais recentemente, quer com o aparecimento de novas questões relacionadas com a elevada diversidade estrutural de lípidos e possível correlação com propriedades funcionais específicas, quer com o aparecimento de resultados experimentais que apontam para um papel extremamente activo da membrana biológica e dos seus componentes nos mais variados aspectos fisiológicos, esta ideia tem sido desafiada, caindo mesmo em desuso.

Apesar do crescente interesse observado na elucidação do papel da membrana biológica na célula, ainda muito pouco se sabe sobre as bases bioquímicas e biofísicas subjacentes aos mais variados processos biológicos. Paradoxalmente, as metodologias experimentais disponíveis não conseguiram ainda acompanhar as necessidades actuais, sendo ainda limitadas em termos da resolução espacial e temporal de que dispõem. Assim, o conhecimento é baseado em princípios e modelos qualitativos que padecem de uma exactidão aquém do pretendido, estando geralmente associados a bases fenomológicas fundamentalmente hipotéticas, o que torna este tipo de conhecimento bastante limitado. Conceitos básicos como a influência do pH sobre a estrutura e a funcionalidade das membranas biológicas são ainda rudimentares, e muitas outras questões, relacionadas com a arquitetura e a fenomologia da membrana celular enquanto entidade estrutural e funcional, continuam por revelar. A título de exemplo, as interacções entre pequenos

péptidos ou proteínas, membranares ou solúveis, com os componentes lipídicos das membranas biológicas, é hoje em dia uma das questões mais amplamente estudadas. Apesar de tudo, uma vez mais, se reforça a inexistência de modelos membranares capazes de elucidar sobre o papel e o mecanismo destas interacções para a célula, de uma forma eficiente e ao mesmo tempo fidedigna. Um dos pontos-chave que precisam urgentemente de ser clarificados passa pelo corroborar da existência de microdomínios especializados de membrana, passíveis de serem funcionais, que se pensa estar implicados nos mecanismos de estabelecimento de interacções do tipo acima supracitadas.

Tendo em conta que a compreensão de muitas destas problemáticas passa numa fase inicial por revelar o papel biofísico destas entidades biológicas, a um nível de detalhe molecular suficiente a uma melhor integração de muito do conhecimento que já existe, com este trabalho propomo-nos a estudar de uma forma integrativa a hipótese de que lípidos aniónicos, nomeadamente, o ácido fosfatídico (PA) pode desempenhar um papel de "pH-biosensing" ao nível da célula. Postula-se que este lípido esteja implicado como um elo de ligação entre o metabolismo lipídico e a disponibilidade de nutrientes, nomeadamente de glucose, no meio ambiente. O grupo experimental de Loewen *et al* conseguiu isolar o PA como o agente participativo no reconhecimento membranar ao nível do retículo endoplasmático (ER) de uma proteína solúvel, a Opi1, sendo que o estabelecimento e manutenção da interacção entre ambos é intrinsicamente dependente do valor de pH do meio. Sendo o PA um fosfomonoéster, tem três diferentes estados de carga (PA^0, PA^{-1} e PA^{-2}), estados estes que estão em constante equilíbrio a um valor de pH perto do fisiológico. Tendo isto em conta e sabendo que o valor do segundo pK_a é cerca de 7 unidades de pH, pensa-se que este lípido pode actuar como um biosensor de pH, ao alterar dramaticamente a sua carga de acordo com pequenas mas rápidas variações do pH intracelular. Assim para valores de pH ligeiramente acídicos, abaixo das 6 unidades de pH, a interacção é suficientemente enfraquecida o que promove a libertação da Opi1 para o citosol e deslocamento desta para o núcleo onde surtirá efeitos regulatórios ao nível de genes implicados no metabolismo geral, nomeadamente no metabolismo dos lípidos, inclusivamente do próprio PA.

Mesmo sendo bem conhecido (apesar de postulado) o mecanismo subjacente a este fenómeno, pouco se sabe, com rigor, sobre a influência da própria interacção PA–Opi1 no valor do pK_a deste lípido e sobre a real influência das interacções electrostáticas e respectiva dependência com o valor de pH do meio. Assim, um dos principais objectivos deste trabalho passou por clarificar quantitativamente a protonação deste lípido aniónico aquando presente numa mistura binária de dois lípidos - DMPA e DMPC. Este é um modelo mais realista da membrana biológica do RE, organelo onde o PA é na verdade um dos mais prevalentes lípidos aniónicos.

Na verdade, as interacções electrostáticas são actualmente tidas em conta como tendo um impacto bastante pronunciado na estrutura e na dinâmica das membranas biológicas. Este facto justifica o porquê do pH ter um papel tão crucial nas propriedades estruturais das membranas que contêem lípidos aniónicos. Para além do pH, a força iónica pode também ter um forte

efeito em bicamadas lipídicas carregadas. Apesar de clara a necessidade de reproduzir o mais biológica e fidedignamente a quantidade e a distribuição de contra-iões que se encontram a solvatar a membrana, a verdade é que este é comummente ignorado. Posto isto, apresentamos neste trabalho uma nova aproximação para estimar a quantidade correta de contra-iões que devem ser adicionados a um sistema numa simulação de MD típica. Através da aplicação de uma metodologia baseada no formalismo de PB para estimar a quantidade "correcta" de iões Na^+ e Cl^- presentes em solução e através da aplicação de um tratamento electrostático adequado (GRF a 0.1 M de forçã iónica), obtivemos bicamadas lipídicas estáveis e reprodutíveis aos vários valores de pH testados. Adicionalmente, fomos também capazes de reportar a transição de fase isotérmica anteriormente reportada. De acordo com Garidel *et al*, para uma bicamada fosfolípida composta pela mistura binária de PA/PC, a uma fracção molar semelhante à por nós estudada (25 % PA/PC), espera-se que esta apresente uma coexistência de ambas as fases gel (organizada) e líquida-cristalina (desorganizada), a um valor de pH rondando as 4 unidades de pH. Já aos valores de pH $\sim$ 7 e pH $\sim$ 12, espera-se que esta se apresente integralmente na fase fluida (L_α). Tendo em conta que os resultados obtidos neste trabalho estão bastante concordantes com aqueles reportados na literatura, conseguimos assim a validação do nosso modelo. De salientar que presentemente estão a ser realizados estudos de uma mesma natureza em modelos de membranas biológicas contendo outras fracções molares de PA/PC, designadamente 50% e 100%, de forma a melhor compreender o efeito deste factor nas várias propriedades estruturais e dinâmicas estudadas.

Com esta tese obtivemos resultados promissores que consideramos ser essenciais para o prosseguimento desta linha de trabalho no sentido de elucidar o papel do lípido aniónico PA no estabelecimento de interacções dependentes do pH com a Opi1. Sabendo que as interacções entre o PA e a Opi1 são conduzidas pela electrostática do sistema e portanto dependentes do pH da solução, a nossa metodologia poderá vir a ser uma das mais capazes em modelar e confirmar a existência de uma interacção significativa PA–Opi1 a determinados valores de pH. Adicionalmente, depois de completa e devidamente validadas as metodologias aplicadas no decorrer deste trabalho, pretendemos amplificar o nosso estudo a outros fosfomonoestéres que se pensa estarem implicados também em funções de reconhecimento e sinalização celulares, como é o caso dos fosfoinositídeos (PIPs) - PtdIns(4)P e PtdIns(4,5)P_2. A longo termo, este trabalho abriu ainda a possibilidade de proceder ao estudo de fenomologias como é o caso da segregação lateral de diferentes componentes lipídicos e consequente formação e manutenção de microdomínios especializados.

Palavras-chave: Ácido fosfatídico, pH, Protonação, Iões, Força iónica, Dinâmica molecular a pH constante, Interacções electrostáticas, Transições de fase

Contents

List of Figures

List of Tables

List of Abbreviations

CE	Continuum electrostatics,
CpHMD	Constant-pH Molecular Dynamics,
DMPA	1,2-dimyristoyl-*sn*-glycero-3-phosphate (phosphatidic acid),
DMPC	1,2-dimyristoyl-*sn*-glycero-3-phosphocholine (phosphatidylcholine),
DSC	Differential scanning calorimetry,
ER	Endoplasmic Reticulum,
FF	Force field,
GRF	Generalized Reaction Field,
LJ	Lennard-Jones,
$\mathbf{L}_\alpha$	Liquid-crystalline (fluid) phase,
$\mathbf{L}_\beta$	Gel (solid) phase,
l-BFGS	Limited-memory Broyden-Fletcher-Goldfarb-Shanno,
MC	Monte Carlo,
MD	Molecular Dynamics,
MM	Molecular Mechanics,
NPT	Isothermal-isobaric ensemble,
NVE	Microcanonical ensemble,
PA	Phosphatidic acid,
PB	Poisson-Boltzmann,
PBC	Periodic Boundary Conditions,
PC	Phosphatidylcholine,
PE	Phosphatidylethanolamine,
PG	Phosphatidylglycerol,
pH	*potentia hydrogenii*,
$\mathbf{pH}_i$	Intracellular pH,

PI	Phosphatidylinositol,
PIPs	Poliphosphoinositodes,
PME	Particle-mesh Ewald,
PS	Phosphatidylserine,
P-LINCS	Parallel Linear Constraint Solver,
RF	Reaction Field,
sMD	Standard Molecular Dynamics,
sn	Stereospecific numbering

Part of the inhumanity of the computer is that, once it is competently programmed and working smoothly, it is completely honest.

Isaac Asimov

Just then I found a strange refuge – "by chance", as they say – though I believe there is no such thing.

Herman Hesse

Preface

Very little is known about the biochemical and biophysical basis underlying most of the biological processes that happen at the cell. Generally speaking, the present knowledge is based on qualitative concepts/ schemes which generally suffer from inaccuracies and uncertainties, rendering this type of knowledge a limited one. Thus, basic concepts such as the influence of pH on the structure and functionality of biological membranes are still obscure, and many other questions remain unanswered. At the same time, the interaction of soluble peptides or small proteins with the membrane is still misunderstood, since key points such as the existence, prevalence and implication of microdomains, with distinct fluidity and lateral organization pattern, has still not been fully clarified. By understanding the physics behind relevant biological systems and processes at an atomistic level of detail, one can further broaden what is known about such events at a macromolecular scale.

The focus of this thesis was built on the hypothesis that anionic lipids such as phosphatidic acid (PA) can play a "pH-biosensing" role in the intrinsic signaling networks of the cell. The (de)protonation behavior of this lipid is thought to be implicated in the crosslink between the lipid metabolism and the nutrient availability through the regulation of the interaction of a specific protein, Opi1, with the membrane of the endoplasmic reticulum (ER). Due to the lack of a study that deals with this problem with significant depth, one of our main objectives was to clarify the protonation behavior of this lipid when in a membrane system composed of a binary mixture of phosphatidic acid (DMPA) and phosphatidylcholine (DMPC). In order to achieve such an objective, atomistic standard molecular dynamics simulations (sMD) and constant-pH molecular dynamics (CpHMD) were employed to study the impact of (de)protonation events of DMPA lipids in a model phospholipid bilayer.

Along the development of this work we had the opportunity to share the results herein discussed at three occasions: one oral communication at the *2nd Portuguese Biomolecular Modeling Meeting* (4 April, 2013) held in Foz do Arelho, Portugal; and by presenting a poster in two conferences, one internally held in CQB, Lisbon, Portugal ("Molecular dynamics simulation of higher complexity lipid bilayer models: PA/PC binary mixtures") at the *CQB-Day 2013* (4 July,

2013) and the other one held in San Sebastian - Donostia, Spain ("Constant-pH MD simulation of higher complexity lipid bilayer models: PA/PC binary mixtures") at the *Iberian Membrane Biophysics Colloquium - Physics Meets Biology at the Cell Membrane* (20-21 September, 2013). In the near future, we will have the opportunity to further extend the exposure of this work by presenting a poster in the *Barcelona BioMed Conference* on "Frontiers in dynamics simulations of biological molecules" to be held in Barcelona, Spain (4-6 November, 2013).

Chapter 1

Introduction

1.1 Biological membranes - the edge of Life

Life is characterized by self-sustaining biological processes, differing from inorganic non-living matter. In one way or another, Life as we know it, depends enormously on the existence of membranes. **(1–3)** Without biological membranes, we simply would not exist. They are one of the most common features of the biological world to be found everywhere, within and around us, and fulfill a pivotal role among other biological entities in the cell's domain, for it is on them that most cellular processes take place. **(2; 4)** Lipid metabolism has a strong impact on cell physiology, and although quite vast, our knowledge and capacity of explaining most of the fundamental biophysical principles that govern such macromolecules is still quite rudimentary. Hence, many important basic questions remain unanswered. **(5)**

1.1.1 Historical Perspective

Even though the cell theory had its origins in the seventeenth century, with the advent of the first microscopic techniques, only more recently, by the early twentieth century, was the structural nature of cell membranes known. It might be surprising that such an essential structure for understanding Life was described, in detail, so late in History. The legacy of a century, with the appearance of multiple hipothetical models (**Figure 1.1**) has led to the present picture of biological membranes as lipid bilayers. **(6)**

The study of the structural and functional properties of membranes goes back at least to the early studies of Benjamin Franklin, in the eighteenth century, a statesman not normally associated with the biology of membranes, whose published empirical experiment on the spread of oils and fats on water, despite passing largely unnoticed, opened the door to the seminal work on the properties of biological membranes done by Lord Rayleigh, Agnes Pockels and

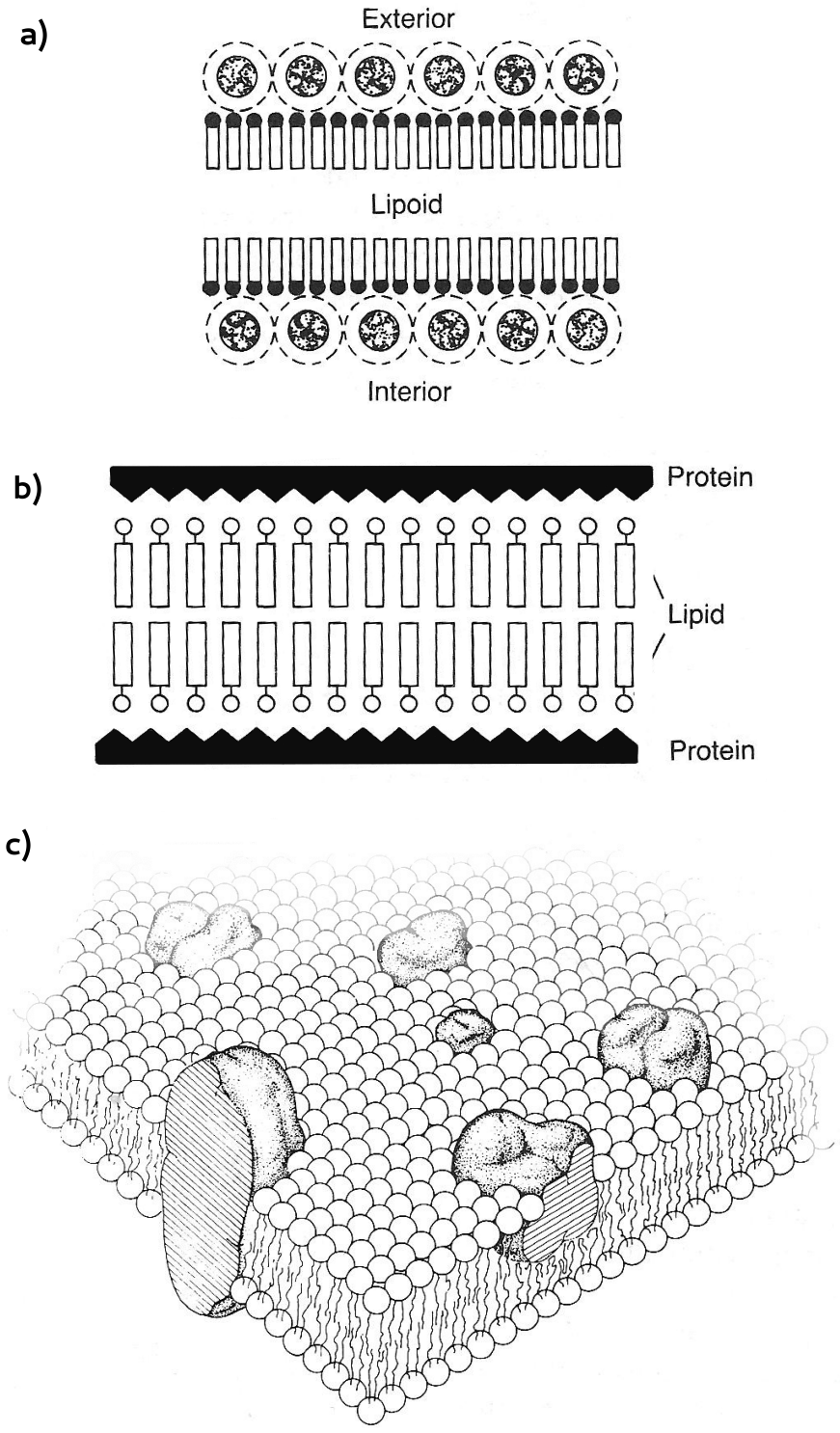

Figure 1.1: Three of the most influential models proposed for biological membrane structure - **(a)** Danielli-Davson's, **(b)** Robertson's "unit membrane", and **(c)** Singer and Nicolson's "fluid mosaic model". See text for further details. All images were adapted from **(7–9)**

Irving Langmuir at the dawn of the nineteenth century. **(6)** The latter of the three proposed that the fatty acid molecules form a monolayer by orienting themselves vertically with the hydrocarbon chains away from the water and the carboxyl groups in contact with the surface of the water. **(10)** Even though not being fully true, it was altogether a key piece in the puzzle of understanding lipid bilayers, and membranes as well.

More recently, less than an hundred years ago, in 1925, Gorter and Grendel proposed from a set of elegant simple experiments that lipids in the eryhrocyte membrane are arranged in the form of a bimolecular leaflet, *"a layer of lipoids just two molecules thick"*. **(11)** Despite hampered by the poor techniques of the time, their conclusions were later on proved to be basically correct.[1] In fact, from this day on, the concept of the lipid bilayer as the structural basis of biological membranes has been dominant - a bilayer of lipids, a fat-like material, arranged with apolar (hydrophobic) hydrocarbon tails opposing each other, end to end, face inward away from the water, and the polar (hydrophilic) heads toward the outside, where they interact with water molecules in the fluid environment of the cell. **(1)**

A decade later, the bimolecular lipid membrane was further elaborated in the Danielli-Davson or *"paucimolecular"* model (**Figure 1.1a**), which postulated that more rigid, globular proteins do coat both inner and outer surfaces of the lipid bilayer. **(12)** Even though it did not account for the functional diversity of membranes, this static structural model was largely sucessful at explaining the rather scarce low-resolution structural data available at the time, hence being the first membrane model to be truly accepted by the majority of scientists for many years. Indeed, it remains the most important generalization ever made in membrane research.

It was not until modern electron microscopy emerged in the late fifties that biological membranes were discovered and confirmed. In 1957, the ultrastructure of the cell membrane was first revealed by Robertson, who proposed that his modified version of the Danielli-Davson membrane model, which he termed the *"unit membrane"* (**Figure 1.1b**), represented the universal structure for all biological membranes. **(13)** According to this model, the two darker outer lines and the lighter inner region of the characteristic *"trilaminar"* appearance of membranes were respectively the protein coat of two apposed lipid monolayers and the lipid bilayer. **(13)** This hypothesis enjoyed acceptance for several years, until in the early seventies, a major change in the understading of membrane structure led to the replacement of the "unit membrane" model.

Even though the fluid mosaic model (**Figure 1.1c**), proposed by biochemists Singer and Nicolson, retained the basic lipid bilayer structure first suggested by Gorter and Grendel and later modified by Danielli, Davson and Robertson, in it, the globular proteins are thought to be *"floating"* within the bilayer rather than forming layers on either sides, some of which do span half way or all the way through the membrane, forming pores or specialized channels,

[1] This is a classical example of a fortuitus error-cancelation event which led to a major breakthrough in Science.

to allow passage of certain molecules through the membrane.[2] **(7)** Hence, the previously stationary structure was replaced by a fluid, dynamical one where the lipid molecules and its embedded "floating" proteins (and other membrane components) are able to move within and along the layers of a completely liquid bilayer, exhibiting rapid lateral diffusion in the plane of the membrane and structural regeneration in response to mild physical stress.

Continued research since 1972 led to minor modifications of the fluid mosaic model. Membranes started to be seen like behaving as an inhomogeneous solution, with the possible segregation of the lipid constituents into different regions, and hence formation of microdomains. **(14; 15)** Still, as of today, it remains the most adopted model worldwide since it is able to explain the current knowledge of membrane structure, serving as the basis for our understanding of membranes dynamics and function.

1.1.2 Structure and Role of Biological Membranes

Biological membranes are self-assembled highly flexible structures, thus having the ability to undergo a vast array of conformational and dynamical transitions. Being essential for many biological functions, these entities play a central role in both the structure and function of all cells, from prokaryotic to eukaryotic, plant and animal. **(2; 3; 9; 16)**

Coarsely, the primary function of biological membranes is to define compartiments, with each membrane setting the boundary between an inside and an outside. **(2; 3)** Whether they surround individual cells, or the organelles inside of eukaryotic cells, the compartmentalization provided by biological membranes was, literally, a key Life-achievement (**Figure 1.2**). But there is a lot more to know about these interesting supramolecular entities. Like all biological membranes, the plasma membrane, a remarkably thin film, with approximately three *nm* thickness of hydrophobic core, not only defines the cell's edges, preserving the cells integrity, providing support and protection, but does so while it controls and regulates the living cell's interaction with its surroundings, determining the nature of all communication established. **(17)** Exhibiting selective permeability, it acts as a screening device, rendering the cell the ability to discriminate in its chemical exchanges, a crucial task in many cellular processes, allowing the passage of some molecules while excluding others. **(18)** Additionally, membranes can act as signal transducers to transmit information about the extracellular environment to the cell or organelle interior. As an example, the plasma membrane contains receptors that enable a cell to communicate with other cells or entities present at the external medium. Some biological processes like electrical excitation either in nerve or muscle cells heavily depend upon rapid changes of permeability to particular ions in response to external stimulli. **(19)** In other cases,

[2] The embedded proteins and other substances, such as cholesterol, give the membrane the look of a mosaic. Therefore the designation of this model.

proteins and glycolipids bound to the cell surface serve as recognition patterns, enabling cells to recognize and communicate with each other, triggering cell to cell interactions. **(20)**

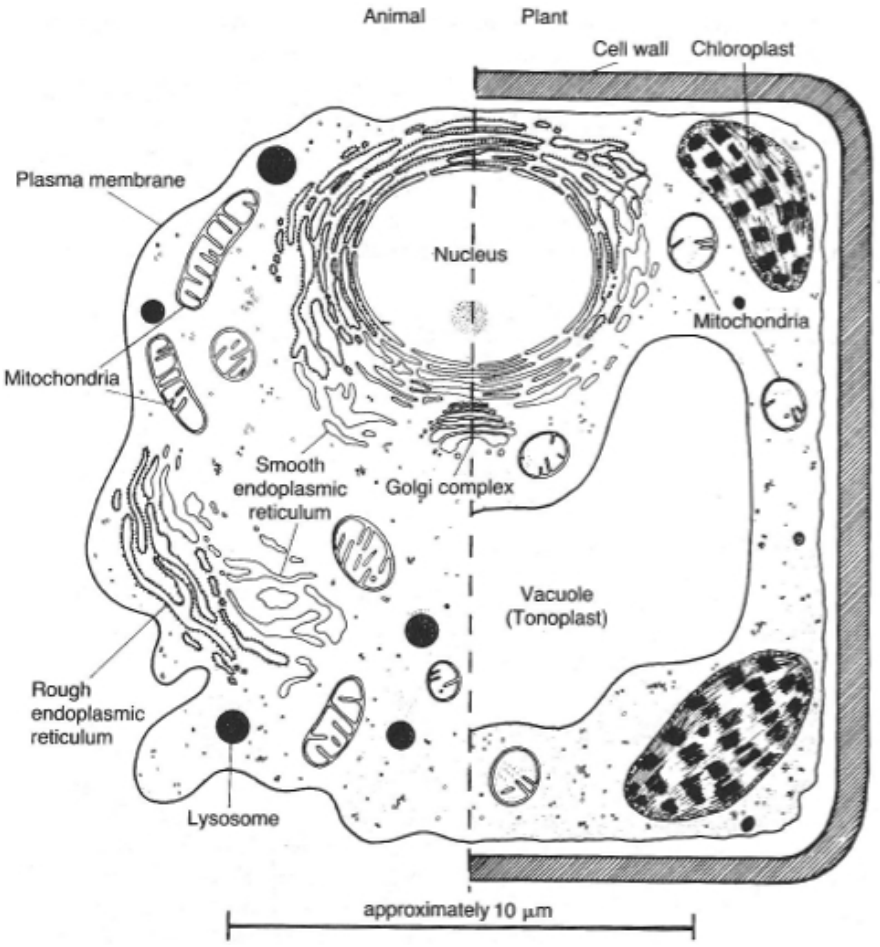

Figure 1.2: Schematic representation showing organelles of eukaryotic animal and plant cells as revealed by electron microscopy. Image was adapted from **(9)**

1.1.3 Lipids - the Primary Building Blocks of Cell Membranes

The most common definition of biological lipids is made solely on the fact that these are easily extracted into organic solvents, such as chloroform and ether, hence having a sparse solubility in water. **(21)** Briefly, fat-like substances, like oils, are one of the body's most important energy storage system, whereas phospholipids, glycolipids and some sterols are the primary building blocks of biological membranes, arising all over the human body.

The essential structural framework of membranes, the matrix, is simply a sheet of lipid bilayer, mainly composed of a wide variety of lipid molecules, where proteins are embbebed. **(2; 3; 9; 21)** Such a structure consists of two self-assembled leaflets of amphiphilic lipid molecules, a structure driven and sustained by weak interactions. The ability of lipids to

assume such a structural organization is dictated by their amphipathic character, which is indicated by the presence of distinct polar (or hydrophylic) head group regions and nonpolar (or hydrophobic) regions, and by the hydrophobic effect, an interaction coined by Tanford. **(22)** When in solution, water's energetically most favorable state, i.e. the one of maximum entropy, leads to the spontaneous segregation of hydrophobic domains away from water molecules, while, at the same time, the hydrophilic portions of phospholipids interact with the aqueous solvent in a manner similar to that of simple salts. **(22)** As a consequence, the net result of such interaction leads to the formation of two fundamental structures, phospholipid bilayers and phospholipid micelles.

Another important property of lipids is their bilayer or nonbilayer prone tendencies. Bilayer prone lipids present a cylindrical shape with the cross-sectional area of the hydrophilic head group and the hydrophobic domain being similar. Such lipids form bilayers and do not induce any curvature stress into the bilayer. In nonbilayer prone lipids the cross-sectional area of the hydrophobic domain is significantly different from the one that is observed at the head group region. But the importance of such structures is still quite obscure. There are a number of other macromolecular nonbilayer structures, which as the name indicates do not readily leads to the formation of bilayers. Due to constraints imposed by individual lipid geometries, these lipids are recurrently associated with fission and fusion events, phenomena where the membrane curvature is important. In pure form, such lipids do not form bilayers but rather a series of inverted micelle structures (hydrophobic domains outside). In mixtures with bilayer prone lipids, nonbilayer prone lipids induce membrane curvature and introduce stress into the bilayer structure due to negative curvature properties. In biological terms, the ability of lipids to self-assemble into an intact, but fluid, permeability barrier is vital, since it permits, among others, the establishment of electrochemical gradients which drive other membrane-mediated transport processes and a proper environment to a functional protein conformation is provided.

For many years, the lipid components of biological membranes have been considered simple passive bystanders with a merely structural/ energetic function as previously stated. **(23)** Nowadays, this idea is no longer blindly accepted and it seems rather inappropriate. Over the past three decades there has been a growing appreciation of the enormous fundamental cellular functions which are membrane-dependent. In fact, mostly all of the fundamental biochemical functions in cells involve membranes at some point - e.g. protein biosynthesis and secretion, ATP generation and hormonal responses. **(24–26)**

The crucial role of lipids in the cell (or at the tissue or organ scales) is demonstrated by a vast array of studies and by many human diseases that involve the disruption of lipid metabolic enzymatic steps or pathways. **(27)** For diseases like cancer, diabetes, neurodegenerative and infectious diseases, these processes are some of the hallmarks of the establishment of the disease. In fact, the role of most lipids as individual entities still pose a great amount of uncertainty

for the scientific community. **(23)** Nevertheless, they play a central role in the plethora of biochemical and biophysical processes such as membrane fusion, membrane-peptide interactions, membrane phase transitions and drug-liposome interactions. **(4)**

Even though each type of lipid has a slightly different structure, they are all primarily non-polar molecules composed of hydrophobic methylene groups and with an hydrophilic functional group at the head region. The fatty acids that compose lipids can be either saturated (*i.e.* inexistence of double bonds, they have as many hydrogens bound to their carbons as possible) or unsaturated (*i.e.* with one or more double bonds connecting their carbons, hence fewer hydrogens bound), giving rise to a fat or an oil at room temperature. Unsaturations in the fatty acid chains usually induces kinks which affects the physico-chemical characteristics of the bilayers since these lipids cannot get close together, resulting in reduced lipid packing and increased membrane fluidness.

Within the biological membranes that make up the cell constituents there is an astonishing amount of lipid diversity. **(28; 29)** According to Raetz *et al*, in an organism such as *Escherichia coli* there exist as many as 100 chemically distinct phospholipids, while in eukaryotes this number can be as many as tenfold higher. **(28)** Nowadays, it is assumed that such diversity must have provided significant evolutionary advantages to the living systems in which they reside, therefore implying specific functional roles for each component. Even so, despite there is an increasing awareness of the multiple roles of lipids in membranes, such roles are not still clear. **(23)** Furthermore, while the distribution of lipids in various membranes does not seem to be random, there is no plausible and conclusive explanation for the observed patterns.

In most eukaryotic and prokaryotic membranes the *1,2*-diacylphosphoglycerid, usually referred simply as phospholipids, are the most common found fatty acid esters of glycerol. These share some structural details namely a glycerol backbone where one of the glycerol hydroxyls (usually *sn*-3) is linked to a polar phosphate-containing group and the other two (*sn*-1 and *sn*-2) are attached to hydrophobic groups, the fatty acids hydrocarbon chains through ester or ether linkages [3]. The acyl chains nearly always have an even number of carbons, ranging from 12 to 24 (typical value being 16 or 18), possessing one saturated chain and one unsaturated chain, whereas the most common unsaturated species are 18:1, 18:2, 18:3 and 20:4. **(30)** Since almost every double bonds are *cis* rather than *trans*, a kink is introduced in the molecule (which is generally disruptive of ordered packing of the chains in the bilayer) leading to naturally occuring fluid states at physiological temperature. **(17)**

According to the element that is attached to the phosphate at the polar head group, lipids can be grouped into several general classes of phospholipids (see **Figure 1.3**) - phosphatidic acid (PA — non-substituted phosphate), phosphatidylcholine (PC — choline), phos-

[3] Glyceride nomenclature is often in terms of the stereospecific numbering (*sn*) system. To obtain a better understanding of such nomenclature the author suggests the reader to consult **(9)**

phatidylethanolamine (PE — ethanolamine), phosphatidylglycerol (PG — glycerol), phosphatidylinositol (PI — inositol), phosphatidylserine (PS — serine) and cardiolipin (CL — bridging glycerol) - each presenting certain specific characteristics, varying both in their structural and functional properties. Even though the specific function of lipids as individual components still has not been clearly revealed **(23)**, the origin of the apparent functional differences is usually pointed out to be the head group chemical structure.

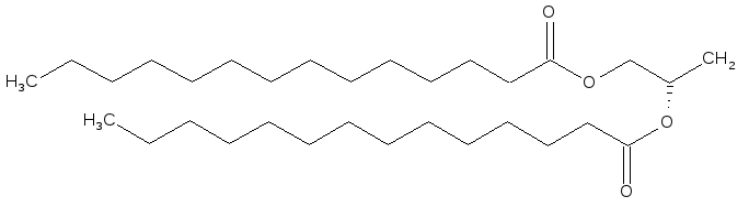

(a) R-group

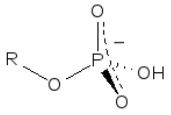

(b) Phosphate

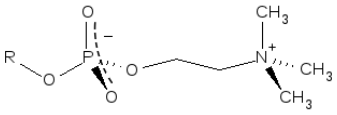

(c) Choline

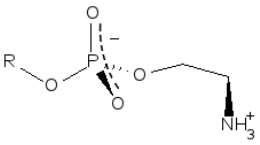

(d) Ethanolamine

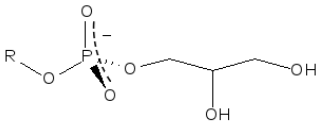

(e) Glycerol

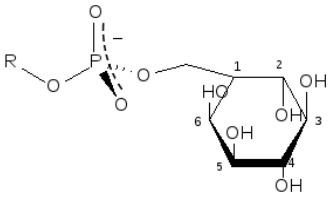

(f) Inositol

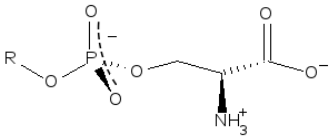

(g) Serine

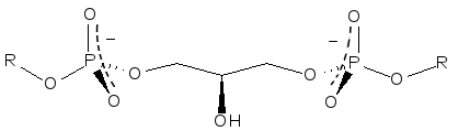

(h) Bridging glycerol

Figure 1.3: Schematic representations of the chemical structures of both alyphatic chain group (herein denoted as R group) **(a)** and polar head groups, associated with the aforementioned lipid classes **(b)**. All structures were obtained by using ACD/ChemSketch and gimp *softwares*.

Apart from phosphoinositodes, phosphatidic acid (PA — 1,2-diacyl*sn*-glycerol-3-phosphatidic acid) is arguably one of the most important regulatory glycerophospholipids. Usually found in trace amounts this lipid is a minor but important phospholipid, being involved in at least three essential and likely interrelated processes — PA is a crucial bionsynthetic intermediate in phospholipid and triacylglycerol synthesis and it has also been implicated in processes concerning membrane dynamics (i.e. fission and fusion events) and cellular signalling (calcium homeostasis, membrane trafficking and cytoskeletal dynamics). **(31)** Despite its relatively simple chemical structure consisting of only a glycerol, two acyl chains and a phosphomonoester headgroup, located close to the headgroup-acyl chain interface, it is thought that it regulates the binding of peripheral and transmembrane proteins — many proteins do have, what seems to be, domains that are specific in their binding of PA. **(32)**

Phosphatidylcholine (PC), 1,2-diacyl-*sn*-glycerol-3-phosphatidylcholine, once given the trivial name *"lecithin"*, is the major lipid constituent of the membranes of most eukaryotes, in animal and plants cells alike, often comprising to almost half of the total membrane lipid content. **(33)** Being a zwitterionic phospholipid over a wide pH range and due to its aproximate cylindrical molecular shape, it spontaneously organizes into bilayers (*i.e.* it does not induce curvature of the membrane). That might explain its enormous abundance on several biological membranes, cell and organelles, mostly in eukariotic organisms. Hence, it is seen as a key building block of membrane bilayers. In addition to its function as a key membrane constituent of membrane bilayers, PC may play an important role in signal transduction as a precursor of PA and PS, lysophosphatidylcholine (lyso-PC) and platelet-activating factor. **(34)**

Phosphatidylethanolamine (PE), 1,2-diacyl-*sn*-glycero-3-phospho-L-ethanolamine, previously named *"cephalin"*, is usually the second most abundant phospholipid in eukaryotic tissues. **(35)** Additionally, through enzymatic transformations it can give origin to PC, hence being seen indirectly as a key building block of biological membranes. This lipid is not only the most abundant on the protoplasmatic leaflet of cellular membranes, but it also has a pivotal role in cellular processes that range from the assembly and folding of membrane proteins to membrane fusion, cell cycle regulation and apoptosis. **(35)**

Phosphatidylinositol (PI) and his poly-derivates, polyphosphoinositodes (PIPs) — mainly phosphatidylinositol 4-phosphate, PtdIns(4)P, and phosphatidylinositol 4,5-bisphosphate, PtdIns(4,5)P_2 — exist in very small amounts in animal cells, due to its very rapid rate of metabolism. Hence, these are minor phospholipid constituents of cell membrane. Nevertheless, PI is especially abundant in brain tissue, where it can make up as much as 10% of the phospholipids, being the primary source of the arachidonic acid required for biosynthesis of eicosanoids, including prostaglandins, which serve as messenger molecules within the nervous system. PIPs are important regulators of processes such as the cytoskeleton organization, membrane trafficking and gene transcription, which are all crucial for polarized cell growth. **(36)** In the particular

case of PtdIns(4,5)P_2, this lipid is implicated in cell responses to its wall perturbations and pheromones metabolism. **(36)**

Phosphatidylserine (PS — 1,2-diacyl-*sn*-glycero-3-phospho-L-serine), is a weakly acidic lipid distributed widely along all living organisms. Interestingly, this lipid is, in general, asymmetrically distributed across the membrane bilayer, being located entirely on the inner monolayer surface of the plasma membrane and other cellular membranes. The exposure of PS on the outside surface of cells is associated with the removal of apoptotic cells and with the initiation of the blood clotting cascade. **(37)** This lipid has an important function since it promotes the stability and the integrity of the cellular membrane, maintaining the cell homeostasis. **(37)**

Cardiolipin (CL — 1,3-bis(*sn*-glycero-3-phosphatidyl)), a cardiolipid, is essentialy a dimeric phospholipid, where two phosphatidyl moieties are linked together through a central glycerol group. **(23)** This anionic lipid is found in significant concentrations in the inner bacterial and mitochondrial membranes and as been directly associated with ATP biosynthesis. **(23)**

The anionic lipids are the ones that exhibit a net negative charge at physiological pH, like PA, PG, CL, PS and PI. Amine-containing lipids are PS, PC and PE, with their head groups having different properties. PC and PE are zwitterions but have no net charge.

Even though the physical properties of membrane lipids are increasingly well-understood, the relation between such properties and the functional roles of lipids remains unclear. **(23)** The next step on achieving a better understanding of the detailed roles of specific lipids in the membrane should clarify the molecular details that are in the basis of the establishment and modulation of lipid-protein interactions and transbilayer signalling phenomena.

In many membranes the fraction of charged anionic lipids is around 10–20%, though it can be as high as 30%, as is the case for mitochondria. **(4; 38)** Hence, variations on the charging pattern of membranes will ultimately have an influence on the electrostatic potential of membranes and therefore on the structure and dynamical features of membrane bilayer systems.

1.1.4 Dynamical properties of Biological Membranes: microscopic description of a two-dimensional fluid

The lipid bilayer in the liquid crystal phase has a very complex structure, being heterogeneous both in the plane of the membrane and transversally. At physiological conditions, orientation of the lipid molecule in the membrane has an order with its molecular axis aligned to the bilayer normal (z-axis), while their in-plane projection (xy-plane) reports a liquid like disordered structure. In addition, lipid molecules have a translational degree of freedom, which makes them able to diffuse in the membrane matrix. **(39)**

We know that cells, as well as organelles, are not static nor rigid and they can undergo size and/ or shape fluctuations during the cells life cycle. In many cases, the cells survival relies on their capacity to move and readjust their shape and volume. Therefore, biological membranes have to overcome a difficult challenge: be plastic and dynamic enough to mechanically adapt to their physical surroundings, but concomitantly provide a stable plataform for the proteins therein embedded to perform their specific functions. **(16)** In addition, membrane fluidity have been shown to have a large impact on the ability of the cell to communicate with the environment - *e.g.* membrane thickness fluctuations have been proposed as a mechanism to regulate pore formation promoting cellular uptake and/ or release events to take place. **(16)**

In addition to their biological relevance, lipid membranes are rather fascinating systems to study since they have interesting thermodynamic properties of their own. The rich variety of chemically different lipids (refer back to **Section 1.1.3**) and proteins leads to a dynamic organization not only across the bilayer - *transversally* -, but also *lateraly*.

As a consequence, in recent years, the model for the membrane architecture evolved from the fluid-mosaic model to a more dynamic structural organization. **(40)** Nowadays, biological membranes are seen like macromolecular entities who present lateral heterogenity. The lateral organization is a key feature for the functioning of a membrane. Usually, biological membranes are thermally disordered, hence dynamic, even at physiological temperatures. This is reflected by an high mobility of lipids and other membrane components in the "two-dimensional liquid matrix", as suggested by Singer and Nicolson in their fluid mosaic model. **(7)** The segregation of the lipid constituints in two or more physico-chemical differentiable regions, may promote the formation of microscopic domains, usually termed microdomains, with different fluidity confered by different protein or lipid concentrations. **(40)**

Usually it is thought that the fluidity of membranes depends largely on the nature of the acyl chain region comprising the hydrophobic domain of most membrane lipids. In addition, membrane systems are able to undergo a transition from a very viscous gel (*frozen*) state to a fluid (*melted*) liquid-crystalline state at certain environmental conditions. **(41)** Such a transition has been studied intensively, since it is thought that the local fluidity of certain regions of the membrane may regulate membrane-mediated processes. Most precisely, at the fluid liquid-crystalline phase, at a temperature above the melting temperature (T_m) of the lipid species, lipid tails are highly fluid, disordered and in constant motion. **(16; 41)** When at the gel phase, at a temperature lower than the respective T_m, lipid tails are fully extended with highly ordered packing being residually fluid. However, at physiological ranges, the temperature varies little ($36.8 \pm 0.7\ ^oC \sim 309.95$ K), and therefore, usually all membrane lipids and the membranes that contain them, are already in a fluid-like state, being highly disordered and in constant motion. As a consequence, transitions dependent on temperature variation are not physiologically relevant. However, other factors, such as pH, can have a crucial role in phase

transitions and microdomain formation under physiological conditions. **(42)**

1.2 Role of pH in the cell

Despite being exceptionally small and one of the most simple chemical species, protons play a central role in the life of cells. Many physicochemical reactions in living cells involve exchange of these hydrogen ions, and changes in its concentration are intimately tied to the charge presented not only by side chains in proteins, but also on the titrable head groups of some ionizable lipids. **(43)** The induction of reversible chemical changes through ionization events, results in substancial electrostatical perturbation, ultimatelly affecting the interaction of the titrable macromolecule with the surrounding enviromnent in a structural, dynamical and functional way. **(43–45)**

Since Life is intrinsically water-dependent, one should expect that the existence of all living things depends strongly on aqueous equilibria, especially acid-base equilibrium. Major fluctuations at the aqueous solution pH should lead to fluctuations of the same magnitude at the cell internal solution, the cytosol. The truth is that although pH effects have a direct impact on the plethora of biological, biochemical and biophysical processes that take place in the cell, through changes in intracellular pH (pH_i), these despite physiological relevant are mostly quite small — cytosolic pH homeostasis is tightly regulated. **(43; 44)** Many of the dramatic phenotypical differences observed in cells at different pH conditions, either at physiological or pathological states, are, in the most cases, solely driven by changes of 0.3-0.5 pH units. In one hand, increases in pH_i are on the basis of growth factor-induced cell proliferation, cell cycle progression and differentiation events, while on the other hand, pH decreasing is usually associated as a non-survival apoptotic signal. **(43)**

Even though events and associations to pH are widely documented, the reasons that sufixe such phenomena are still misunderstood. The importance of gaining a detailed understanding of protonation-conformation coupling and its modulation by pH should be, as today, a topic of major concern. Proteins and lipids are sensitive to modifications of the proton concentration in their environment. For proteins, this dependence is well established since pH is one of the main regulators of the activity of several key enzymes and metabolic pathways. **(43–45)** In the case of lipids, the role of pH is usually not considered to be relevant, because most biophysical experiments use models based on pure zwitterionic lipids. If pH has limited impact on these lipids, the same does not apply when dealing with even small content of anionic lipids. In fact, a large number of biological membranes have anionic lipids in their constitution, which render them pH-sensitive. **(46; 47)**

1.3 Phosphatidic Acid, a Signalling Lipid

Recognition of lipids by proteins is important for their targetting and activation in many signalling pathways, but the mechanisms that regulate such interactions are largely unknown. **(48)** Even though PA is the simplest membrane phospholipid, at least from a purely structural point of view (**Figure 1.4a**), it occupies a key position in many metabolism and biogenesis related processes in plants, animals and microorganisms. **(32)** Recently, PA was established as a pH biosensor (**Figure 1.5**). **(46; 49)** In yeast, under nutrient depletion conditions (acidic pH), the negative transcriptional regulator Opi1 is released from the ER membrane to the cytosol to inhibit membrane biogenesis. A rapid and significant decrease in intracellular pH results in increased protonation of its phosphomonoester, thereby reducing the strength of the electrostatic interactions with the effector. **(48)** pH-modulated PA binding of Opi1 is the basis of the coupling between membrane biogenesis and general metabolism. **(49)** This anionic lipid has a complex pH titration behavior where it can capture/release two protons, and probably exhibit different mixtures of charges (0, -1 and -2) at physiological pH. Having two pK_a values, one of which expected to be in the physiological pH range, PA varies significantly its protonation state according to small changes in solution pH, and therefore bind proteins in a pH-dependent manner. **(47)**

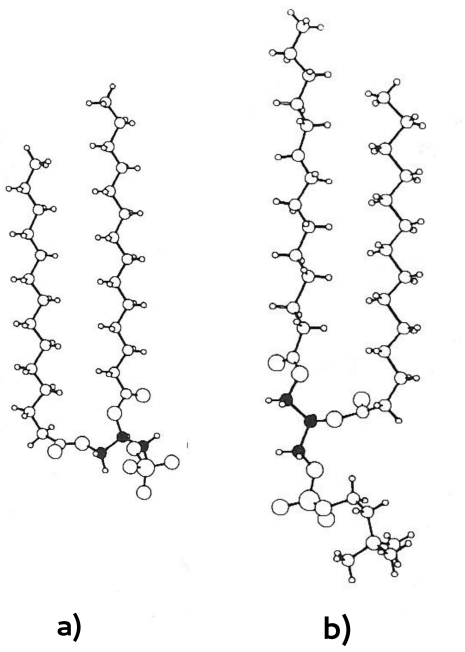

Figure 1.4: Single crystal structures of DMPA (a) and DMPC (b) phospholipids. Image adapted from **(9)**.

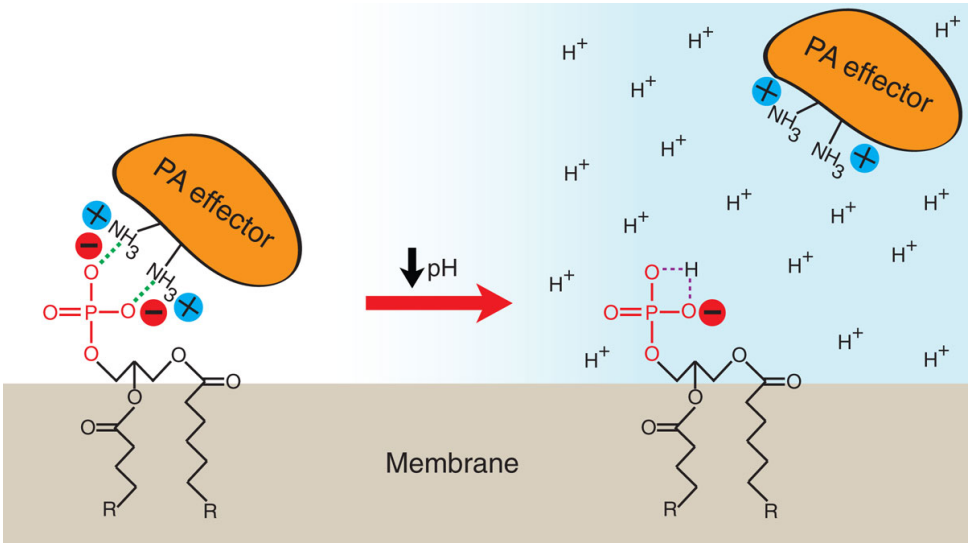

Figure 1.5: Phosphatidic acid as a pH biosensor. Diagram representing the mechanism by which effector proteins bind PA at acidic pH values proposed by Shin and Loewen. **(48)** Image was retrieved from **(48)**

There is limited experimental data concerning PA/PC binary mixtures. **(42; 50)** However, Garidel and coworkers published a comprehensive study of pseudobinary phase diagrams PA/PC mixtures at several pH values and at an ionic strength of 0.1 M. **(50)** In this study, the author suggests that some of these mixtures undergo phase separation under certain pH conditions. From these, we obtained the lipid phases of our 25% PA/PC bilayer at three different pH values (pH 4.0, pH 7.0 and pH 12.0), which were pivotal to validate our approach.

The experimental data reported by Träuble and coworkers **(42)** refers to a pure PA-containing membrane, at ionic strength of 0.0 and 0.5 M. These do not correspond to physiological conditions and hence we could not take real immediate advantage of it. However, in the near future this data will be useful to further validate our results.

Chapter 2

Theory and Methods

2.1 Molecular Mechanics/ Molecular Dynamics (MM/MD)

Biological membranes can be investigated by various experimental techniques, including X-ray diffraction, fluorescence methods, and nuclear magnetic resonance (NMR) spectroscopy. These macromolecules assemblies, being inherently complex both on its structure and dynamics, do exist, in a physiological form, in a liquid crystalline (fluid) state. This implies a relatively high degree of disorder, a characteristic feature of lipid bilayers, which greatly limits the nature of the structural data that can be obtained experimentally **(51)**. In addition, experimental measurements cannot always give an unambiguous picture of individual lipids and their interactions since either structural or dynamical properties are obtained as averages over a large number of lipids and over a given time interval, leading to a lack of resolution power. **(52)** All these factors, as well as differences in the space and time scales that both experimental and theoretical molecular dynamics (MD) techniques can intrinsically probe, make the investigation at an atomic level of detail of the structure and dynamics of biological membranes challenging, or even inacessible, for most experimental techniques.

Biological systems, in general, are very complex, and experimental data is often at too low resolution to infer details at an atomic level, hence, the opportunity to use molecular modeling to predict molecular properties that are otherwise difficult to observe experimentally. Often, those who do it, find themselves in a paradoxical situation where the predictions obtained cannot be validated. Nevertheless, for the past decades, MD simulation methods have become a valuable and well established primary tool used in the theoretical study of biological membrane models at an near-atomic or atomic level. **(53; 54)** [1]

[1] An in-depth detailed description of MM/MD can be found in **(55)** and **(56)**.

In contrast with quantum mechanical methods, in molecular mechanics (MM) the nuclei and electronic motions are assumed to be independent (Born-Oppenheimer approximation). Due to such simplification, by averaging out the electronic motion (the electrons are assumed to be at their optima positions), the potential energy of a system can be calculated seldomly as a function of nuclear positions. This leads to a considerable reduction of the required computational and time cost of the calculations.

Through the integration of Newtonian, classical equations of motion, with respect to time, one is able to compute the instantaneous forces acting on the system and hence the velocities and the trajectory of the particles in the system can be determined atom by atom. By trajectory one refers to the description of the positions of the particles - atoms or molecules - over time. Globally, the characterization of the time evolution of the molecular structures, their fluctuations and interactions, one is able to investigate the kinetic and thermodynamical properties of a system **(57)**.

In more detail, the forces can be calculated from the negative gradient of the potential energy function, $-\nabla_i U$, which describes energy terms from the bonded and non-bonded interactions between the particles:

$$-\nabla_i U = E_{bonded} + E_{non-bonded} \tag{2.1}$$

The potential energy U in the GROMOS force field (FF) **(58; 59)** is a function of the positions of all atoms in the system. The forces $\mathbf{F}_i$ of each atom i in the system can be related with changes in their position, $\mathbf{r}_i$, over time (t):

$$-\nabla_i U(\mathbf{r}_i) = \mathbf{F}_i = m_i \mathbf{a}_i \tag{2.2}$$

$$\mathbf{F}_i = m_i \frac{\mathrm{d}\mathbf{v}_i}{\mathrm{d}t} = m_i \frac{\mathrm{d}^2 \mathbf{r}_i}{\mathrm{d}t^2}, \tag{2.3}$$

where the acceleration $\mathbf{a}_i$, together with the prior position $\mathbf{r}_i$ and velocity $\mathbf{v}_i$ of each atom i of mass m_i, determines their new position after a given time step.

Revisiting the potential energy function (**Equation 2.1**), the energy of a given molecule with a certain conformation can be obtained from the interatomic interactions within a system. In most FFs used for MD simulations, the potential energy function of a given system in a certain configuration has the following general form:

$$U = U_{bonds} + U_{angles} + U_{dihedrals} + U_{impropers} + U_{vanderWaals} + U_{electrostatics}, \tag{2.4}$$

where the first four terms parameterize the interactions of atoms chemically bonded to each other (intramolecular or internal terms), while the last two terms (nonbond, intermolecular, or external terms) describe the van der Waals and electrostatic interactions between atoms, respectively. In more detail:

$$U_{\text{bonds}}(r_{ij}) = \frac{1}{4}k^b_{ij}(r^2_{ij} - (r^0_{ij})^2)^2 \tag{2.5}$$

$$U_{\text{angles}}(\theta_{ijk}) = \frac{1}{2}k^\theta_{ijk}(cos(\theta_{ijk}) - cos(\theta^0_{ijk}))^2 \tag{2.6}$$

$$U_{\text{dihedrals}}(\zeta_{ijkl}) = k^\zeta[1 + cos(n\zeta_{ijkl} - \zeta^0_{ijkl})] \tag{2.7}$$

$$U_{\text{impropers}}(\xi^{ijkl}) = \frac{1}{2}k_\xi(\xi_{ijkl} - \xi^0_{ijkl})^2 \tag{2.8}$$

$$U_{\text{LJ}}(r_{ij}) = 4\epsilon_{ij}[(\frac{\sigma_{ij}}{r_{ij}})^{12} - (\frac{\sigma_{ij}}{r_{ij}})^6] \tag{2.9}$$

$$U_{\text{electrostatic}}(r_{ij}) = \frac{1}{4\pi\epsilon_0}\frac{q_i q_j}{\epsilon_r r_{ij}}, \tag{2.10}$$

corresponding to the sum of several contributions, namely - U_{bonds}, the bond stretching between two covalently bonded atoms i and j (r_{ij} – interatomic distance (bond length); ;k^b_{ij} – bond force constant; r^0_{ij} – equilibrium length); U_{angles}, the bond angle bending between atoms i j k (θ_{ijk} – bond angle; θ^0_{ijk} – equilibrium angle); $U_{\text{dihedrals}}$ (k^ζ – force constant; n – dihedral multiplicity; ζ_{ijkl} – proper dihedral angle (phase factor); ζ^0_{ijkl} – reference proper dihedral angle) and $U_{\text{impropers}}$ (k_ξ – force constant; ξ_{ijkl} – improper dihedral angle; ξ^0_{ijkl} – reference improper dihedral angle), the proper and improper dihedral potential, respectively (all these bonded atoms contributions are represented by two-body, three-body, four-body terms, based on bond distances and bond and dihedral angles); the last two terms correspond to non-bonded interactions, usually described by pairwise interactions, where $U_{\text{vanderWaals}}$ (σ_{ij} – collision distance; ϵ_{ij} – well depth) and $U_{\text{electrostatics}}$ (ϵ_0 – electric permittivity of vacuum; ϵ_r – relative dielectric constant) correspond to the van der Waals attractive/repulsive interactions (modelled by using a Lennard-Jones 12-6 potential) and the electrostatic interaction (modelled by a Coulombic potential).

By considering an isolated system of fixed N particles in a constant volume V, and at constant energy E, we are dealing with the most fundamental statistical mechanics description of a system, the microcanonical ensemble (NVE). **2** A system simulated with such an ensemble will evolve towards temperature, T, and pressure, P, equilibrium, whose equilibrium values are difficult to estimate *a priori*.

A more realistic, and convenient, approach is to study a system where T, P or both thermodynamical parameters are kept constant. In our case, let us consider the statistical mechanics

2 In fact, even though the total energy E is conserved, potential and kinetic energies do vary with time.

principles regarding the isothermal-isobaric (NPT) ensemble - the one used in this work. In the NPT ensemble, the number of molecules (N), the pressure (P) and the temperature (T) are kept constant, throughtout the entire simulation trajectory. In this ensemble the volume variations are used to adjust pressure.

An important approximation has to be taken into account regarding the non-bonded interactions. Electrostatic interactions are treated in molecular mechanics by pairwise calculation using the Coulomb Law. With the increasing size of the systems of interest, and especially by the inclusion of explicit water molecules, the calculation of all possible interactions is prohibite, making simulations unfeasible. These scale with the size of the system by a factor of 2^N, where N is the total number of particles. Since the systems of interest are usually of large proportions such calculations are prohibitive. **(57)** Hence, we rely on the use of cutoff methods with long-range electrostatic treatments. Despite such limitation, the importance of an accurate representation of electrostatics cannot be overemphasized, since it has profound consequences on the accuracy of classic FFs.

Initially, long-range interactions in macromolecular simulations were usually treated by means of truncation schemes in which the electrostatic interactions are computed up to some cutoff distance. Based on the fact that the Coulombic potential decreases monotonically with atomic distance and that the aqueous solution provides an high dielectric screening, truncation of electrostatic interactions was rather usual. In fact, due to the lack of sufficient computational power, the usage of such aproximations was mandatory. However, simulations with electrostatic cutoffs soon revealed to give rise to the reproduction of severe unphysical behavior in the structure, dynamics, and thermodynamics of the system under investigation. **(57)**

Many authors defend that when modeling biological membranes, the Ewald as well as its variant, the Particle-mesh Ewald (PME) algorithm **(60)**, are the most appropriate methods to be used in the treatment of electrostatic interactions. In fact, when modeling biological membranes these are the most commonly used methods. This method calculates electrostatic potential beyond a chosen cutoff distance by the solution of a PB equation for a solute in a continuum bath. The electrostatic potential within cutoff distance is calculated as Coulomb forces. However, PME presents a considerable limitation when dealing with charged systems, namely, the need to have our microscopic system neutralized. With densely charged systems, this implies the use of a fixed lower limit counterion number, independent of the desired ionic strength. In order to overcome this problem, we opted for the continuum-based reaction field (RF) approach **(61)**, which present both the computational eficiency and the possibility to treat non-neutral systems. In addition, the Generalized Reaction Field (GRF) allows the inclusion of an implicit ionic strength. **(62; 63)** In this method, the interactions of the molecule inside a sphere of radius given by the cutoff distance are calculated explicitly, and the environment outside this sphere is modeled by a homogeneous medium with a given dielectric constant.

2.1.1 Force fields (FF) development for lipid bilayers

As stated in the previous section, a proper parametrization of the FF defining interatomic, and hence molecular interactions, is an ongoing problem in molecular simulations. Ideally, a FF should provide agreement with all available experimental data, within the simulation and experimental uncertainty. Even though uncertainties caused by the equilibration stage and statistical error are decreasing with the acessible longer timescales, the experimental techniques are improving concomitantly and at some point, the FF which earlier provided satisfactory agreement with experimental data, may begin to show significant discrepancies.

For the past decades (or years, in the case of lipid bilayers simulations), many were the alternative parameter sets that have been proposed by the most renowned names in the field, most of them based on the united-atom force field GROMOS **(59)**, and on the all-atom force fields CHARMM **(64)**, AMBER/GAFF (Generalized AMBER FF) **(65)** and OPLS **(66)** [3]. Here I give account to some of the most recent developments that have been critical for improving the application of the GROMOS FF to lipids, the FF used in this thesis.

Since the earliest GROMOS parameter sets developed in the mid eighties, the GROMOS FF has undergone continuous revision and has been refined so that a broader range of experimental data could be reproduced with a sufficient degree of accuracy. Among such refinements are the reparameterization of van der Waals interactions for nonpolar groups and the introduction of a twin-range 0.8 nm/1.4 nm for both electrostatic and van der Waals interactions (GROMOS 43A1), a correction of the torsion-dihedral parameters and the refinement of third-neighbor van der Waals interactions (GROMOS 43A2), the reparameterization of the Lennard-Jonnes parameters of aliphatic carbons (GROMOS 43A3), and the extension to lipids (phosphatidylcholines (PC)), carbohydrates and nucleic acids (GROMOS 45A4). An extensive reparameterization of nonbonded interactions involving polar groups based on the free enthalphy of hydration and apolar solvation of a range of model molecules was undertaken and led to GROMOS 53A5 and 53A6.

A common feature of all these diverse GROMOS FF was that they simply failed to reproduce, in an appropriate manner, the properties of a pure phosphatidylcholine (PC) - a major component of biological membranes - in its fluid (L_α) phase. **(51)** Later, Kukol *et al* proposed a correction to the GROMOS 53A6 parameters for lipids, suggesting changing the atom type used for the carbonyl carbons in PC **(67)**. It involved artificially enlarging the van der Waals radius of the carbonyl carbon in the glycerol backbone in order to increase the water penetration into the bilayer, while maintaining the remainder of the force field consistent.

[3] One can proceed to the investigation of such alternative parameter sets for lipids by looking at the Lipidbook database, a public repository containing the entirety of all published lipid force fields: **lipidbook.bioch.ox.ac.uk/**

From the group of Alan Mark came a second correction to GROMOS 53A6. **(68)** The authors increased the repulsion between the choline methyls and the nonester negatively charged phosphate oxygens. This was done by increasing the van der Waals radius for this particular interactions (introduced by a new atom type for the charged -CH_3 group whose repulsive Lennard-Jones (LJ) (C^{12}) is higher for the phosphate free oxygens). Pushing away the positively charged cholines diminishes the shielding of the repulsion between phosphates, and consequently, increases the area per lipid. The recent GROMOS 54A7 FF parameter set adopted the Alan Mark correction which results in a great improvement of the fluidity of PC lipid bilayers. **(51; 68)**

All the recent GROMOS based FF use the partial atomic charges calculated by Chiu *et al.* **(69)** Even though the high level of accuracy achieved by the latest 54A7 GROMOS FF, there is plenty to improve and our need to model the protonated versions of several phospholipids forced us to evaluate the atomic charges present in these force fields.

2.1.2 MD simulations of Membranes

Structural information about the molecular organization of the lipid bilayers and their interactions with small molecules, peptides, and proteins is essential for the understanding of a growing number of relevant biological systems. **(70)**

MD simulations have been used to elucidate the structural properties of the lipid bilayers at the atomic level. **(70–73)** With this information, the study of structure-function relationship of the lipid bilayers, and their proteic partners, is now a feasible topic. With increasing computational power, at the cutting edge of technology, it is now possible to simulate very large systems with a large number of interacting particles, for longer timescales (hundreds of *ns* to some *ms*). **(74)** This had led to tremendous increase of the number of research on the computational modeling of lipid bilayers.

Nowadays, the main limitation in the study of more realistic lipidic mixtures with MD simulations is the lack of proper methodologies. Besides PC, most lipid molecules are poorly parameterized and "simple" physico-chemical properties, like pH, remain a computational challenge.

2.2 Continuum Electrostatics (CE)

Continuum Electrostatics (CE) are simplified methods that can describe the electrostatics of a solute as a continuous function in space **(75–78)**. We used one of such methodologies, the Poisson-Boltzmann (PB) model **(79–82)** to obtain the electrostatic potential needed for

p$K_a$calculations. In PB models (**Figure 2.1**), the solute is described with atomic detail (coordinates, radii and charges) with a low dielectric constant (2 is used within the Constant-pH MD (CpHMD) framework) within an implicit solvent continuum with a higher dielectric constant (80 for water). These dielectric constant approximations try to describe the instantaneous reorganization of dipoles of the different environments.

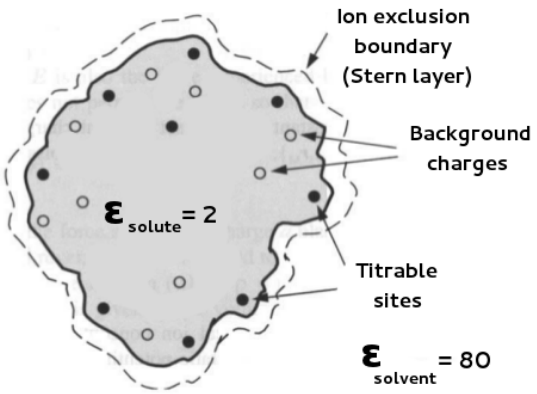

Figure 2.1: General continuum electrostatics model. Image was adapted from **(83)**

The protonation free energies can be calculated using a thermodynamic cycle (**Figure 2.2**) which reduces an intrinsically complex quantum mechanical problem of bond formation to a simple problem of free energy of solvation. With the protonation free energies and the pairwise interactions, we can calculate the protonation states of protonable groups in our systems using a Monte Carlo (MC) method. **(55; 56; 84; 85)**

$$\begin{array}{ccc} \mathrm{A^{sol}} + \mathrm{H^+} & \xrightarrow{\Delta G^\circ{}_{\mathrm{sol}}(\mathrm{A}\rightarrow\mathrm{AH})} & \mathrm{AH^{sol}} \\ \Big\downarrow{\scriptstyle \Delta G^\circ{}_{\mathrm{sol}\rightarrow\mathrm{M}}(\mathrm{A})} & & \Big\downarrow{\scriptstyle \Delta G^\circ{}_{\mathrm{sol}\rightarrow\mathrm{M}}(\mathrm{AH})} \\ \mathrm{A^M} + \mathrm{H^+} & \xrightarrow{\Delta G^\circ{}_{\mathrm{M}}(\mathrm{A}\rightarrow\mathrm{AH})} & \mathrm{AH^M} \end{array}$$

Figure 2.2: Thermodynamic cycle involving membrane and model compounds.

The use of continuum electrostatics methods for the p$K_a$calculations in proteins has received considerable interest from the scientific community for over three decades. However, these methodologies have scarcely been used to characterize the electrostatic potential of lipid bilayers **(86)**. Recently, several authors started using this approach to do p$K_a$calculation of simpler systems like micelles **(87–89)**. The choice for addressing micelles over lipid bilayers resides in the fact that most methods are not able to deal correctly with the periodic boundary conditions needed to model a lipidic patch. In our CpHMD method, we can now include periodic boundary conditions (PBC) in the PB calculations, which resulted in a better description of the electrostatic potential used in p$K_a$calculations, but also became very important in the

PB calculations of strongly charged membranes, that are needed for the explicit ion estimation procedure.

Changes in pH can generate high charges on a lipid membrane patch being simulated. These "infinite" charged surfaces are particularly sensitive to ionic strength and the counter-ions present. A good physical representation of these membranes requires an "a priori" estimation of the correct number of ions to be present in order to stabilize the charges at the surface, as these will have a major impact on the protonation and conformation of the bilayer. The ion distribution at a given ionic strength can be estimated using the PB formalism - **Figure 2.3**.

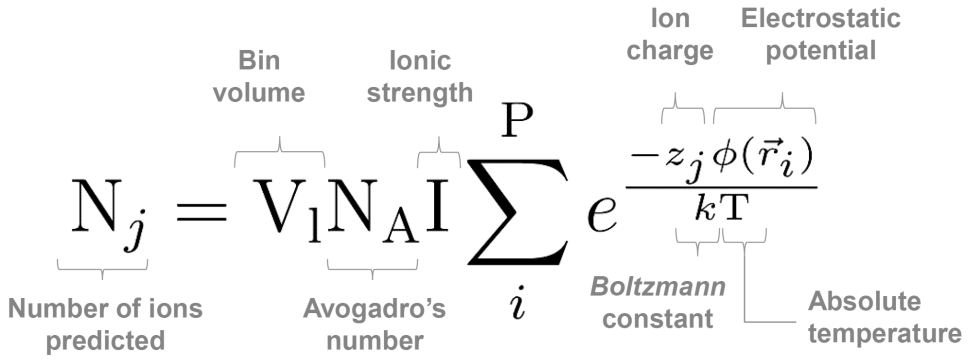

Figure 2.3: Rearranged Poisson-Boltzmann (PB) equation

To estimate the number of ions accessible to the membrane, we can sum all contribution from the grid points that are beyond the Stern layer (ion exclusion layer) but still within the cutoff of long-range electrostatic treatment in the MD simulations.

2.3 Computational details of MD simulations

All the standard Molecular Dynamics (sMD) simulations were performed with the GROMOS 54A7 force field **(90)** for a modified version of GROMACS distribution (version 4.0.7) **(63; 91)** and with the SPC water model **(92)**. The atomic partial charges of the lipid molecules were parametrized following the procedure of Chiu *et al* **(69)** (for details see **Section 2.5**). PBC with the usual minimum image convention were used in all three dimensions, with a tetragonal/ rectangular prism boxtype.

Two Berendsen's temperature couplings to baths at 310 K and with relaxation times of 0.1 ps were used for both the membrane and solvent **(93)**. Therefore, the temperature of the bilayer and water molecules plus counterions was controlled separately.

The temperature of the system was set at 310 K. The gel-liquid crystal phase transition

temperature of DMPC is situated at around $T_m \sim 297$ K [4], while the correspondent transition temperature for DMPA is around $T_m \sim 325$ K. **(50; 94)**

A Berendsen's pressure coupling **(93)** was used to scale the box semiisotropically (*i.e.*, the extension of the simulation box in the bilayer normal direction (z) and its cross-section area in the bilayer plane (xy) could vary separately) at the constant pressure of 1 bar using a relaxation time of 5.0 *ps* and a compressibility of 4.5×10^{-5} bar^{-1}.

The bond lengths of all molecules were preserved using the Parallel Linear Constraint Solver (P-LINCS) algorithm **(95)**. The equations of motion were numerically integrated using a time step of 2 *fs*, for all simulations.

Nonbonded interactions were treated with a twin-range cutoff, with short— and long—range cutoffs of 8 Å and 14 Å, respectively. The neighbor pair list was updated every 5 steps. Long—range electrostatics interactions were treated using the Generalized-Reaction-Field method **(62)**, with a relative dielectric constant of 54.0 and and ionic strength of 0.1 M, being treated as an external parameter. **(63)** For a set of simulations to test different long—range electrostatic interactions treatments we also used PME **(60)** to treat these type of interactions. In the case of PME, a grid spacing of 1.0 Å was used, and the short-range interactions were calculated using a nonbond pairlist with a single cutoff of 10 Å. The PME neighbor pair list was updated every 10 steps.

Our lipidic systems are composed of 128 lipid molecules (100% PC or 25% PA/PC), a varying number of water molecules and Na^+/Cl^- counter-ions (see an example in **Figure 2.4**). The hydration of the bilayer depends on the average A_L to assure the existence of a small bulk-like water region above the defined cutoff (**Figure 2.5**). The number of counter-ions used depends on the ionization of the system at the ionic strength of 0.1 M. We used a PB-based formalism to estimate the number of counter-ions which were explicitly added to each system. The systems were equilibrated under the new counter-ion regime and the distribution of ions was evaluated to assure self-consistency. If that is not the case, the number of ions needs to be corrected and a new evaluation cycle begins. The convergence criteria needs to be below one ion because a significant difference of the number of ions used can lead to artificial bilayer conformations. The counterion distribution in the MD snapshots was measured using an in-house tool that is able to compute the number of atoms within two cutoffs. In this case, we only limited the higher cutoff to 14 Å, the value used in the long-range electrostatics treatment. This tool was also used to evaluate the ions distribution along the membrane normal, using a 0.1Å-thick layers.

An energy minimization procedure consisting of 10.000 steps was performed using the steepest descent algorithm (unconstrained) followed by another 10.000 steps using the low-memory

[4] Since DMPC would be the major lipid molecule existent in our membrane systems, an absolute temperature of 310 K would be high enough to attain a lipid bilayer in the liquid-crystalline phase state

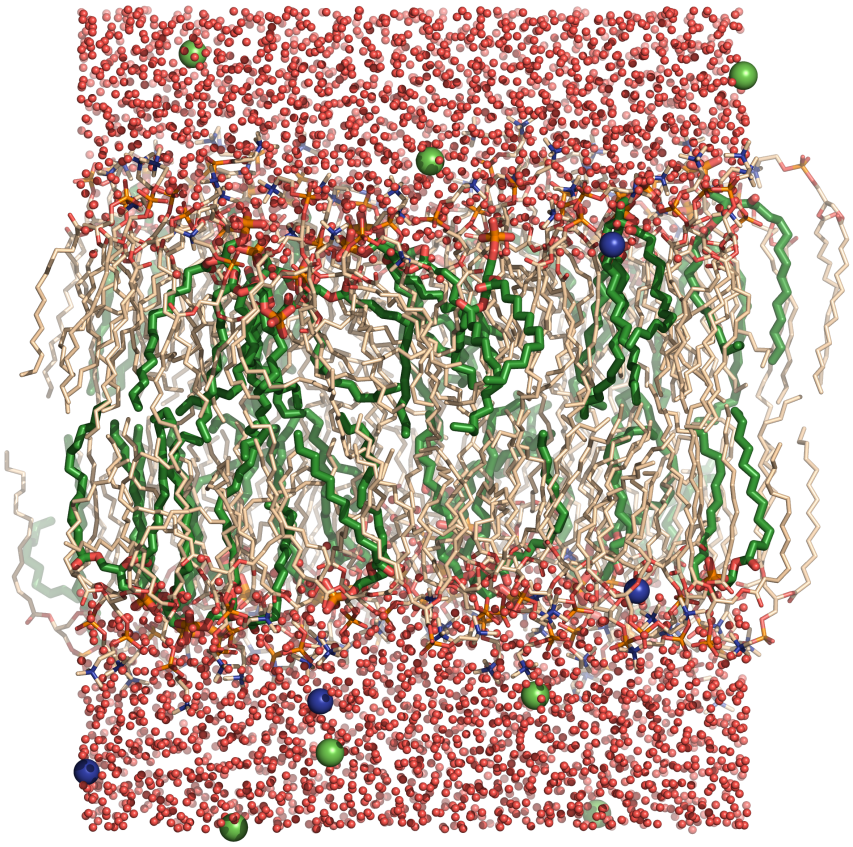

Figure 2.4: Snapshot of an equilibrium configuration of the hydrated bilayer system consisting of 128 lipids at a 25% molar fraction of DMPA over DMPC and 3946 water molecules as taken out from the computer simulations. Color-coding is the following: carbon atoms are either wheat or green when from aliphatic chains of DMPC and DMPA lipid molecules, respectively; water oxygens are red (water hydrogens were omitted for clarity); lipid oxygens are dark red; phosphorus atoms are orange, and nitrogens are blue. Na^+ and Cl^- ions are here represented as spheres, in blue and green, respectively.

Broyden—Fletcher—Goldfarb—Shanno (*l-BFGS*) integrator (unconstrained), and yet another 10.000 steps using again the steepest descent algorithm (with all bonds constrained).

The initiation of all systems consisted of a 50 ps simulation with all of the heavy atoms harmonically restrained to their respective fixed reference positions with a force constant of 1000 $kJnm^{-2}mol^{-1}$. This first initiation step was followed by three other initiation steps of 100 *ps*, 150 *ps* and 200 *ps* simulations, respectively. Throughout these three last initiation steps, the positions restraints where applied differently to phosphorus atoms and all the other heavy atoms. Hence, the force constants where 1000, 100 and 10 $kJnm^{-2}mol^{-1}$ for the phosphorus atoms pertaining to the phosphate headgroups of all lipids, whereas all other heavy atoms motion potentials where restrained with force constants of 100, 10 and 0 $kJnm^{-2}mol^{-1}$. Such restraints are usually applied during equilibration in order to avoid drastic rearrangements of critical parts of the studied biomolecule, *e.g.* to restrain motion in the lipids that are mostly

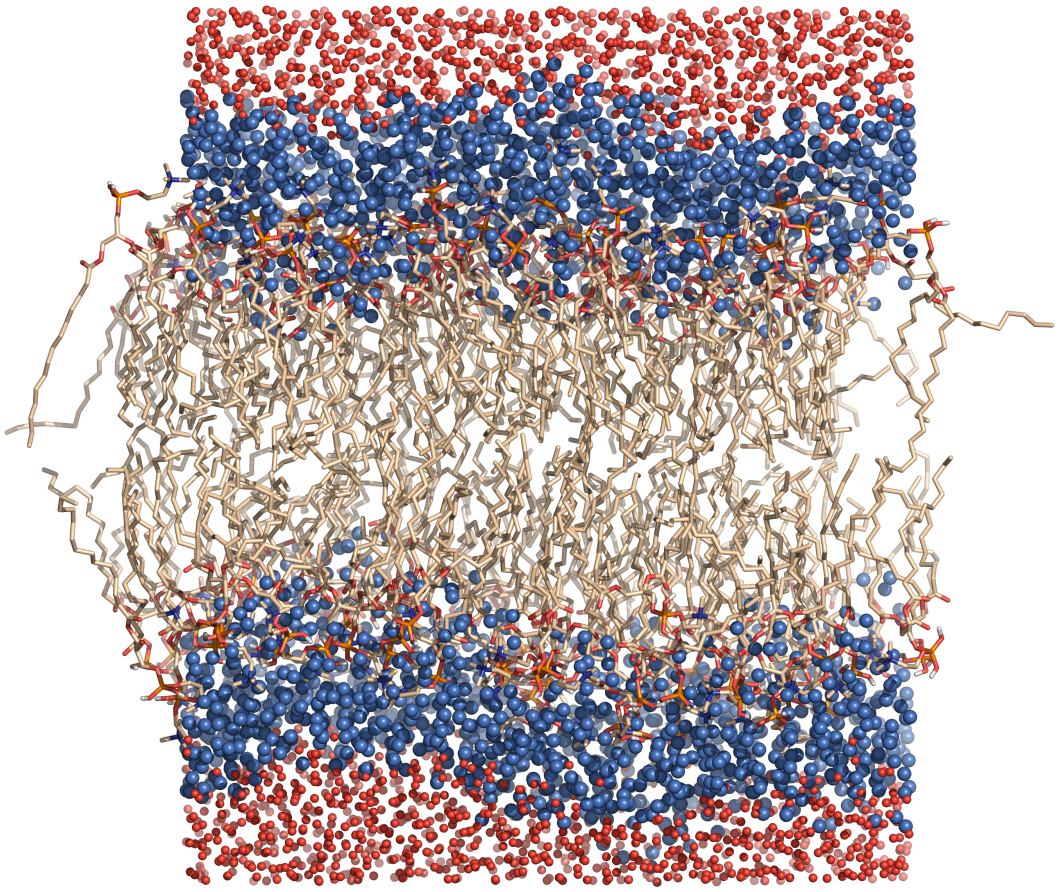

Figure 2.5: Snapshot of an equilibrium configuration of the hydrated 25% bilayer system portraiting the waters pertaining either to the membrane-water interface (local waters) - inside the 1.4 Åcutoff - in blue or to the bulk (bulk waters) in red.

subjected to large solvent forces when the solvent is not yet equilibrated. Special potentials are used for imposing restraints on the motion of the system, either to avoid disastrous deviations, or to include knowledge from experimental data.

The MD simulations of all billayer systems were pre equilibrated for 100 ns, at which point, three replicates where then started for 100 ns equilibrated runs. The first 20 ns were disregarded and the last 80 ns were used to assess equilibration.

These equilibrated sMD systems were used to initiate our CpHMD simulations. An *"a priori"* estimation of the ionization at a given pH was needed to choose the correct sMD system. **Tables 2.1** and **2.2** comprise all the sMD systems equilibrated.

Table 2.1: Lipid compositions of several one-component (pure) lipid membrane containing the zwitterionic lipid DMPC at different charge states

PA/PC (%)	DMPC	Charge	Composition	
			$DMPC^{+1}$	$DMPC^{0}$
0.00	128	0	0	128
		+6	6	122
		+12	12	116

Table 2.2: Lipid compositions of various two-component lipid membranes containing DMPC and DMPA at a molar fraction of 25%. The charge state of DMPC was fixed to $DMPC^{0}$, while DMPA lipids is present at several charge states.

PA/PC (%)	DMPA	DMPC	Charge	Composition		
				$DMPA^{0}$	$DMPA^{-1}$	$DMPA^{-2}$
25.00	32	96	0	32	0	0
			-8	24	8	0
			-16	16	16	0
			-24	8	24	0
			-32	0	32	0
			-40	0	24	8
			-48	0	16	16
			-56	0	8	24
			-64	0	0	32

2.4 Computational details of CpHMD simulations

The constant-pH MD method used was the implementation for the GROMACS package of the stochastic titration method previously described **(63; 91)**. This method relies on three sequential blocks (**Figure 2.6**):

1. First, using Poisson—Boltzmann/Monte Carlo (PB/MC) calculations, the protonation states of the titrable sites of the molecule of interest are evaluated and assigned;

2. Following the protonation changes (charge modifications) there is a short solvent relaxation MM/MD simulation of the system with the solute molecule frozen sufficient time (0.2 ps) for the water molecules to accomodate around the newly charged solute;

3. And finally, a full MM/MD simulation (20 ps) of the unconstrained system will produce a trajectory with the assigned set of protonation states. The last snapshot of the simulation will be used in the first block of the following cycle.

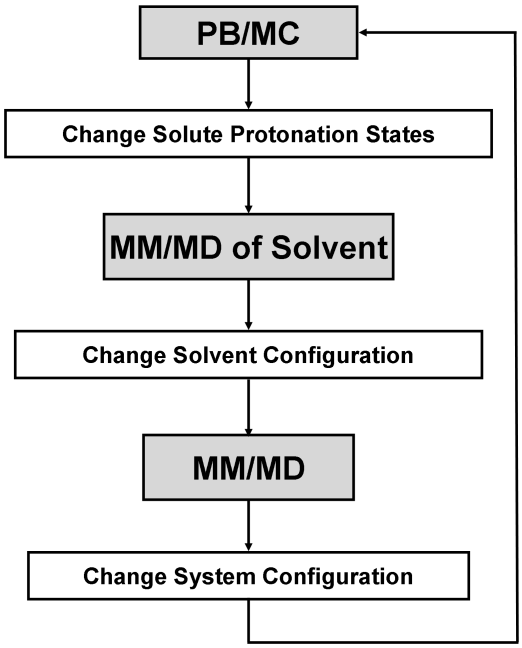

Figure 2.6: Scheme of the Stochastic CpHMD algorithm. Image adapted from **(91)**

The PB and MC calculations were done using the programs DelPhi (v5.0) **(96)** and PETIT (v1.6) **(97)**, respectively. The radii used in the PB calculations were derived **(98)** from the GROMOS 54A7 force field. **(90)** All PB calculations consisted of finite-difference linear and non-linear PB calculations at a temperature of 310 K, a molecular surface defined with a solvent probe radius of 1.4 Å, and a Stern layer of 2.0 Å. The dielectric constants were 2 for the membrane and 80 for water. **(99)** A two-step focusing procedure was used, with consecutive grid spacings of $\sim$ 1.0 Å and $\sim$ 0.25 Å. The larger grid had its spacings varying over time due to variations in the *xy* vector sizes. PBC were applied in this first PB calculation with the box size being the same as in MD. MC runs were performed using 10^5 MC cycles, one cycle consisting of sequential state changes over all individual sites and also all pairs of sites with at least one interaction term above 2 p$K_a$units. The model compound used for DMPC was dimethylphosphate, which has a p$K_a$value of 1.29. **(100)** In the case of DMPA, we used the monosubstituted methylphosphate, which has two p$K_a$values of 1.54 and 6.31. **(100)**

Relatively long equilibration periods (20-50 ns) were done in our CpHMD simulations, followed by 70-90 ns of production runs **Table A.2**. All CpHMD analysis were performed on these trajectories.

2.5 Deriving atomic partial charges for PA and PC lipids

All QM calculations were performed with the computational chemistry software program Gaussian 03 **(101)**. The geometry optimizations were done at the DFT level using a combination of Becke's three-parameter hybrid exchange functional and the Lee-Yang-Parr correlation functional (B3LYP). **(102–104)** The 6-31G(d) basis set was used in all calculations. **(105–111)** The electrostatic potential used in the subsequent RESP fitting procedure was obtained at the Hartree-Fock level in order to mimic the original approach by Chiu and coworkers. **(69)** The RESP fitting was done using a modified version of Amber Tools 1.3 RESP program. **(112–114)** We applied this procedure (**Table 2.3**) to the two charge states of PC (**Figure 2.7**) and to the three charge states of PA (**Figure 2.8**). The tautomers used in the CpHMD simulations shared the charge set of the equivalent charge state. The charges obtained for the deprotonated DMPC are very similar to those of Chiu *et al* **(69)**, for which the GROMOS force fields have been parametrized (**Table 2.3**). Therefore, we are confident of the transferability of this approach to DMPA and to the protonated form of DMPC.

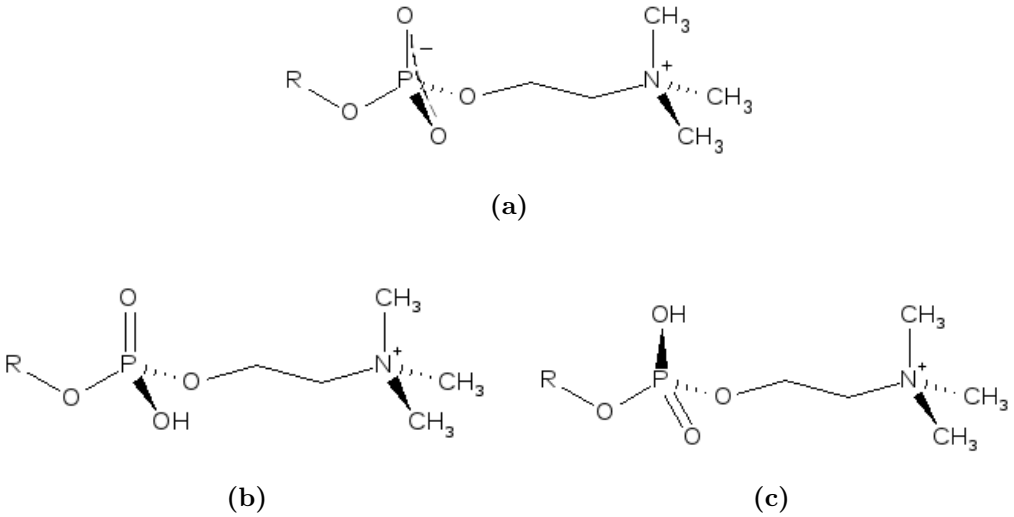

Figure 2.7: Charge states of a DMPC lipid molecule - **(a)** $DMPC^{0}$ and **(b,c)** $DMPC^{+1}$. All structures were obtained by using ACD/ChemSketch and gimp *softwares*.

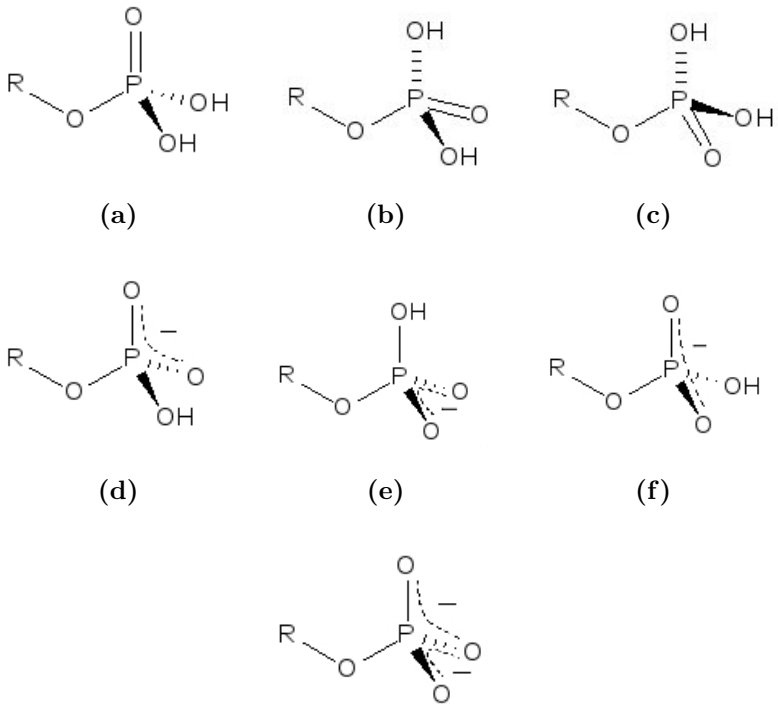

Figure 2.8: Charge states of a DMPA lipid molecule - **(a, b, c)** $DMPA^0$, **(d, e, f)** $DMPA^{-1}$, and **(g)** $DMPA^{-2}$. All structures were obtained by using ACD/ChemSketch and gimp *softwares*.

2.6 Analyses details

2.6.1 Area per lipid - A_L

A key structural quantity the average interfacial area per lipid molecule, along the bilayer's surface, commonly referred simply as area per lipid, A_L, is one of the most fundamental properties of a lipid bilayer, being one of the most commonly used properties to attest the correct liquid crystalline phase behavior in lipid bilayers. When the area per lipid properly converges, other structural properties (lipid lateral diffusion, density distributions, NMR bond order parameters) tend also to converge. **(52)** In addition, the A_L parameter is a direct measure of lateral organization (*packing*) of lipid systems **(115)**, while indirectly, it carries some transverse information, therefore playing an essential role in the description of membrane structure and function.

Given a simulation of a bilayer patch consisting of a single lipid component, the A_L can be easily and readily captured from the evaluation of the *xy* dimensions of the simulation box, assuming that the bilayer remains intact and that the limits of the membrane patch coincide with the box limits, troughout all the simulated trajectory. Hence, to compute this parameter,

Table 2.3: Charge sets computed by Chiu *et al* **(69)** and those computed by us for the charge states of DMPA and DMPC. The atom nomenclature was based on the atom names of DMPC in GROMOS 53a6 force field. **(68)**

Atom	**DMPC**$_{\text{Chiu}}$ ***et al***	**DMPC**$_{\text{Derived}}$		**DMPA**$_{\text{Derived}}$		
		DMPC^{+1}	**DMPC**^{0}	**DMPA**^{0}	**DMPA**$^{-1}$	**DMPC**$^{-2}$
C_{methyl}	0.40	0.42	0.40	-	-	-
N	-0.50	-0.58	-0.58	-	-	-
C_B	0.30	0.32	0.32	-	-	-
C_A	0.40	0.55	0.39	-	-	-
O_A	-0.80	-0.74	-0.69	-0.72	-0.91	-0.97
P	1.70	1.71	1.71	1.17	1.54	1.47
O_B	-0.80	-0.68	-0.90	-0.63	-0.80	-0.97
H_B	-	0.44	-	0.48	0.43	-
O_G	-0.80	-0.83	-0.90	-0.63	-0.51	-0.97
H_G	-	-	-	0.48	-	-
O_D	-0.70	-0.45	-0.61	-0.15	-0.35	-0.56
C_D	0.40	0.21	0.21	0.21	0.21	0.21
C_E	0.30	0.42	0.42	0.42	0.42	0.42
O_E	-0.70	-0.75	-0.75	-0.75	-0.75	-0.75
C_{1A}	0.70	0.85	0.85	0.85	0.85	0.85
O_{1A}	-0.70	-0.73	-0.73	-0.73	-0.73	-0.73
C_Z	0.50	0.41	0.41	0.41	0.41	0.41
O_Z	-0.70	-0.56	-0.56	-0.56	-0.56	-0.56
C_{2A}	0.80	0.83	0.83	0.83	0.83	0.83
O_{2A}	-0.60	-0.68	-0.68	-0.68	-0.68	-0.68

one should apply the following mathematical treatment:

$$A_L = \frac{x \times y}{\mathrm{N}}, \tag{2.11}$$

where x and y correspond to the box dimensions over the x- and y-axis along the simulation, and N is the number of lipids contained in one leaflet. However, the inherent simplicity of A_L for homogeneous bilayers is challenged and even lost, when the membrane system of interest is a mixture of two or more components, lipids or not. In mixtures, the well defined and unique measure of parameters (such as A_L) of individual molecular components precludes necessarily the application of the classical physical chemical concept of partial molar parameters (*e.g.* specific area per lipid or specific volume per lipid). Conventional approaches for simple one-component membrane systems cannot be easily applied to more complex systems where the A_L turns to be fairly heterogeneous, which can be attributed to the variety of different interactions among bilayer constituents - local perturbations on the molecules that are neighbors with. Hence, not only one should take in consideration that such mixtures are prone to experience

local inhomogeneity, but they can also give rise to the formation of microdomains, which are characteristic of heterogenous mixtures.

Although it is a difficult mathematical treatment, when compared to the formalism presented above, one can deal with the problem by computing the partial-specific-area for the several components, individually. In our system, we deal with a bilayer containing a mixture of two lipid components (binary mixture) of DMPA and DMPC, in a isothermic-isobaric (NPT) ensemble where the size of the simulation box is allowed to fluctuate in the *xy*-plane and *z*-direction separately (semi-isotropic). One can then define the area per total lipid *A(x)* as a function of the mole fraction of DMPA over DMPC (x), defined as:

$$x = \frac{\#_{\mathrm{DMPA}}}{\#_{\mathrm{DMPC}} + \#_{\mathrm{DMPA}}}, \tag{2.12}$$

$$A(x) = (1 - x) \times A_{\mathrm{DMPC}} + x \times A_{\mathrm{DMPA}}, \tag{2.13}$$

where $\#_{\mathrm{DMPA}}$ and $\#_{\mathrm{DMPC}}$ correspond to the number of either DMPA or DMPC lipid molecules in the system, and A_{DMPC} and A_{DMPA} are both variables dependent of x, corresponding to the partial specific areas of both DMPC and DMPA lipids, respectively. This rationale is followed by the premise that $\mathrm{A_{DMPA}}$ (x) can be estimated as the slope of the tangent in a plot of A(x)/(1-x) versus (x/(1-x) and $\mathrm{A_{DMPC}}$ (x) as the intercept of the tangent with the y-axis, as follows:

$$\frac{A(x)}{1 - x} = A_{\mathrm{DMPA}} \times \frac{x}{1 - x} + A_{\mathrm{DMPC}}, \tag{2.14}$$

Even though, we could have performed such an analysis, this approach would require us much needed time in order to simulate multiple membrane systems at several molar fractions and ionization values. Since we expect to be able to obtain equivalent information with other structural parameters (such as order parameter, thickness and diffusion, for instance), we have not explored extensively such an option. In that sense, such analytical treatment goes beyond the scope of this thesis and hence the A_L was computed as firstly presented. Nevertheless, for those eager to explore such a strenuous approach we suggest the reader a recent article where the authors propose a partial-specific area formalism, stated as an appropriate method to ascertain a canonical quantity to report from simulation of mixtures in contraposition to the Voronoi method for instance. **(115)**

2.6.2 Volume per lipid - V_L

The volume per lipid (V_L is one of the most accurate physical datum pertaining to the structure of bilayer systems. **(116)** Making the same assumptions intrinsic to the area per lipid determination, the V_L can be readily obtained from MD simulations by evaluating the volume of the simulation box, according to the following equation:

$$V_L = \frac{V_b - n_w V_w}{n_l}, \tag{2.15}$$

where V_b is the box system volume varying over time, V_w is the (presumably constant) volume of a single water molecule (this volume was estimated from an independent simulation of bulk waters), and finally, n_l and n_w correspond to the number of lipid and water molecules, respectively. By subtracting the volume occupied by the n_w water molecules from the total volume (*box system volume*), we are able to compute the volume of the membrane, and hence the volume of a single lipid molecule. **(117)** Notice that, again, for simplicity, we chose not to discriminate the volume of a single DMPA or DMPC molecule, but instead to compute the average volume of a single lipid molecule irrespective of its nature.

2.6.3 Order Parameter

Lipids in a fluid bilayer should not be seen as static components of the membrane, but instead as highly dynamic entities. **(118)** Many dynamical movements on different timescales are taking place, from rotation around chemical bonds and trans-gauche isomerisations, taking a few ps, to events such as lateral diffusion and flip-flop across the bilayer that take place in a superior timescale of *ms* to *s*. Most of these movements tend to influence in a significant manner the hydrocarbon lipid chains. **(118)** Therefore, when trying to elucidate the functional properties of membranes, it is important to study the way that the interfacial lipid headgroups behave, but also to focus on the study of the conformation and dynamics of lipid acyl chains, since these can modulate some macromolecular characteristics of the membrane, leading to structural effects on the membrane's surface.

The order parameter, S_{CD}, provides an indispensable measure of both disorder and fine-structure in lipid bilayers, and it can be experimentally measured by deuterium NMR experiments and by ESR-spectroscopy using spin-labelled lipids as spectroscopic probes. Even though it can se assessed by computer simulations, this interpretation is not entirely straightforward, and values computed through simulations do not necessarily correspond to quantities that can be measured. To assess the ordering effect in our PA/PC binary mixtures at several ionizations values, we have computed the order parameter profiles and hence their respective hydrocarbon chain order parameter, one of the most common and most important quantities to characterize

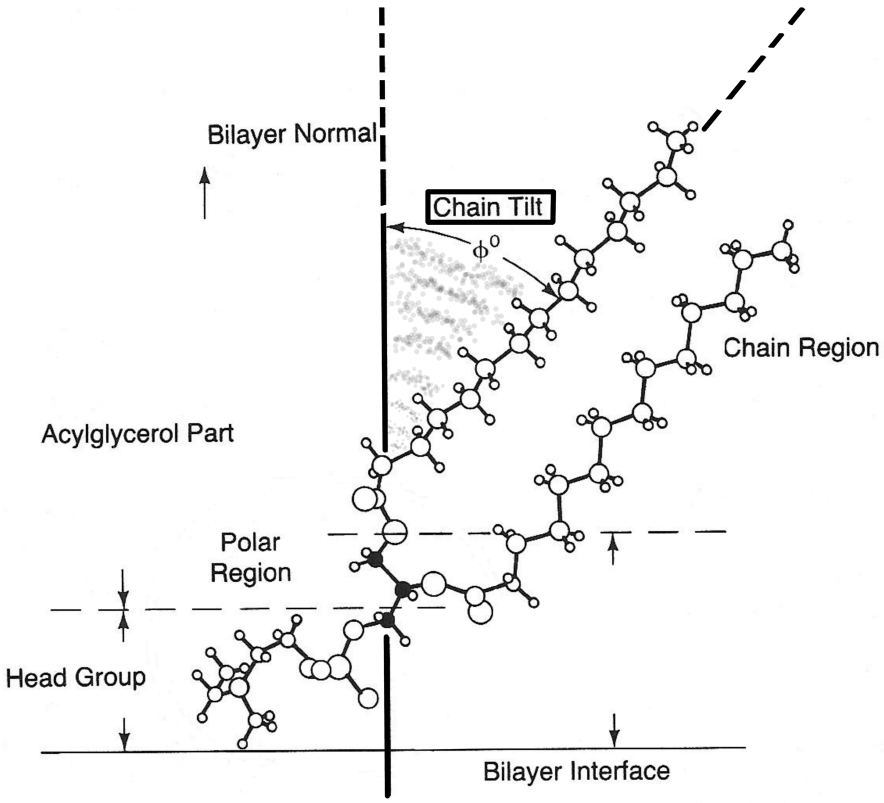

Figure 2.9: Schematic of a tilted PC lipid molecule showing the structural notation defining various regions . Figure adapted from Hauser, H. I. *et al* **(119)**

the state of the L_α-phase. **(117)** In this liquid-crystalline phase, the hydrophobic lipid chains do not form a rigid and well behaved tridimensional lattice, but instead are highly disordered, having almost free mobility and high content of *gauche* defects (resultant from high *trans-gauche* isomerization, only hindered by their close neighbors).

The deuterium order parameter, S_{CD}, is measured from ^{2}H-NMR experiments. This parameter reports the degree of disorder of the hydrocarbon region in the interior of the lipid bilayers by measuring the orientation of the hydrogen dipole of the methylene groups with respect to the perpendicular axis to the lipid bilayer.

We employed a standard approach for calculating the S_{CD} value which takes into consideration the fact that we use an united atom force field that does not provide in a direct manner the atomic coordinates of the hydrogen atoms - these atoms are incorporated into a mesoscopic particle known as united-atom containing both carbon atoms and the collapsed hydrogen atoms which are directly bonded to such atoms. **(120)** Since the hydrogens of the lipid methylene groups (CH_2) have not been taken into account, explicitly, in our simulations the order parameter on the i+1 methylene group was defined as the normal unitary vector to the vector defined from the *i* to the *i+2* CH_2 group and contained in the plane formed by the methylene groups *i*, *i+1* and *i+2*, as depicted in **Figure 2.9**.

Thus, S_{CD} on the *i-th* of the CH_2 group can be estimated by Molecular Dynamics simulations, as follows:

$$-S_{\mathrm{CD}} = \frac{< 3cos^2(\theta) - 1 >}{2} \tag{2.16}$$

where θ corresponds to the time-dependent angle between the unitary bond CD vector, defined above, and a reference axis, in this case, the bilayer normal, herein considered as the z-axis. In that sense, we can report the angular deviation (anisotropy) of the n^{th} segmental vector with respect to the chain axis in the *all-trans* state. **(94)** The angular brackets denote a time and ensemble average over all thermodynamically accessible configurations of the lipid chains.

2.6.4 Trans-gauche isomerizaton

As earlier stated, lipids in a fluid bilayer are highly dynamic. **(118)** Most of their dynamical behavior results from the existence of many possible states or conformations associated with their alyphatic chains. The richness in simple C-C bonds allows many degrees of freedom to emerge, and hence the appearance of many different structural organizations, including *kink* and *jog* conformations, and *trans/gauche* conformers originated from *trans-gauche*-isomerization events. **(39)** Proper dihedral angles can be classified in *trans* (t), *gauche*$^+$ (g^+) and *gauche*$^-$ (g^-) when its value is within the following ranges: $\measuredangle = 180 \pm 60^o$, $\measuredangle = +60 \pm 60^o$ or $\measuredangle =$ -60 $\pm 60^o$, respectively. **(39)**

2.6.5 Membrane thickness

The thickness of biological membranes is known to vary, both in time and in space - *e.g.* the bilayer can adjust its thickness in order to diminish the mismatch observed between the bilayer and the hydrophobic surface of embedded proteins. **(121)** Hence, understanding how a membrane modulates its thickness is an essential part of unraveling the relation between structure and function of biological membranes.

In order to compute the thickness of our membrane systems, we have obtained the mass density profiles across the bilayer, in respect to the phosphorus atoms of the phosphate headgroups of all lipids (DMPA and DMPC). These were calculated by separately analyzing each frame of the simulation, along the entire production time length. The center of the bilayer (*i.e.*, its z-component) was first determined by computing the center of mass (COM) for the two monolayers, accordingly to the phosphorus atoms z- cartesian coordinates. The positions of all phosphorus atoms were then corrected with respect to the respective COM. Since the system possesses a close to mirror-symmetry, all positions with z < 0 have been symetrized to z > 0

to improve sampling and hence reduce statistical error. In the case of DMPC, we also did this calculation for the nitrogen atom present in the choline groups. Finally, the thickness of the bilayer was defined as twice the distance between the peak of the phosphorus atoms density profile and the origin. **(122)**

2.6.6 Lateral Diffusion

The lateral self-diffusion of lipids, one of the best studied dynamical process occurring in membranes (**Figure 3.22**), can be measured by several techniques, from the most commonly used fluorescence spectroscopy methods (*e.g.* FRAP - fluorescence recovery after photobleaching - sensitive at the *ms* time scale), which compute the diffusion coefficient of lipids by the temporal displacement of fluorescence probes, to the more recent NMR and neutron scattering experiments (sensitive at the *ps* range). These types of experiments are limited by their time resolution, and the recorded displacements are really averages over some time window. Additionally, different techniques work at different time scales, and thus, the existence of a very wide range of experimentally determined coefficient values.

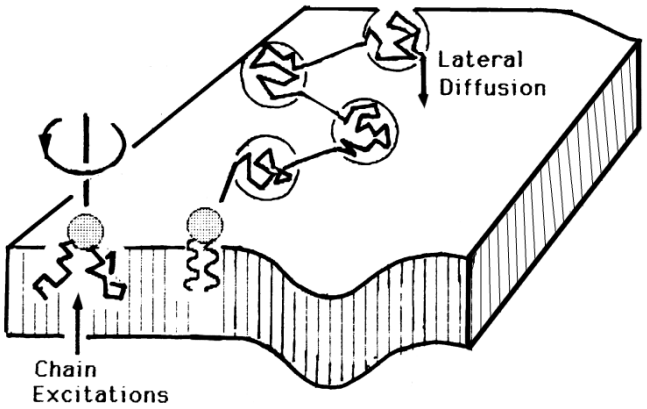

Figure 2.10: Thermal motions in membranes comprising chain conformational transitions, chain defects and rotational diffusion of lipid molecules about the long axes **(a)**, and in-plane lateral diffusion **(b)**. Figure adapted from E. Sackmann **(123)**

Since neutron scattering experiments measure on a much shorter time scale than FRAP, this technique led to the determination of diffusion coefficients that are significantly higher than others techniques working at longer time scales. After some unsettled times, the source of such a phenomenon was postulated to be the existence of two completely different types of lipid lateral diffusion taking place at different time scales. Hence, it was proposed that the in-plane motion of the whole lipids consists of two sequential stages: at shorter timescale, the lipid molecules diffuses locally within their solvent cage (one can see a local diffusion of a lipid molecule in its microenvironment, as it 'rattles in the cage' under the boundaries of their neighbors) and at

longer timescales, the well known long range diffusional jumps between adjacent sites (the lipid will start to conditionally hop between adjacent 'cages'), leading to the determination of much smaller diffusion coefficients, the so called asymptotic diffusion coefficient. **(124)**

When dealing with lipid chain and whole-lipid dynamics, MD simulation techniques have the advantage of being able to cover most of the essential time scales needed to calculate a dynamic property like diffusion, directly from stored atomic coordinates or velocities. In our case, by knowing the *xy*-positions as a function of time, and after obtaining the linear portion of the time dependency of the mean-square-deviation (MSD) for the analyzed trajectory, through a linear least square regression, we have computed the self-diffusion coefficient. As a side note, one should be cautious and perform the regression not over all the time range obtained, but rather on the maximum amount of data where the graphic behavior is linear and concomitantly where the observation time is long enough that we have reached the long-time asymptotical behavior. Even though it's not an objective of this work, the nonlinearity at short times makes this approach inappropriate to determine the fast diffusion without an additional fitting to a nonlinear expression. **(125)**

The lateral diffusion coefficient, D, can be computed using the Einstein relation, in two dimensions (the z-axis is collapsed into the xy-plane in order to account only with the lateral displacements over the membrane plane), by measuring the slope of MSD over time:

$$D = \lim_{t\to\infty} \frac{1}{4}\frac{\mathrm{d}}{\mathrm{d}x}\langle[r(t+t_0) - r(t_0)]^2\rangle_{t_0}, \tag{2.17}$$

where the self-diffusion coefficient, D, is related to the MSD of a particle as a function of observation time t ($[r(t+t_0) - r(t_0)]^2 \sim \langle r^2\rangle$). The angled brackets indicate that an ensemble average has been taken. The ensemble average is an average over all molecules in the simulation and all time origins - by origins we mean that any time step can be considered the time zero (t_0) because it is only looking at elapsed times rather than absolute times (for further information we suggest the reader to consult **(125)**).

2.6.7 Protonation

The lipid protonation was evaluated from the CpHMD simulations at different pH values. Even though the phosphate group was modeled taking in consideration the existence of conformational tautomers, we only needed to consider the different charge states in the total charge calculations. These were done by simply averaging over all lipids, over time, and over replicates.

2.6.8 Error analysis

All the errors presented in this work were computed as the correlation corrected standard deviation of the average, taking as correlation time the value at which the autocorrelation goes below 10%..

The mean and standard deviations obtained provide, in principle, estimates of the mean bilayer structure and the fluctuations of the bilayer around the mean. Knowing that on short timescales, bilayer configurations are highly correlated, and thus unsuitable for statistical analysis, we aimed at sampling interval to be long enough to assure a collection of uncorrelated bilayer configurations (**Table A.2**).

Chapter 3

Results and Discussion

3.1 Equilibration and Validation

3.1.1 Inclusion of the effect of ionic strength in membranes

Since electrostatic interactions, and consequently pH effects, can be significantly affected by ionic strength (I), the inclusion of this effect on our bilayer systems simulations (either sMD or CpHMD) was essential to obtain realistic data from such an ensemble. Altered pH effects wil lead to a different modulation on the molecular structure (conformation), stability and function of our system of interest. **(126; 127)** In the case of bilayers containing anionic lipids titrating at pH values around physiological pH, the existence of multiple titrable sites which are not only being subjected to different environments, but also coupled to one another, leads to emerging complex pH effects. Therefore, electrostatic interactions have a major effect on the structure and dynamics of membranes, especially on those containing anionic lipids. **(128)** This implies a proper treatment of electrostatics. The Generalized Reaction Field (GRF) method **(62)**, with the possibility of including I as an external parameter **(63)** opened the possibility do deal implicitly with I in MD simulations. Unfortunately, the screening effect given by the bulk I might be insufficient when in the presence of strongly charged systems. The obvious way to deal with charges is by adding counterions, similarly to what has been done when using PME as a long range electrostatic treatment. **(129–132)** The problem is that PME requires the neutrality of the system, which limits the use of counterions to express a certain I. The GRF method, on the other hand, does not require the system's neutrality and, therefore, can be used with a number of counterions typical of a certain I. To estimate the "correct" number of counterions to add, we used an approach based on the Poisson-Boltzmann (PB) formalism (see details in **Section 2.2** and in **Section 2.3**).

As a general rule, all sMD and CpHMD simulated systems, achieve self-consistency after

Table 3.1: Computed amount of Na^+ and Cl^- ions for the various sMD simulation systems at different molar fractions of PA/PC and different ionization values

PA/PC (%)	DMPA	Charge	Predicted		Actual		Evaluation	
			Na^+	Cl^-	Na^+	Cl^-	Na^+	Cl^-
0.00	0	0	5.52	8.21	6	8	5.97	7.33
		+6	5.31	8.52	5	8	4.93	7.38
		+12	4.91	8.27	5	8	4.85	8.22
25.00	32	0	4.60	6.37	5	7	5.00	6.32
		-8	4.99	6.26	6	7	5.99	5.78
		-16	5.86	6.75	6	7	5.99	6.31
		-24	6.54	6.56	7	7	7.00	5.95
		-32	7.24	6.57	8	7	7.99	6.06
		-40	8.19	6.40	9	6	9.00	4.79
		-48	9.21	6.35	9	6	9.00	5.11
		-56	10.68	6.52	10	6	10.0	4.98
		-64	11.89	6.36	12	6	12.0	4.60

Table 3.2: Computed amount of Na^+ and Cl^- ions for the various CpHMD simulation systems with a 25% molar fraction of PA/PC at different pH values

System	pH	Charge	Predicted		Actual		Evaluation	
			Na^+	Cl^-	Na^+	Cl^-	Na^+	Cl^-
PC	0.0	+ 8.73 ± 1.15	5.27	8.83	5	8	4.88	7.45
	1.0	+ 2.53 ± 0.46	5.42	8.24	6	8	5.91	7.31
	2.0	+ 0.42 ± 0.10	5.50	8.11	6	8	5.94	7.22
PA/PC	0.0	+12.75 ± 0.82	4.83	7.84	5	7	4.93	6.75
	1.0	- 0.35 ± 1.38	5.05	7.37	5	7	4.96	6.69
	1.5	- 5.21 ± 1.04	5.24	7.19	6	7	5.94	6.17
	2.0	-11.21 ± 1.35	5.87	7.10	6	7	6.00	6.50
	3.0	-19.00 ± 0.55	6.22	7.14	7	7	6.99	6.17
	4.0	-28.02 ± 0.69	7.18	6.77	8	7	7.99	6.11
	5.0	-31.60 ± 0.66	7.24	6.85	8	7	8.00	6.16
	6.0	-36.34 ± 0.46	7.80	6.89	8	7	8.00	6.33
	7.0	-46.71 ± 0.57	9.56	6.45	10	6	10.00	4.78
	8.0	-57.91 ± 0.48	11.29	6.39	12	6	12.00	4.45
	9.0	-62.79 ± 0.31	11.79	6.43	12	6	12.00	4.63

a finite number of cycles, and we were able to capture all the Na^+ predicted with the PB formalism approach (**Tables 3.1** and **3.2**). With Cl^- ions, there is systematically on average one ion that diffuses away from the membrane towards bulk. We could have corrected this with an extra iteraction step, but we knew *a priori* that Cl^- ions interact weakly with anionic membranes and have little to negligible impact on its conformation. **(126)**

As expected, there seems to be a direct relationship between the negative ionization of the membrane and the number of Na^+ ions (**Figure 3.1**), added to stabilize it. In addition, with membrane charging, the number of expected Cl^- ions tend to decrease at a slower pace (**Figure 3.1**).

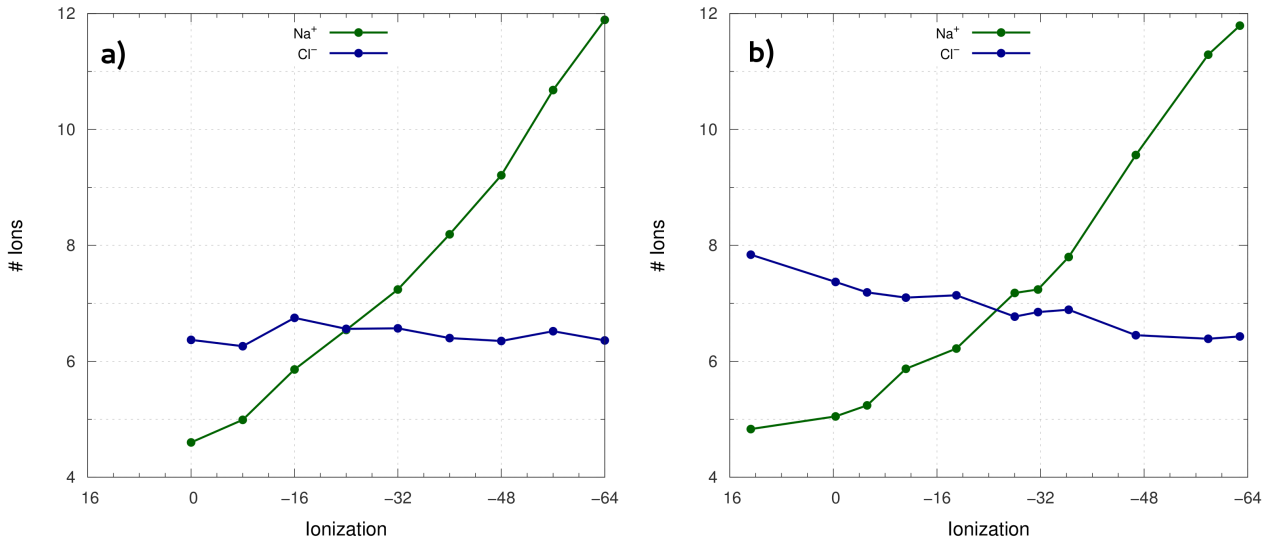

Figure 3.1: Ion abundance at various ionization values from either sMD simulations (a) or CpHMD simulations (b). Notice that # Ions plotted in **(b)** refers to the PB-formalism estimated number of either Na^+ or Cl^- ions

3.1.2 Area and Volume per Lipid and Protonation over Time

The A_L and V_L values were followed over the entire simulation time, for all the studied systems (see **Annex B**), with doing both sMD (at several molar fractions of DMPA over DMPC and diverse ionization values) and CpHMD (for a bilayer system of 25% PA/PC at pH values ranging from 0 to 9).

Figure 3.2 shows A_L over time for the pure PC and 25% PA/PC bilayer systems, with fully neutral and fully ionized PA lipids. All systems are equilibrated throughout the whole 100 *ns* runs. From the results, one can also see that the presence of DMPA can have stabilizing or destabilizing effect on the binary mixture bilayer, depending on is ionization state. The CpHMD simulations (**Figure 3.3** and **Annex B**) started from the previous sMD systems were

equilibrated right from the beginning of the simulations for most pH values. Nevertheless, at lower pH values, equilibration was achieved more difficutly, probably due to PC protonation that was not taken in account in sMD simulations. At pH 0.0, for instance, the 25% PA/PC system is only equilibrated after 80 *ns*. At this pH value, a small fraction of DMPC is protonated, thus leading to a formal charge of +1 per DMPC lipid molecule, and consequently, one expects that the repulsive forces between charged lipids will lead to an increase in the A_L parameter until an equilibrium state settles in.

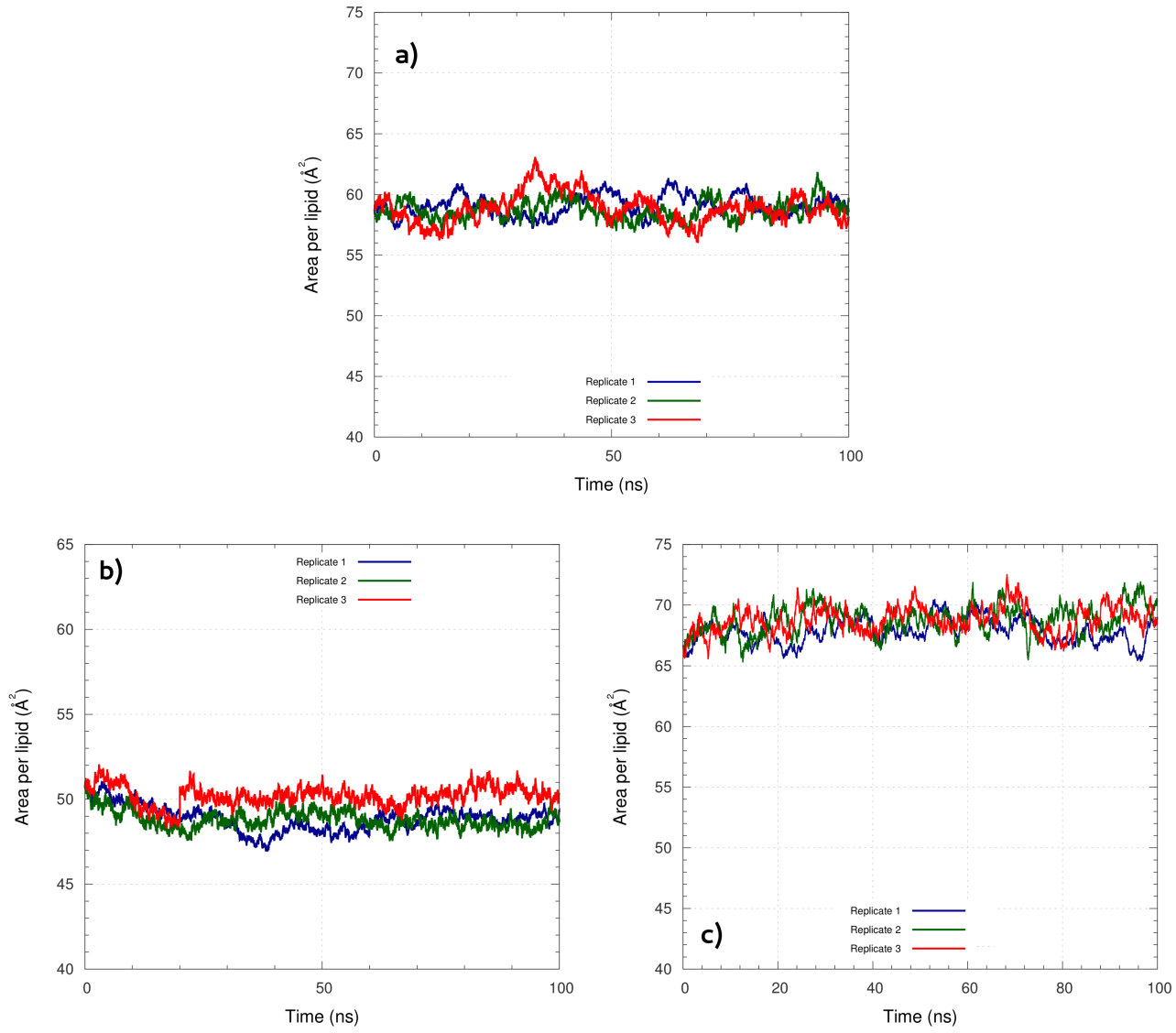

Figure 3.2: Area per lipid at 310 K and 0.1 M NaCl, for the sMD simulations of bilayer systems of pure neutral DMPC **(a)**, and 25% PA/PC with PA fully neutral **(b)** or fully ionized **(c)**.

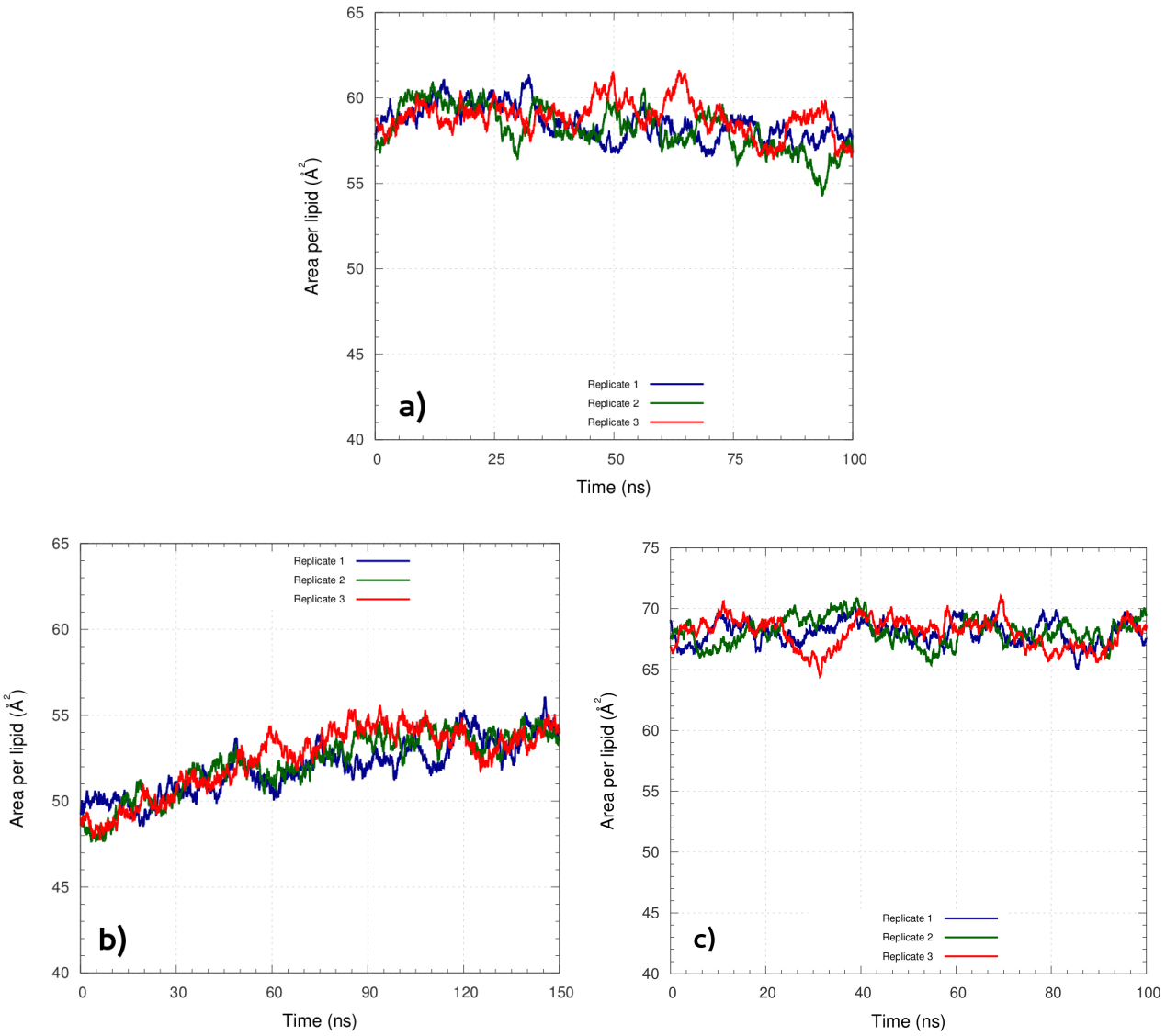

Figure 3.3: Area per lipid at 310 K and 0.1 M NaCl for the CpHMD simulations of bilayer systems of 0% PA/PC at pH 0.0 **(a)** and 25% PA/PC at pH 0.0 **(b)** and pH 9.0 **(c)**.

Similarly to the A_L, the V_L property displays a strong dependence on the pH value, and hence, on the ionization degree of the membrane (**Figure 3.4** and **Figure 3.5**) and present better equilibrations at higher pH values (*i.e.*, higher ionization degrees).

As stated by Anézo *et al*, the V_L is a very important quantity to take into consideration when comparing simulation and experimental data, as it not only shows fewer and smaller fluctuations but it also converges faster than area per lipid. **(133)** Nevertheless, as observed for the A_L, at pH 0, a 25% PA/PC bilayer is only equilibrated after $\sim$ 80 *ns*, probably due to the protonation of the phosphate headgroups of DMPC lipids. More simulation time was required to achieve proper equilibration.

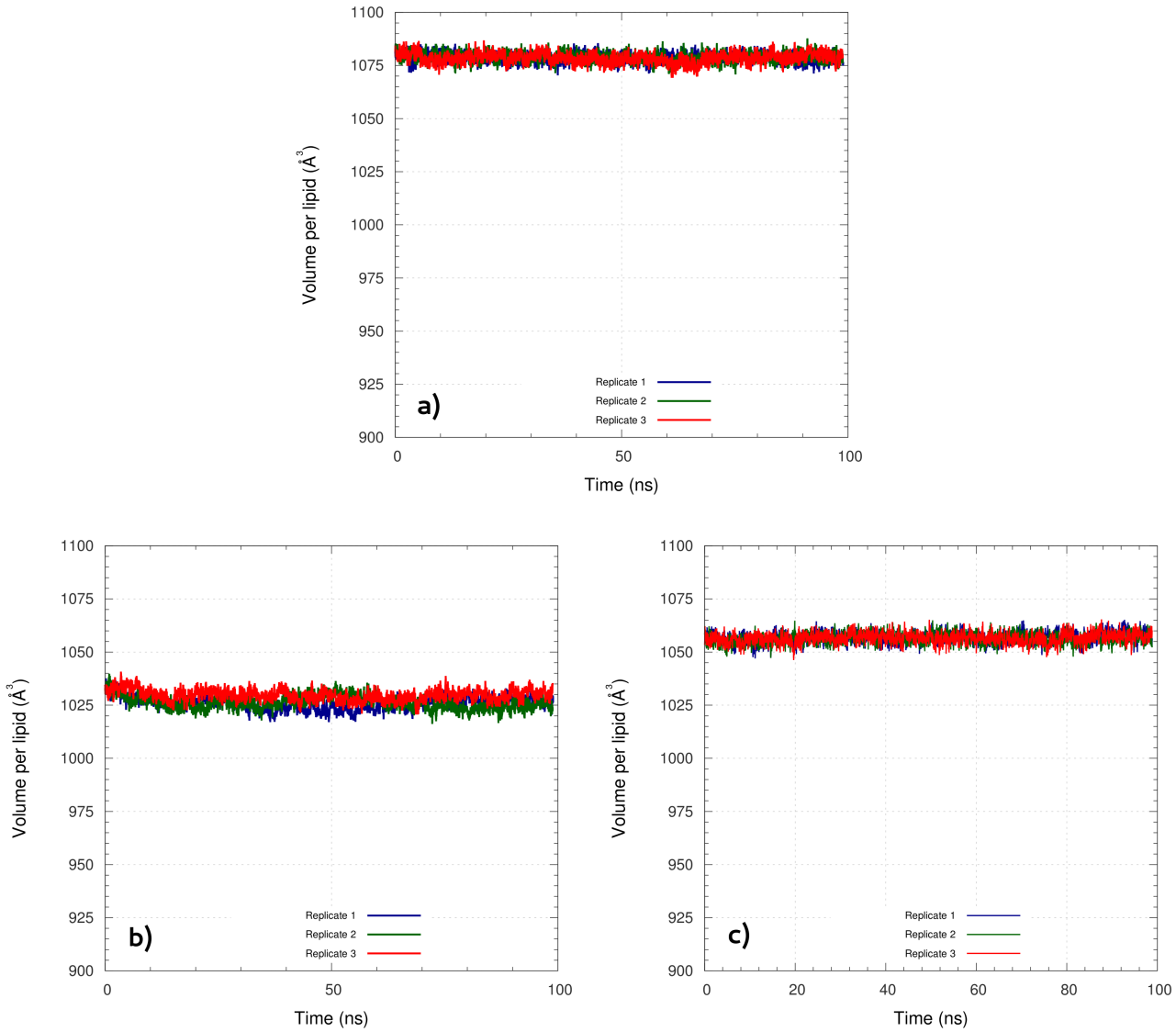

Figure 3.4: Volume per lipid at 310 K and 0.1 M NaCl, for the sMD simulations of bilayer systems of pure neutral DMPC **(a)**, and 25% PA/PC with PA fully neutral **(b)** or fully ionized **(c)**.. A floating window average of 500 *ps* was applied for clarity.

In addition to both A_L and V_L parameters, the protonation was followed over the entire simulation time, for all the studied CpHMD systems (**Figure 3.6** and **Annex B**). By computing the population fraction of the three charge states of DMPA over time, one is able to see that despite the large fluctuations observed, this property equilibrates as fast as both A_L and V_L time evolutions. In fact, all these properties should equilibrate in a similar timescale, because they are tightly coupled.

To conclude, both A_L and V_L reached an equilibrium behavior for the sMD and CpHMD simulations and were stable throughout the production runs. The same behavior is reported for protonation over time for the CpHMD simulations. Only these equilibrated segments will hereafter be used in the characterization of the lipid bilayers.

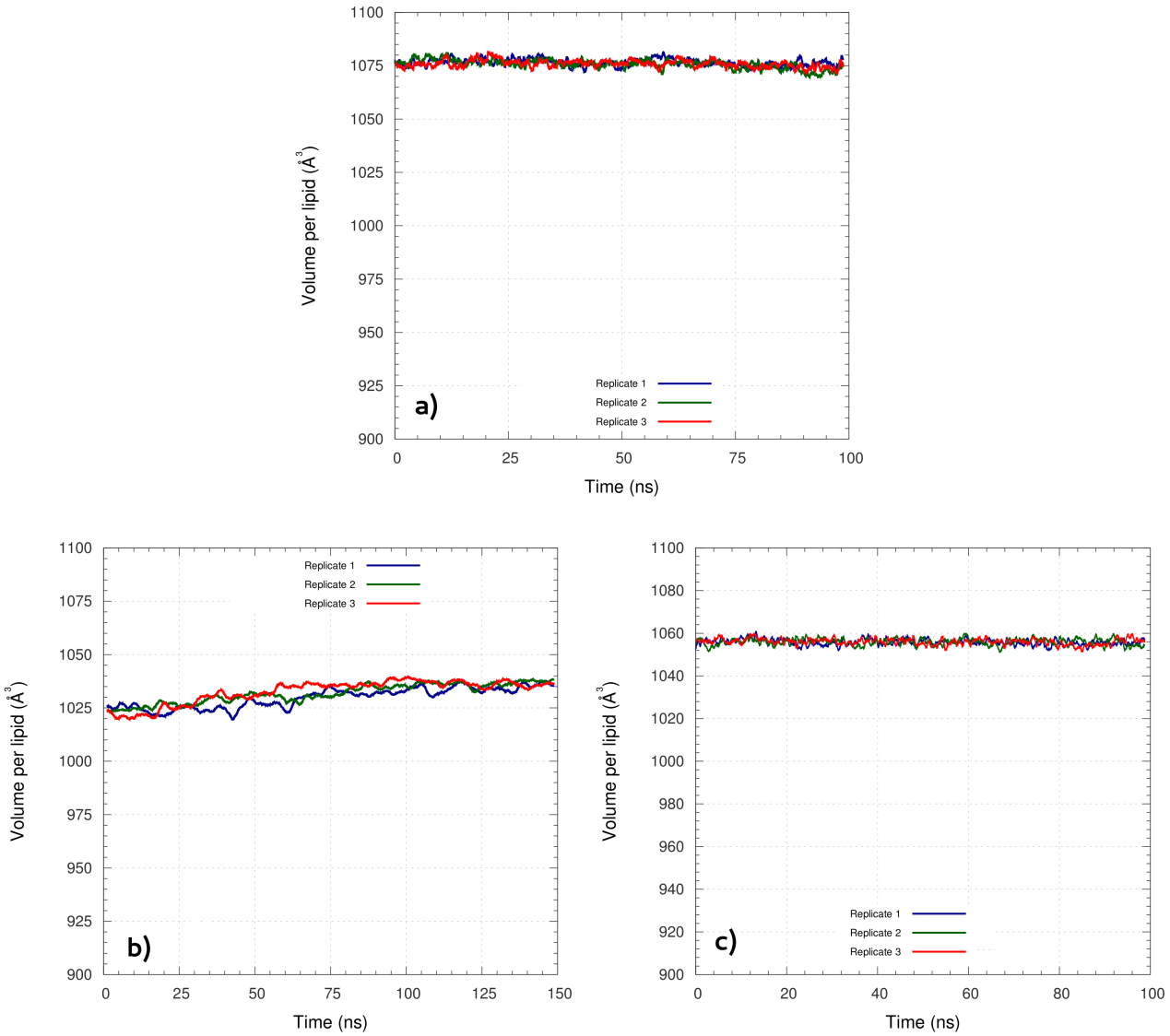

Figure 3.5: Volume per lipid at 310 K and 0.1 M NaCl for the CpHMD simulations of bilayer systems of 0% PA/PC at pH 0.0 **(a)** and 25% PA/PC at pH 0.0 **(b)** and pH 9.0 **(c)**. A floating window average of 500 *ps* was applied for clarity.

3.2 Modelling a 25% PA/PC membrane with CpHMD

In order to evaluate the behavior of a two-component bilayer containing phosphatidic acid (PA) as anionic component we have decided to use the 25% PA/PC bilayer system to proceed with our studies. The choice of this molar fraction was due to the fact that some authors, despite stating that anionic phospholipids are a minor residual part of the lipid population presented in the cell and organelle membranes, in certain occasions, do report that their concentration rapidly increases up to $\sim$ 30 %. **(4; 38)** In that sense, we have chosen this bilayer system to mimic those occasions when PA is relevant to the cell.

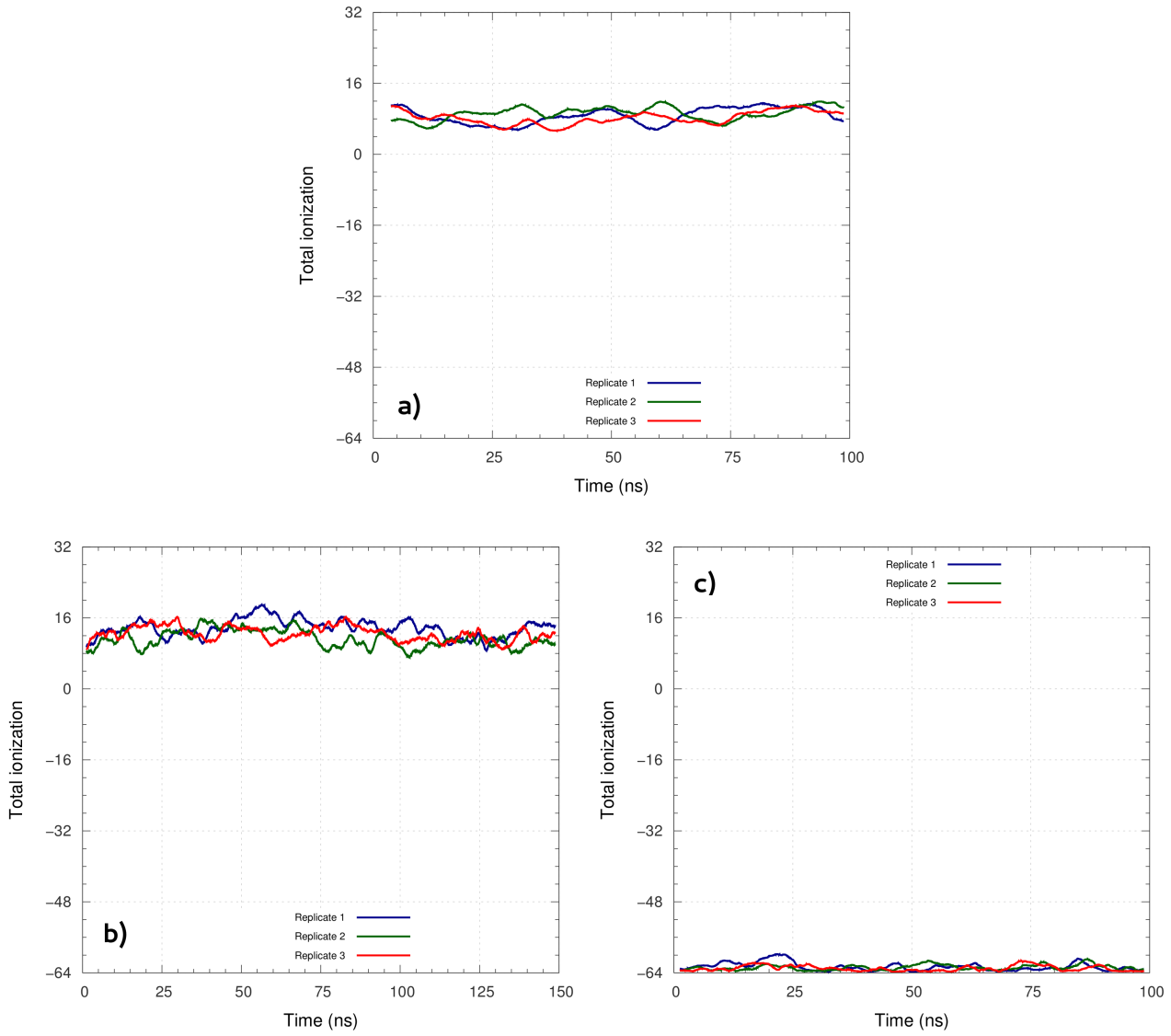

Figure 3.6: Protonation at 310 K and 0.1 M NaCl for the CpHMD simulations of bilayer systems of 0% PA/PC at pH 0.0 **(a)** and 25% PA/PC at pH 0.0 **(b)** and pH 9.0 **(c)**. A floating window average of 500 *ps* was applied for clarity.

3.2.1 pH titration

One of the most important characteristics of anionic membranes is its dependence on pH. The CpHMD simulations allowed us to study the pH titration of the PA/PC binary mixture. The simulations were performed at pH values from 0.0 to 9.0 with increments of 1.0 pH units. Additionaly we have simulated our system at pH 1.5 to improve our sampling on this pH region where a significant conformational transition seems to take place. The titration was computed by averaging at each tested pH value the occupancy states of all titrable sites over the final equilibrated segments.

As can be seen, the titration curve shows two inflection points (**Figure 3.7**) typical for

a chemical entity containing two ionogenic groups that in aqueous media exchange protons. The first inflection point $\sim$ 2.5 pH units, corresponding to the first pK_a value, precludes the conversion of fully protonated, H_2PO_4, to the monobasic acid, HPO_4^{1-}. At around neutral pH ($\sim$ 7.0 pH units), one can see a second inflection point, corresponding to the second value of pK_a from the conversion of the monobasic acid to the fully deprotonated species, PO_4^{2-}.

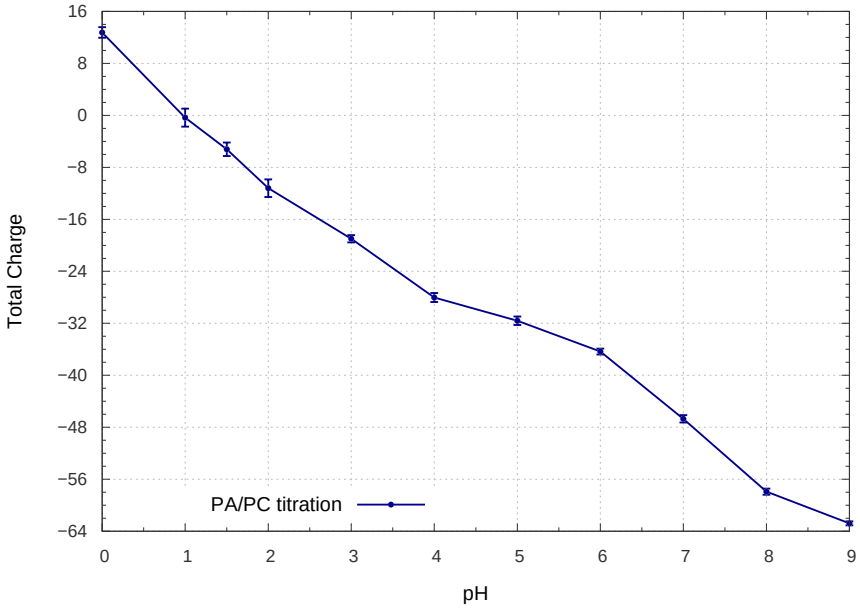

Figure 3.7: Titration curve of the 25% PA/PC lipid bilayer. The positive charge is due to PC protonation.

The deconvolution of the titration curve, gives the titration for both lipid components, DMPC and DMPA, separately (**Figure 3.8**). One can see that for pH values ranging from 0 to 4, there is a positive contribution from DMPC to the overall total charge. In fact, when looking at the relative abundance of the PC charge state populations over the tested pH range (**Figure 3.9(a)**), we can see that, at the most acidic tested pH value (0.0 pH units), the PC positive charge state makes up for 15 % of the total PC present in the mixture. Thus, even though its contribution is small, PC has an effect on the first pK_a value observed.

In respect to the fractions of PA populations (**Figure 3.9(b)**), we did not observe a single pH value among the tested range, where only one of the charge states exist exclusively (**Table A.3**). Nevertheless, we can theoretically predict that for a 25% PA/PC bilayer, at very acidic pH values (pH $<$ 0.0) and very basic pH values (pH $>$ 9.0), the fully protonated or the doubly deprotonated forms is the unique charge state present in solution, respectively.

From pH 4.0 to pH 7.0, one can see a coexistence of the three charge states - PA^0, PA^{1-} and PA^{2-} -, an event never suggested by other authors. At physiological pH, from the observation of **Figure 3.9(b)**, one should expect an equal fraction of PA^{-1} and PA^{-2}, a fact that was proposed in the literature. **(48)** Here, we find a significant advantage of using CpHMD instead

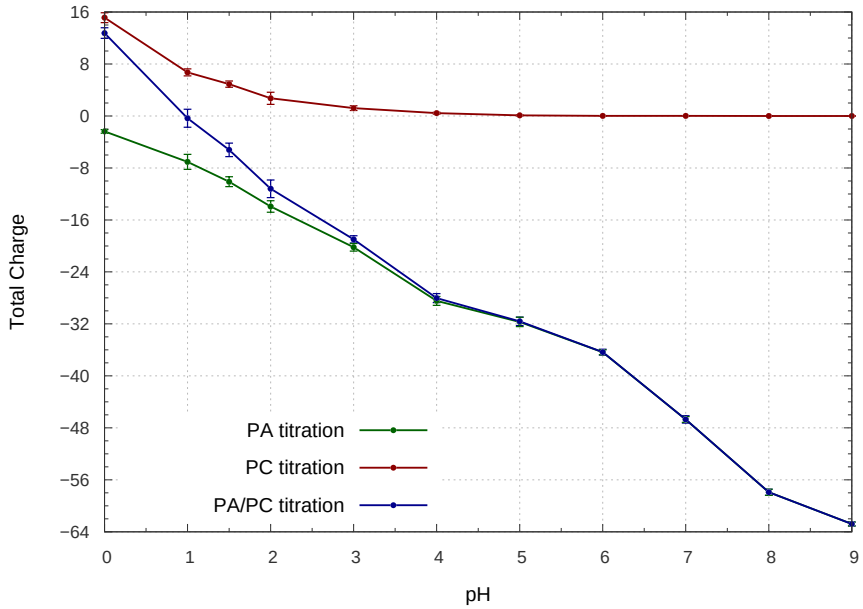

Figure 3.8: Titration curves of the 25% PA/PC lipid bilayers - global titration curve shown in blue, PA titration curve shown in green and PC titration curve shown in red.

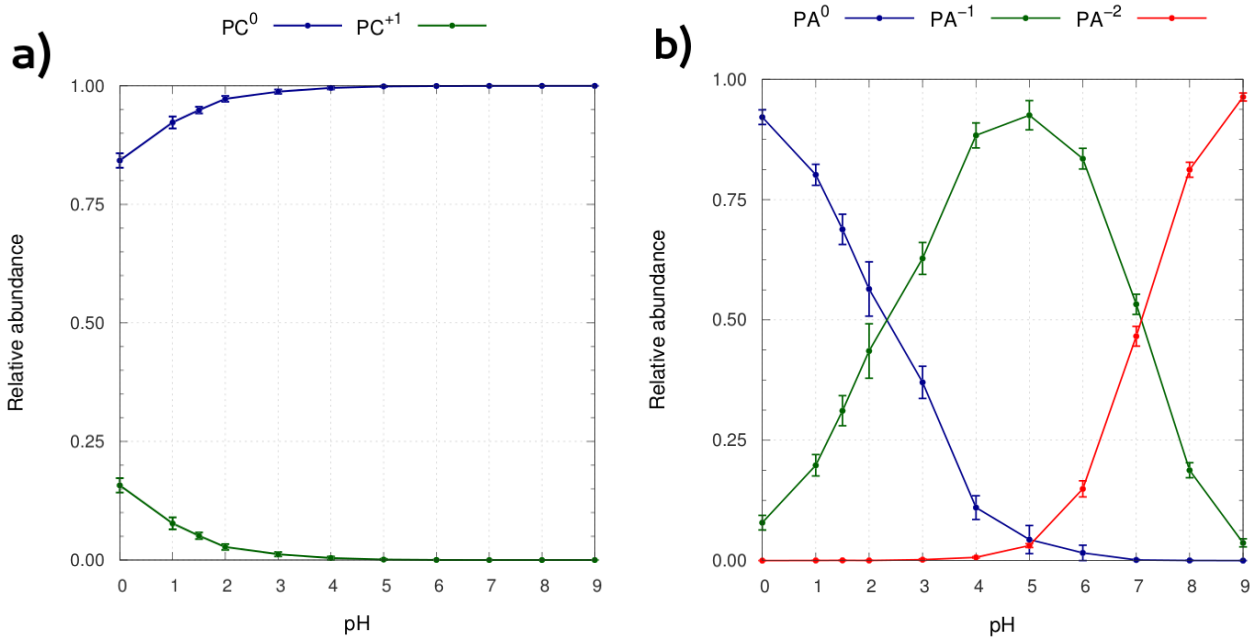

Figure 3.9: Relative abundance of (a) DMPC and (b) DMPA lipid molecules charge states at several pH values for the binary mixture 25% PA/PC.

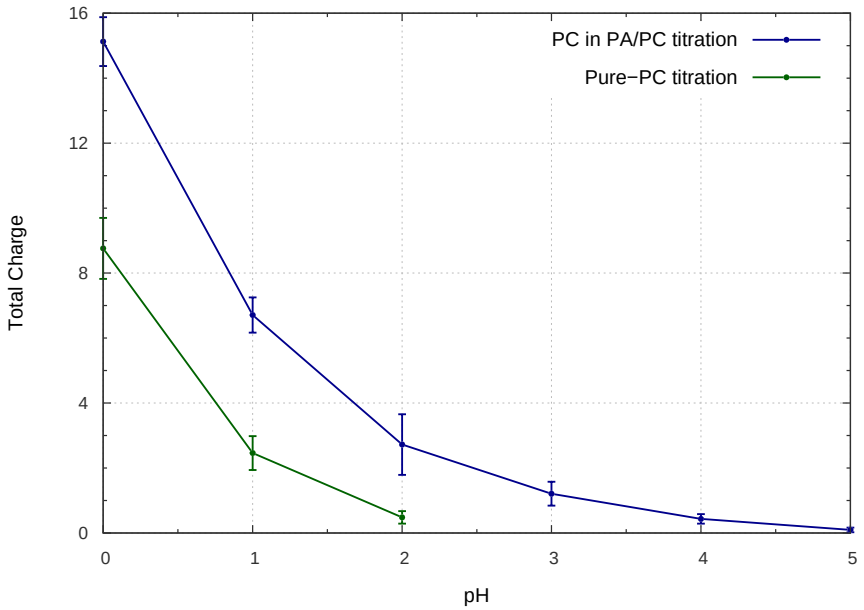

Figure 3.10: Theoretical titration curves for a pure DMPC lipid bilayer, in blue, and for a 25% binary mixture PA/PC bilayer, in red.

of sMD methodologies alone, as it reveals that at pH $\sim$ 7.0, any slight changes in the solution pH will lead to significant changes on the charge densities of the membrane.

In the cell, because of the "crowding effect", a bilayer of the same composition as ours would never be fully isolated. Therefore, interaction with biomolecules, such as peptides or proteins will certainly modulate its local electrostatic potential, leading to shifts in the pK_a and charging events not entirely predicted by the present results.

Interestingly, when comparing the titration curve of the PC lipid in a pure membrane and in a mixture at a 25 % PA/PC (**Figure 3.10**), it is patent the shift which is really significant over the first pH values from 0.0 to 2.0. It seems that PC in a pure membrane is difficult to protonate, while when in the presence of an anionic lipid, it retains protons at higher pH values. The anionic lipid favors the positive protonated DMPC species which can be reasoned in terms of electrostatics.

3.2.2 Area and Volume per lipid

Lipid bilayers in the liquid crystalline phase, also known as the L_α or liquid disordered (L_d) phase, are generally considered to be relevant for models of biological membranes. The liquid ordered (L_o) phase is described as an intermediate state between the L_α and the L_β (gel) phase, usually associated with bilayers containing cholesterol. Since lipids can influence the structure and function of membrane proteins and the way that they interact with

soluble proteins, and in turn membrane proteins have an influence on the lipid dynamics, it is of utmost important to be able to characterize the structure and dynamics of a lipid bilayer. **(118)**

We have computed the values of the average area per lipid and volume per lipid for all pH values (**Table 3.3** and **Figure 3.11**). At increasingly ionization values of the membrane, due to higher pH values, we observe a lateral expansion, a consequence of the charges repulsion between the phosphate headgroups, which also resulted in an increase of the volume per lipid. In fact, we seem to model accurately an isothermal pH-induced gel-to-fluid phase transition, a well known and moderately reported event. **(134)** For this, we simply assumed the A_L range values corresponding to the gel and liquid-crystalline (fluid) phases (Lα) of a pure DMPC membrane to be $\sim$ 48 - $\sim$ 52 Å^2 and $\sim$ 58 - $\sim$ 65 Å^2, respectively. **(51; 135–137)**

We state that our membrane is representative of a DMPC pure bilayer in its fluid, liquid-crystalline phase. Nevertheless, the computed area per lipid value (58.67 $\pm$ 0.35 Å^2) pertaining to the DMPC pure lipid bilayer at the highest tested pH value (pH = 2.0 $\sim$ 7.0) is marginally inside the lower limit correspondent to such a phase. It seems that the charge set that was used in order to simulate our DMPC membrane systems led to a decreased A_L. When using Chiu charge state at similar conditions, Machuqueiro *et al* have obtained a value that is in best agreement within the experimental range. **(117)** Additionaly, at this pH value, the computed value of V_L concerning the pure DMPC lipid bilayer (1077.30 $\pm$ 0.40 Å^3) is slightly lower than the values obtained previously **(117)**, in our case, a consequence of the relatively low value obtained for A_L.

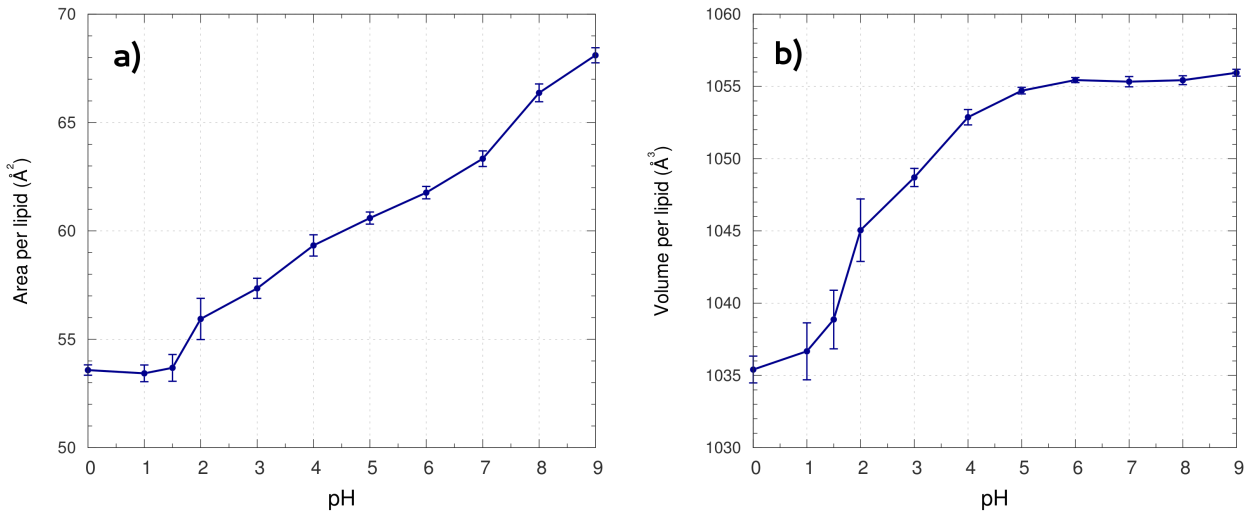

Figure 3.11: Area **(a)** and volume **(b)** per lipid dependency with the pH value for the 25% PA/PC lipid bilayer.

At the lowest pH values, pH < 2.0, the membrane is close to a gel-phase, reported by the A_L of a value below 54 Å^2. Then from pH 2.0 to pH < 4.0, still at acidic pH, there is a

Table 3.3: Area per lipid and volume per lipid dependence with the pH value for both the pure DMPC lipid bilayer and the 25% PA/PC lipid bilayer.

System	pH	Charge	Ions		A_L /Å^2	V_L /Å^3
			Na^+	Cl^-		
100 % PC	0.0	+ 8.73 ± 1.15	5	8	58.51± 0.79	1076.04 ± 1.51
	1.0	+ 2.53 ± 0.46	6	8	58.59 ± 0.36	1077.58 ± 0.19
	2.0	+ 0.42 ± 0.10	6	8	58.67 ± 0.35	1077.30 ± 0.40
25 % PA/PC	0.0	+12.75 ± 0.82	5	7	53.58 ± 0.24	1035.41 ± 0.93
	1.0	- 0.35 ± 1.38	5	7	53.43 ± 0.39	1036.67 ± 1.97
	1.5	- 5.21 ± 1.04	6	7	53.68 ± 0.62	1038.87 ± 2.03
	2.0	-11.21 ± 1.35	6	7	55.94 ± 0.95	1045.05 ± 2.16
	3.0	-19.00 ± 0.55	7	7	57.35 ± 0.46	1048.70 ± 0.63
	4.0	-28.02 ± 0.69	8	7	59.33 ± 0.49	1052.87 ± 0.53
	5.0	-31.60 ± 0.66	8	7	60.59 ± 0.28	1054.71 ± 0.23
	6.0	-36.34 ± 0.46	8	7	61.77 ± 0.29	1055.44 ± 0.18
	7.0	-46.71 ± 0.57	8	7	63.33 ± 0.36	1055.33 ± 0.35
	8.0	-57.91 ± 0.48	12	6	66.37 ± 0.41	1055.43 ± 0.31
	9.0	-62.79 ± 0.31	12	6	68.11 ± 0.35	1055.95 ± 0.24

region of coexistence of both gel (liquid ordered state, L_o) and fluid (liquid disordered state, L_d) phases, named coexistence region. In this exact region, although DMPC lipid molecules become disordered, DMPA lipid molecules still keep their ordered state. For pH values higher than 4.0, and until pH 8.0, the A_L is contained in the fluid phase range of DMPC **(51; 135–137)**, and we postulate that the membrane transite from a gel ordered phase to a liquid crystalline fluid phase, where the disorder of the lipid alyphatic chains may have a major impact on the overall structure of the lipid bilayer. At around pH $\sim$ 9.0, and supposedly afterwards, the membrane enters a super-fluid region where the increasing unstability of the membrane will inevitably lead to its disruption - this behavior was not fully explored, but we postulate its existence on a 25% PA/PC lipid bilayer. The gel-to-fluid phase transition observed is in very good agreement with experimental results (**Figure 3.12**) obtained by Garidel and coworkers. **(50)**

3.2.3 Impact of different electrostatic interactions treatments on the membrane conformation

Standard Molecular Dynamics (sMD) were performed to investigate the effect of different electrostatic treatments on the structural stability of a two-component bilayer system composed of the binary mixture with 25% PA/PC at 310 K and 0.1 M ionic strength. Four different electrostatic schemes were considered: a regular generalized reaction field (GRF) at 0.1 M without any explicit counterions, the same GRF at 0.1 M with the amount of Na^+

and Cl^- ions predicted by the Poisson-Boltzmann formalism, and GRF at 0.1 M with enough counterions to neutralize the system. Additionaly, a PME method was also evaluated within a neutralized system. In order to evaluate the structure of the membranes that resulted from all four schemes, we ran three replicates of 100 *ns*, and computed their average area per lipid.

Figure 3.12 shows the experimental phase diagrams for PA/PC at pH 4.0, 7.0 and 12.0. **(50)** From the data, we can extract the specific phases for our simulated molar fraction, using the CpHMD ionizations as references for the three pH values **Figure 3.13**. The results show that altough its simplicity and low computational cost, GRF without explicit counterions renders the system too unstable at higher ionizations. Both neutral systems (using 0.1 M GRF or PME) are relatively insensitive to ionization and, therefore, to pH variations. Only using a PB-estimated number of counterions in the system, we can correctly predict the phase transition observed experimentally. **(50)**

The disappointing results obtained for the neutral systems (especially with PME), with an almost total insensitivity of the membrane structure to pH, has another nefarious consequence, the insensitivity to the I used. Therefore, we consider that, even thought PME is very popular in Molecular Modeling nowadays, it is completely inadequate for our purposes.

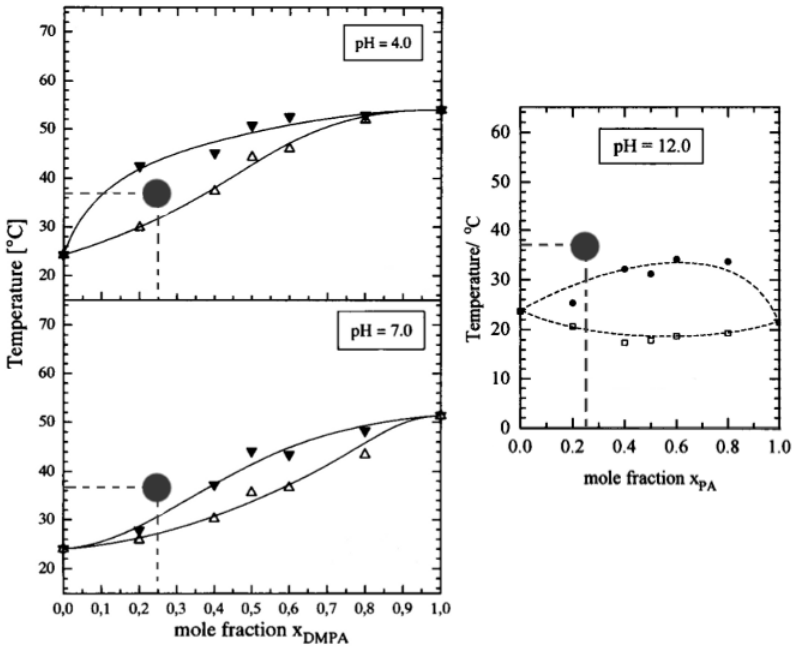

Figure 3.12: Pseudobinary phase diagrams for the PA/PC mixtures obtained by Garidel *et al* (50) at **(a)** pH 4, **(b)** pH 7 and **(c)** pH 12. Graphical interpolation for the 310 K ($\sim 37^o$C) at 25% PA/PC is also shown.

We can conclude that by considering the I as an external parameter, defining its value, and concomitantly adding explicitly the amount of Na^+ and Cl^- ions predicted by the formalism of PB, it is possible to correctly predict the phase state of our binary mixture at different

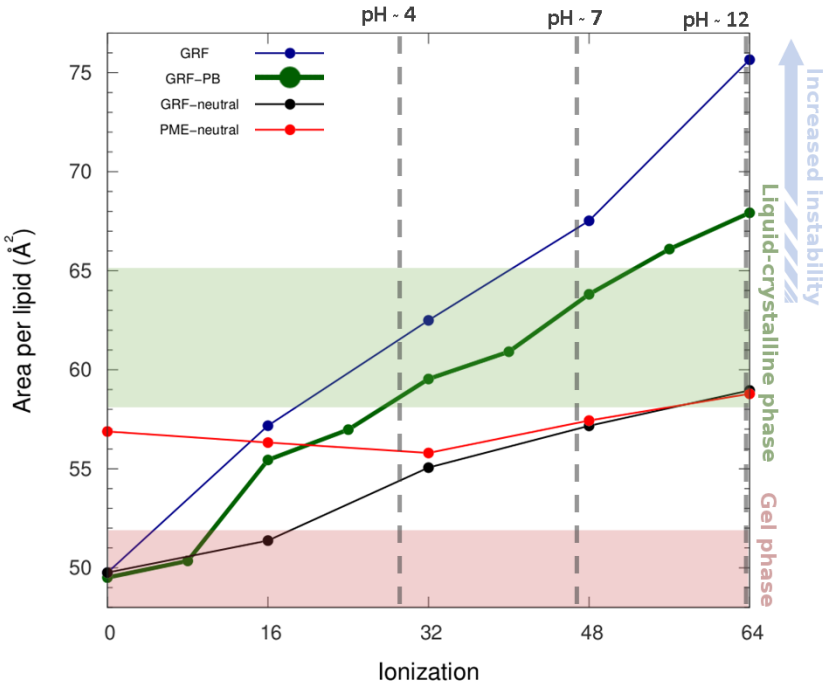

Figure 3.13: Area per lipid dependency with the ionization when using different electrostatic treatments.

pH values, and to postulate about a possible phase transition from the gel state to a liquid-crystalline phase (**Figure 3.14**), induced not by temperature but by pH, and consequently ionization states alone.

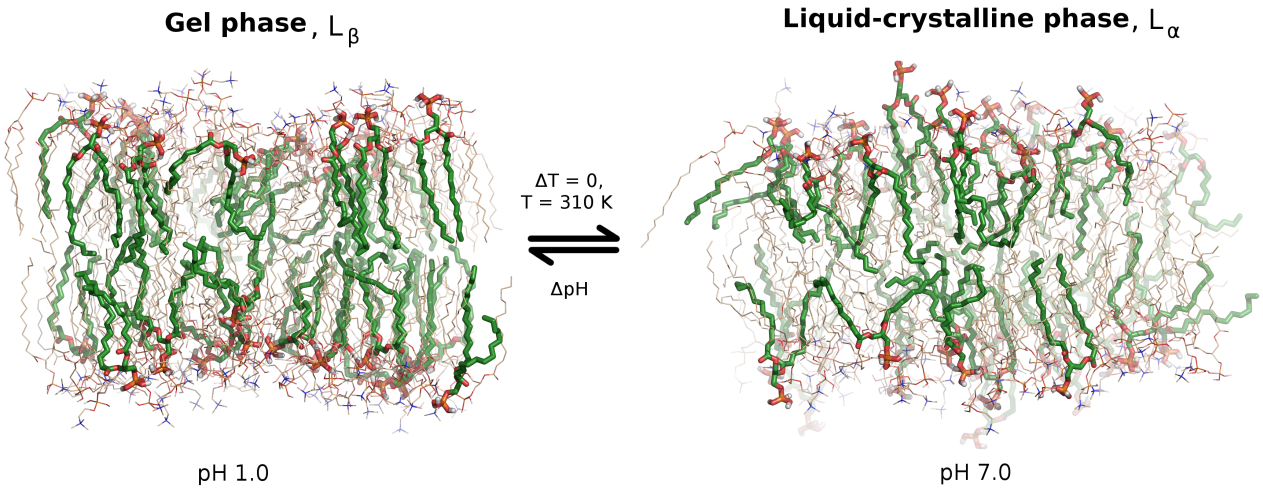

Figure 3.14: Isothermal gel-to-fluid phase transition at 310 K and 0.1 M. Image was acquired with PyMOL software.

Our methodology not only is able to maintain stability for the entirety of the ionization range

possible values, but we were also able to reproduce, in very good agreement, the isothermal phase transition reported by Garidel. **(50)**

3.2.4 Order parameter

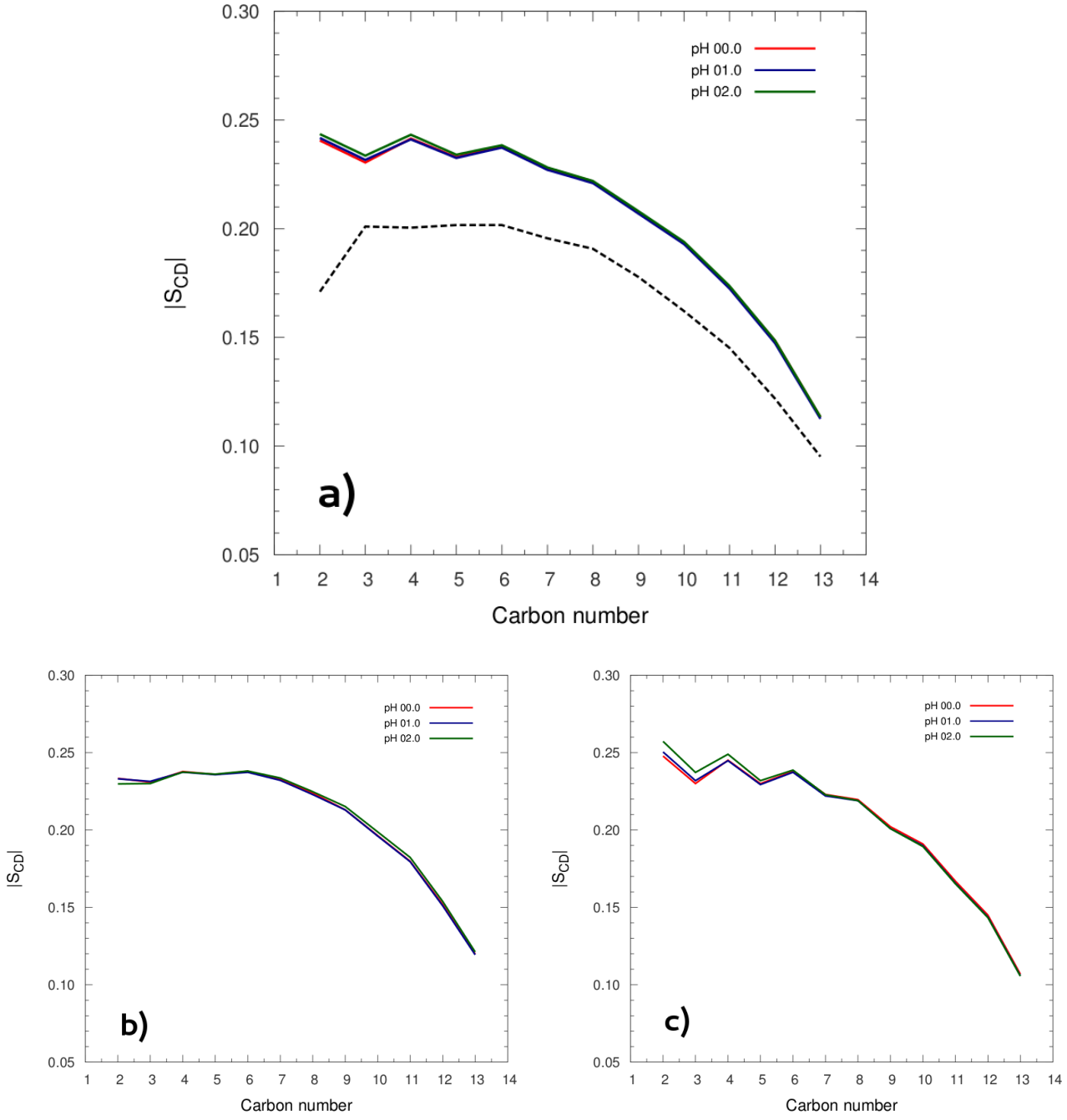

Figure 3.15: Order parameter of DMPC aliphatic lipid chains dependency with the pH value for the 25% PA/PC lipid bilayer - **(a)** *sn*-1 and *sn*-2 chains; **(b)** *sn*-1 chain; **(c)** *sn*-2 chain

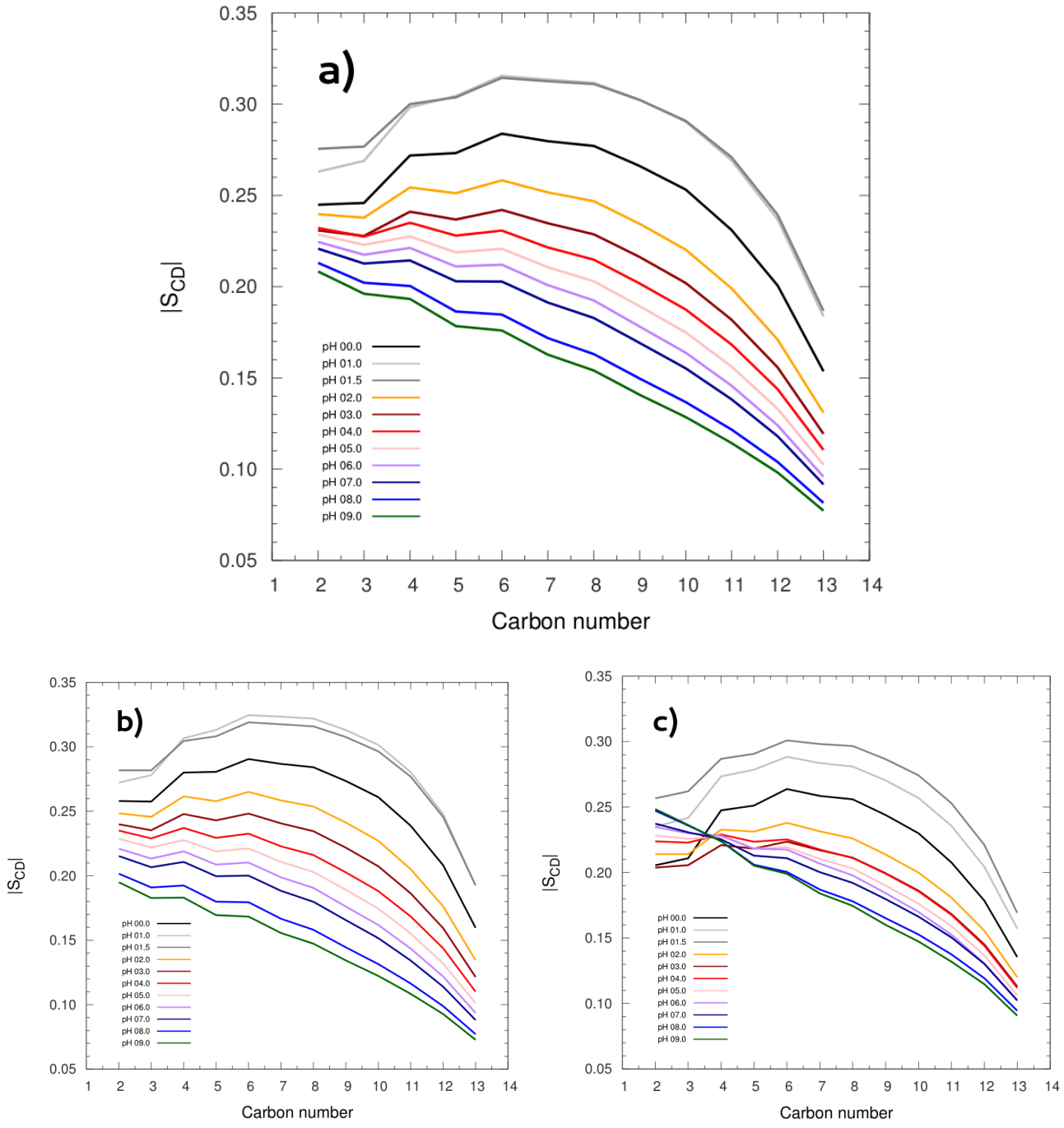

Figure 3.16: Order parameter of DMPA and DMPC aliphatic lipid chains dependency with the pH value for the 25% PA/PC lipid bilayer - **(a)** *sn*-1 and *sn*-2 chains of both DMPA and DMPC lipid molecules; **(b)** *sn*-1 and *sn*-2 chains of DMPC; **(c)** *sn*-1 and *sn*-2 chains of DMPA

We have computed the order parameter, S_{CD}, for all carbon atoms in both chains (*sn*-1 and *sn*-2) by averaging over all equivalent atoms in both DMPC and DMPA lipid molecules. **Figure 3.15** shows the order parameter profile from the CpHMD simulations of pure DMPC lipids. It exhibits a plateau for the first five to six CH_2 groups following the ester group and is relatively insensitive to the pH range studied. In the 25% PA/PC binary mixture, the plateau varies with pH reaching even the first eight methylene group (**Figure 3.16**). After such plateaus, one can see that the order parameter decreases rapidly towards the terminal methyl group. Therefore the acyl chains are reasonably ordered close to the head group, while conformational disorder becomes more and more apparent towards the center of the bilayer. This was expected, since in general, order decreases from the central glycerol region to the bilayer center **(118)** The reported behaviour is a consequence of the motional restrictions of the chain segments at the glycerol region - the constraints present in the head group region will induce ordering over the methylene groups. **(118)**

Figure 3.15a shows a somewhat increased ordering behavior when comparing the computed order parameter profiles, at either pH value, with the experimental one. It should be noted that the experimental results were linearly interpolated at the desired temperature of 310 K from the three available temperature sets (303 K, 323 K and 338 K). **(138)** By knowing that the computed mean area per lipid stands marginally inside the experimental range at the lower limit, one is able to predict that our membrane has an excess degree of ordering, a result of the charge set used. Therefore, the aforementioned behavior was expected. In **Figure 3.15b** In **Figure 3.15b** and **Figure 3.15c**, we also see that both chains have similar order profiles, even though *sn*-2 (**Figure 3.15c**) exhibited an already reported "odd-even" effect **(118)**, characteristic of these lipid chains, likely a result of the chain's tilt.

Figure 3.16 shows a clear loss of order with increasing pH. This becomes even clearer when plotting the value of the order parameter at the plateau (arbitrarily chosen as the sixth CH_2 group following the ester group), for both DMPA and DMPC lipid molecules, and in addition for DMPC lipid molecules when in a pure bilayer (**Figure 3.17**). At higher pH values, with the increase of A_L and higher fluidity of the membrane, the lipid chains can move more freely and hence accomodate to its neighbours, rotating rapidly around their normal axis, leading to a decrease of the order parameter.

Unlike A_L, the order parameter is easily deconvoluted in its two major contributions, DMPC (**Figure 3.16b**) and DMPA lipid molecules (**Figure 3.16c**). At increasing pH values the order parameter decreases over the entire span of pH values for the DMPC lipid molecules, while DMPA lipid molecules seem to be less sensitive. Interestingly, by computing the order of the 6^{th} carbon (following the ester group) for DMPC lipid molecules in the pure bilayer, and for DMPA and DMPC lipid molecules in the 25% PA/PC lipid bilayer, we observe that, even though the pH-induced ionization is generated in DMPA lipids, it is the DMPC lipid order

that is more sensitive to pH (**Figure 3.17**). These results suggest that protonated DMPA is interfering with the electrostatic network of DMPC leading to its high sensitivity to pH.

At acidic pH values (pH $\leq$ 2), the DMPC lipid molecules when present in a pure bilayer are less ordered than when in a binary mixture, for the same pH values. This difference can only be explained by the presence of DMPA (**Figure 3.17**).

Revisiting **Figure 3.16c**, we might have noticed an unexpected ordering effect at the interfacial lipid headgroups of DMPA lipid molecules. At increasing pH values, higher than 3.0, for the first three methylene groups, there is a clear gain of order. This might be explained by the following rationale: at increasingly high pH values, DMPC lipids tend to disorder more and more for the entireity of the pH range tested. As stated earlier, with the decrease of lipid packing, the acyl chains of lipid molecules can move more freely and hence adapt their conformation with the immediate neighbours in a isomer not mandatorily in an all-trans conformation (see **Section 3.2.5**). This accomodation will not only affect the interior of the lipid bilayer but also its global form, since with the increase of A_L, a decrease in the membrane thickness is expected (see **Section 3.2.6**). Postulating that, as seen here, the effect will be felt by DMPC lipid molecules, a reason that might be on the basis of this "artificial" gain of order is a "bootleneck" effect derived from the entrapment of a budding DMPA lipid molecule between their most common neighbours - DMPC lipid molecules. Implicitily, this will force the initial part of the acyl chains to be more constrict in space and therefore to lose its ability to span various conformers, leading to the capture of an higher order at these constrained methylenes.

3.2.5 Trans-gauche fraction

There is abundant data indicating that the terminal methyl groups have considerably more freedom than groups near the polar end of the molecule. Because of the greater rotational freedom, one expects the methyl termini to occupy a much larger effective volume than that of methyl groups near the surface, much more organized and closely-packed. **(118)** In addition, a perfectly ordered acyl chain in an *all-trans* conformation has a global energy minimum around the *trans (t)* region, which seems reasonable based on steric considerations. **(39; 118)** However, when in the presence of a disordered membrane we expect an enrichment on the *gauche* isomers fraction.

After evaluating the profile of the order parameter for either DMPA or DMPC lipid molecules when part of a 25% binary mixture, we have opted to complement this study with an evaluation of the probability distribution of the torsion angles for the lipid alkyl tails (**Table A.4** and **Figure 3.18**). By reporting the *trans-gauche* fractions correspondent to a given membrane system, one is able to infer about the degree of (dis)order of the system, using a complementary methodology.

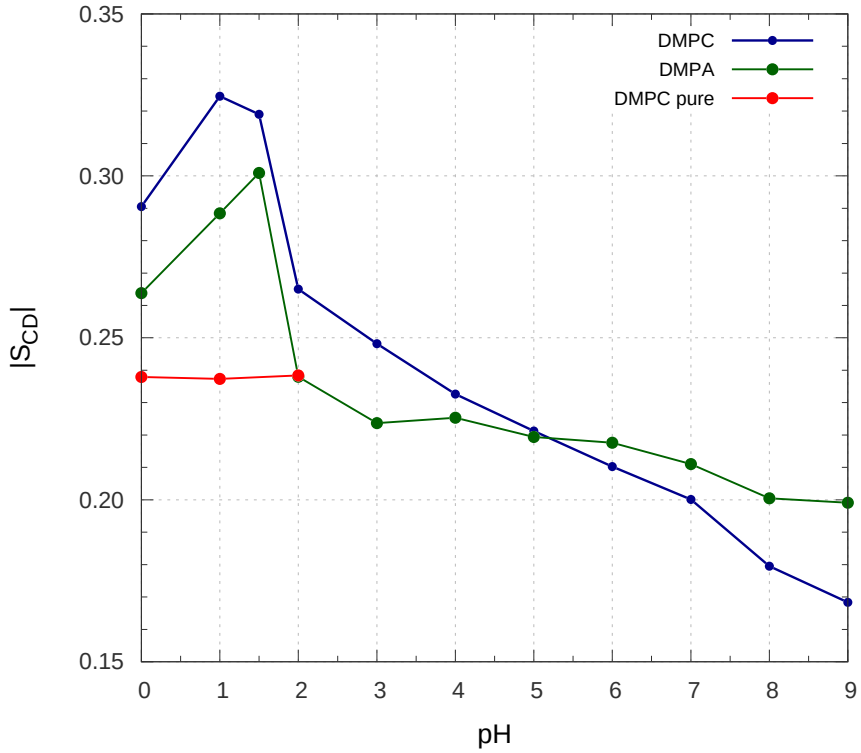

Figure 3.17: Order parameter plateau (sixth CH_2 group) dependency with the pH value for PC lipid molecules at the pure PC bilayer and for both DMPA and DMPC lipid molecules at the 25% PA/PC lipid bilayer.

By observing **Figure 3.18** we conclude that DMPC lipid molecules report different order degrees when in a pure PC lipid bilayer and when in a mixture. In fact, when in a pure mixture (**Figure 3.18a**), for the tested pH values, PC lipid molecules seem to be irresponsive to the alterations of pH value of the solution. As previously stated, since the protonation behavior of these lipids does not varies significantly in the tested range, (dis)ordering effects are not expected. On the other hand, in **Figure 3.18b**, when changing the solution pH from a very acidic value (pH = 1.0) to around physiological pH (pH 7.0), there is an enrichment of the *gauche* isomers in almost $\sim 12\%$, an event that clearly reveals disorder of the lipid bilayer.

3.2.6 Membrane thickness

The thickness of the bilayer is here defined as the headgroup spacing, D_{HH}, *i.e.* twice the distance between the peak of the phosphorus atoms density profile and the origin (for further methodological details refer back to **2.6.5**). Based on the aforementioned definition proposed by Pearson *et al* **(122)**, we have plotted the mass density profiles respective to the phosphorus atoms of either DMPA and DMPC lipids at various pH values. Both the pure DMPC lipid bilayer (**Figure 3.20**) and our 25% PA/PC membrane system (**Figure 3.21**) were analyzed.

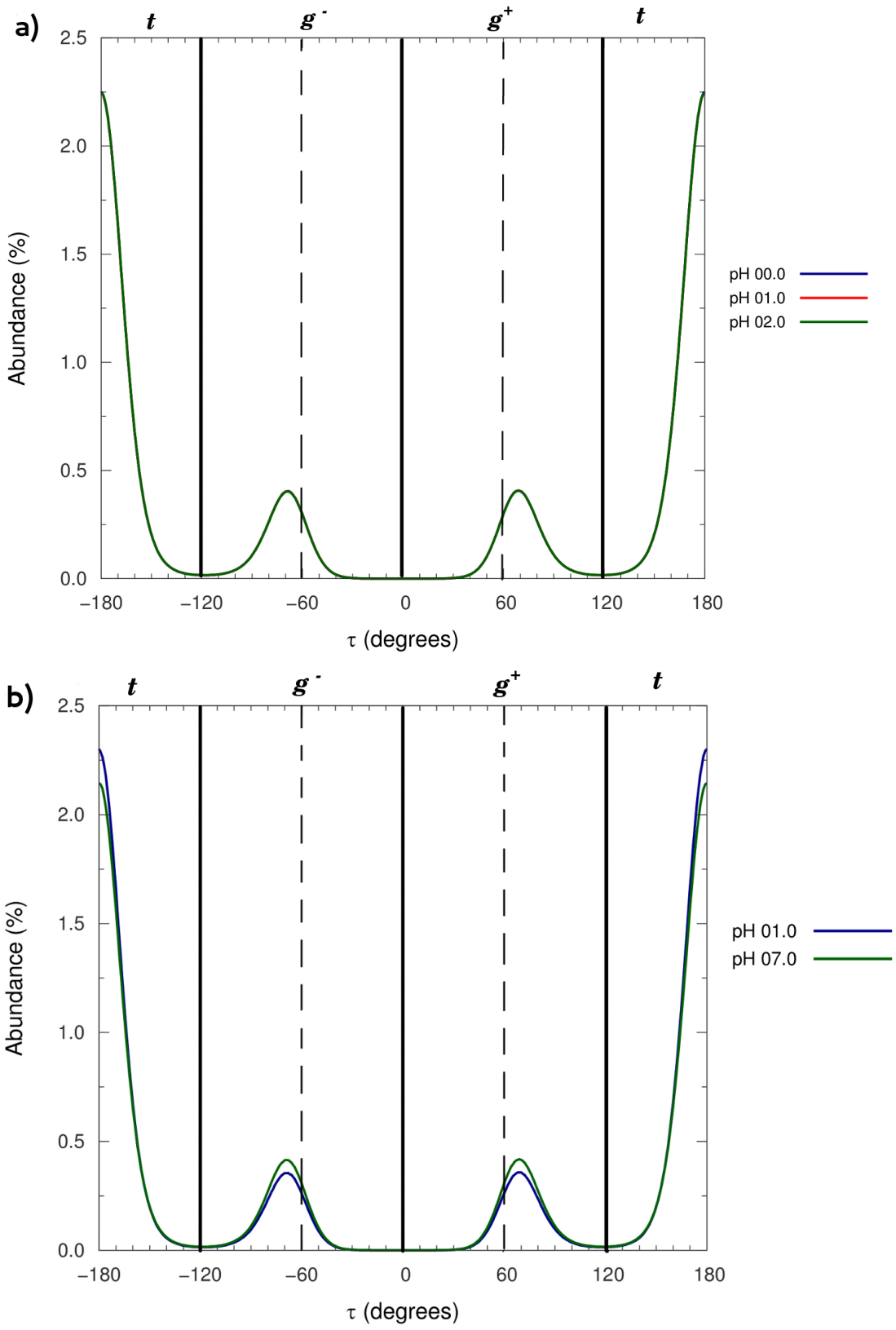

Figure 3.18: Distribution of propers dihedrals for the lipid alkyl tails of DMPC lipid molecules when **(a)** in a pure PC lipid bilayer, and when **(b)** in the 25% PA/PC lipid bilayer.

From **Figure 3.20**, we can see that despite the pH variation from pH 00.0 to 02.0 the thickness of the membrane stays nearly the same, being almost insensitive to pH, at around 36.3 ± 0.01 Å. This value is in excellent agreement with the one experimentally obtained by Kučerka *et al* **Figure 3.19** - 36.1 ± 0.70 Å. **(139)**

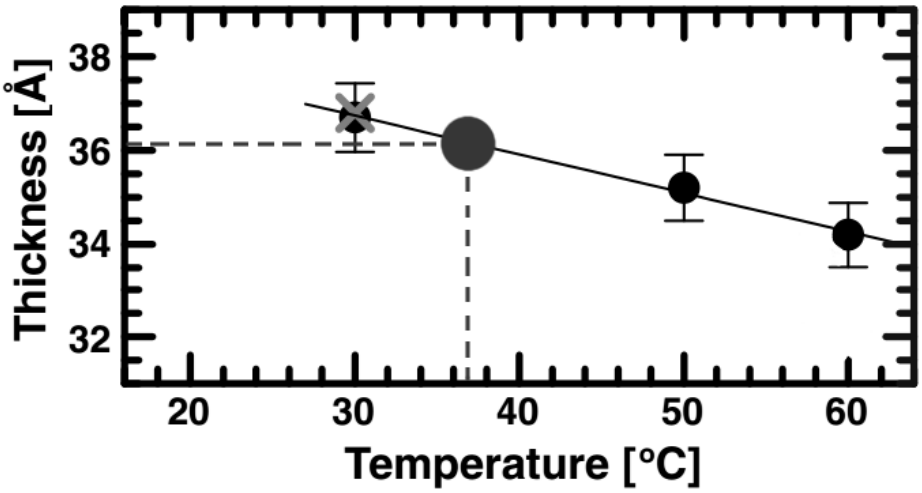

Figure 3.19: Temperature dependence of DMPC bilayer thickness. Image was adapted from **(139)** - the data shown is from the analysis of ULVs, while data at 30°C (gray X) is from joint refinement of ULV and ORI samples, both experimental procedures carried away by Kučerka and coworkers. Graphical interpolation for the 310 K (∼ 37°C) is also shown.

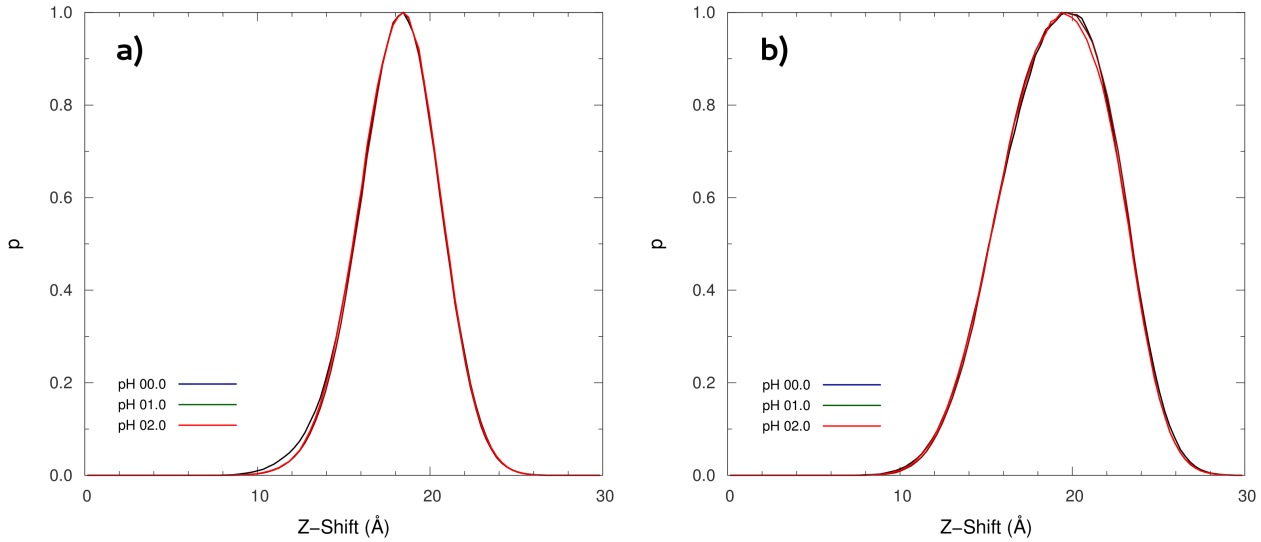

Figure 3.20: Membrane thickness for the pure DMPC bilayer at pH values from 00.0 to 02.0. The thickness was calculated using both the phosphorus **(a)** and nitrogen **(b)** atoms as references.

As for the 25% PA/PC bilayer system (**Figure 3.21**), the phosphorus atoms of the DMPA lipids, independently of the ionization presented by the membrane at the several tested pH

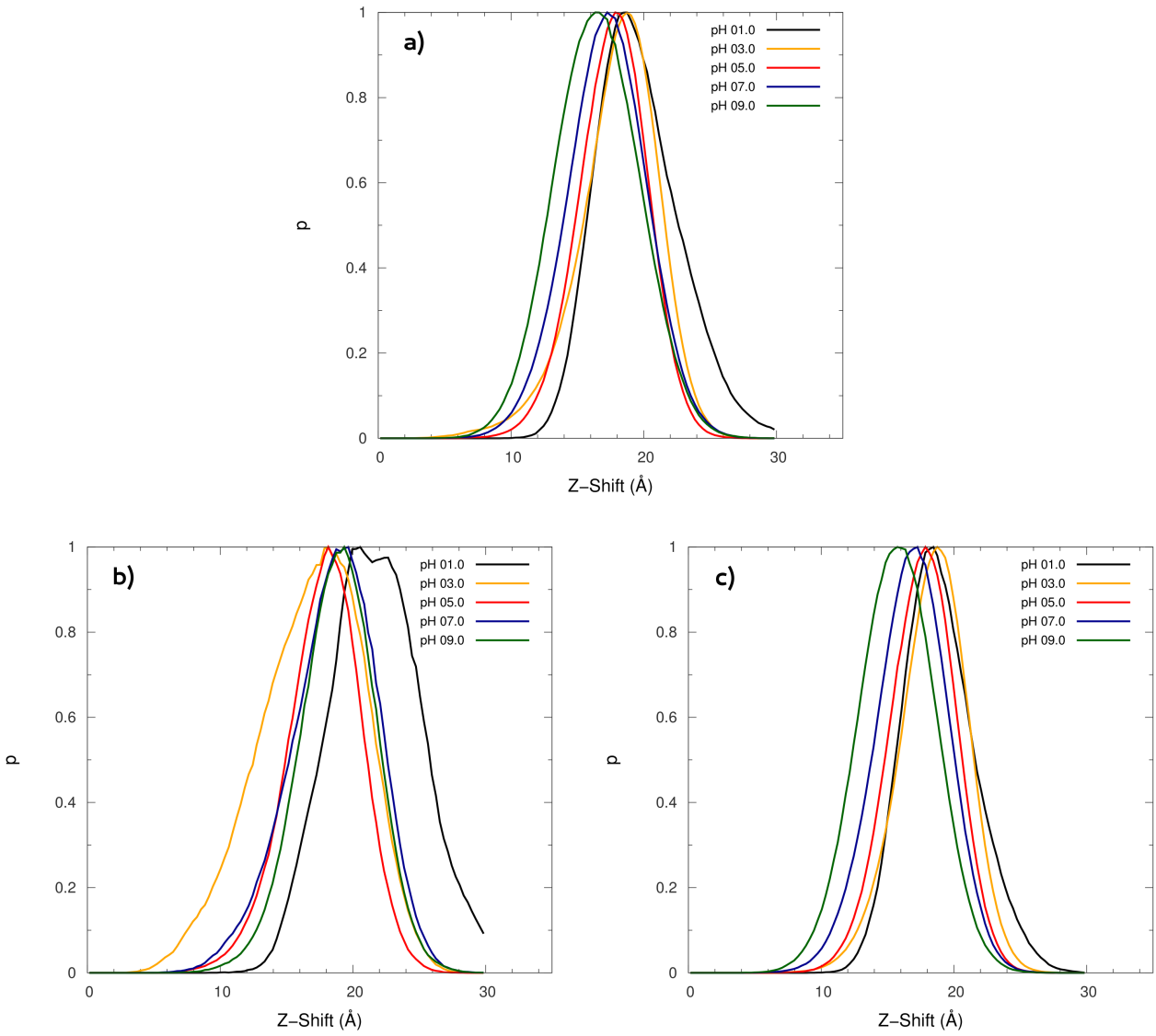

Figure 3.21: Membrane thickness of 25% PA/PC mixture at odd pH values from 01.0 to 09.0. The calculations with the phosphorus atoms as reference were done on all lipids **(a)**, and either on PA **(b)** or PC **(c)** lipids alone.

values, are on average at a similar distance from the bilayer center, hence varying little with the solution pH. On the other hand, it seems that DMPA lipids lead to a membrane transversal condensation, which was captured when analyzing the distribution of the phosphorus atoms of DMPC lipids, where at increasingly higher pH values we can see that these are getting closer and closer to the bilayer center, thus leading to a decreased membrane thickness. By ionizying the DMPA lipids, one is promoting the disordering of neighboring DMPC lipids and therefore leading to a fluid membrane. However, preliminary data obtained within this work suggests that the magnitude and direction of such condensation effect depends on the DMPA lipid molar fraction (*data not shown*).

Interestingly, we observed that the destabilization induced by pH, mainly at pH 09.0 (31.5

± 0.4 Å), is higher than the one observed by Kučerka, for instance, at 60^{o}C (34.2 ± 0.7 Å) (**Figure 3.19**). Therefore, we conclude that in a mixture with the same composition as ours, varying the solution pH in an isothermal fashion, leads to a larger structural disorder than when raising the temperature to non-physiological values. Again, with this result one can see how much pH can influence the structure and hence functionality of biological membranes.

3.2.7 Lateral Diffusion

Today, picturing a biological membrane as an extremely dynamical entity is no longer just a reasonable assumption but rather a fact. These soft macromolecular aggregates are quite flexible and their dynamical behavior is determined by a whole hierarchy of rapid motional events (**Figure 3.22**) with correlation times within a broad spectrum, ranging from a few *ps* to as much as some *ms* or even *s*, time scales usually associated with local conformational changes in the hydrocarbon chain and long wave length bending undulations of the bilayer, for example, respectively.

Table 3.4: Summary of the lateral diffusion constants averaged over three replicates for all the CpHMD systems, computed for distinct time intervals, with a time step of 10 *ps*. The errors were determined as the highest difference between the reported diffusion and the two diffusions calculated from two equal halves of the time interval.

System	pH	D (10^{-8} cm^2 s^{-1})			Time intervals		
		DMPA	DMPC	Global	DMPA	DMPC	Global
PC	0.0	-	5.91 ± 0.92	5.91 ± 0.92	-	5-50	5-50
	1.0	-	5.34 ± 0.65	5.34 ± 0.65	-	5-70	5-70
	2.0	-	4.35 ± 0.40	4.35 ± 0.40	-	10-40	10-40
PA/PC	0.0	4.51 ± 0.42	5.10 ± 0.54	4.68 ± 0.21	10-30	5-45	5-30
	1.0	3.98 ± 0.50	4.54 ± 0.91	3.26 ± 0.54	15-30	5-25	15-35
	1.5	4.08 ± 0.21	4.41 ± 0.65	4.42 ± 0.73	10-25	5-25	5-25
	2.0	6.49 ± 0.68	6.18 ± 0.44	6.44 ± 0.51	10-30	5-30	5-30
	3.0	6.33 ± 0.24	6.61 ± 0.14	6.34 ± 0.66	10-35	5-50	10-60
	4.0	6.63 ± 0.78	7.12 ± 0.10	6.63 ± 0.80	10-30	5-35	10-40
	5.0	7.60 ± 1.88	8.41 ± 0.16	8.34 ± 0.31	10-40	5-30	10-30
	6.0	10.08 ± 0.20	8.79 ± 0.55	9.24 ± 0.38	10-50	10-60	10-60
	7.0	7.30 ± 0.63	8.15 ± 0.15	8.10 ± 0.19	10-70	10-60	10-50
	8.0	9.75 ± 0.27	8.22 ± 0.56	8.50 ± 0.33	5-75	10-30	10-30
	9.0	8.06 ± 0.55	8.36 ± 0.72	8.61 ± 0.46	5-25	10-30	5-25

We have computed the lateral diffusion coefficient, D, by plotting MSD for both lipids or for either DMPA or DMPC lipid molecules over elapsed time (**Figure 3.22** and **Table 3.4**; for further methodological details refer back to **2.6.6**).

From **Figure 3.22a** it is clear that the DMPC lipid molecules in a pure DMPC bilayer are not very sensitive to the solution pH, dinamically speaking, even though for pH 2.0, the complete deprotonation of the phosphate headgroups of DMPC lipids led to a small decrease of the lateral diffusion of this lipid. Nevertheless, the differences are small and within the error measured. This insensitivity to pH is in agreement to what was observed for all the structural parameters previously discussed for this system.

As for the 25% PA/PC lipid bilayer system (**Figure 3.22b**), we observed that at increasing pH values, the membrane tends to become more fluid. This result is in agreement with the A_L, V_L, D_{HH} and order parameter analysis already presented, where at higher pH values this model membrane presented a lower lipid packing and hence higher fluidity. With the augmentation of the A_L, and higher fluidity of the membrane, the lipid chains can more freely accomodate themselves, rotating rapidly around their normal axis. In addition, with the lower lipid packing lipid molecules have more free space to diffuse along the membrane plane. This higher fluididity of the membrane seems to be potentiated by the presence of the DMPA lipid molecules, since for pH values higher than 2.0, inclusively, one can see that all the diffusion coefficients respective to the DMPC lipid molecules (**Figure 3.22c**) are consistently higher than the ones obtained when in a pure membrane (**Figure 3.22a**).

In addition, we have plotted the MSD time dependency for the DMPC lipid molecules either in the pure bilayer system or in the 25% PA/PC membrane, at pH values 0.0, 1.0 and 2.0. The difference between the two diffusion coefficient values at the three pH values is mainly a reflexion of the different ionization of DMPC when in the absence or presence of the tested molar fraction of DMPA (**Figure 3.22d**).

Furthermore, from the observation of **Figure 3.23**, the existence of two different diffusion regimens, one at shorter times and another at longer times, can be postulated. At a shorter timescale, even though the lipid is trapped by its nearest neighbors, not being able to diffuse freely along the lipid matrix, it does have some local motility in the free area to which it is confined, exhibiting fast hydrocarbon chain fluctuations. Graphically, this effect is reported by a nonlinearity behavior at short times in the MSD time evolution (a behavior commonly named "rattle in a cage") **(124)**. **Figure 3.23** illustrates these rapid motions for different carbon atoms along the alyphatic chains. From these results, we observed that, even though the diffusion coefficients obtained are very similar, the MSD ranges sampled by the different atoms vary according to their conformational freedom. At longer timescales, the lipids are able to diffuse and switch places with each other, jumping bettween adjacent sites, giving rise to a diffusion whose value is limited by the liquid-viscuous properties of the lipid bilayer under analysis.

Altogether, the diffusion coefficients, obtained from the linear portion of the respective MSD curve, at longer times (refer back to **Table 3.4** for considered time intervals), were found to

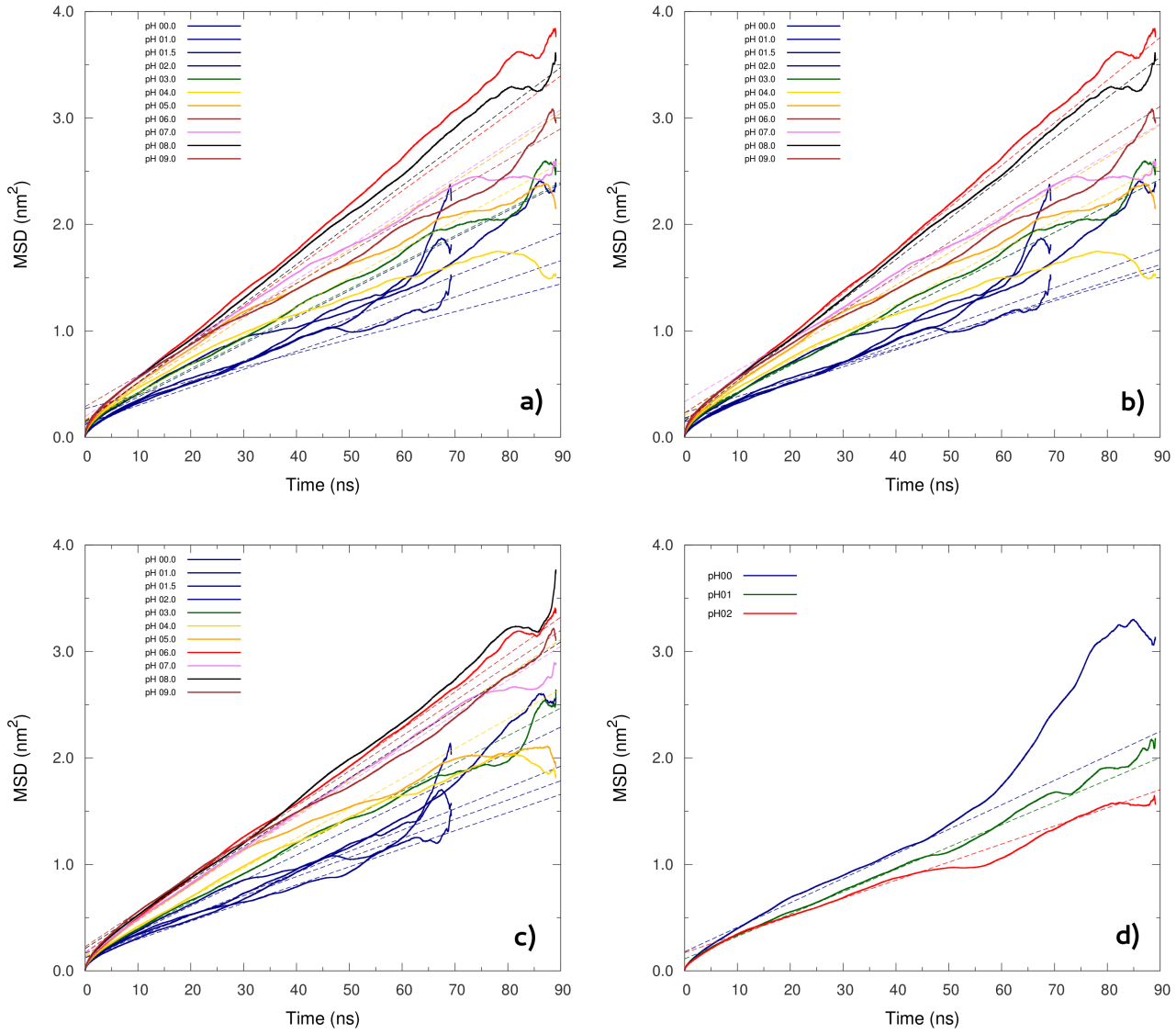

Figure 3.22: Mean square displacement as a function of time for all pH values studied in either the 25% PA/PC binary mixture (a,b,c) and pure DMPC membrane (d). The diffusions related to the PA/PC mixture **(a)** were calculated either for PA **(b)** or PC **(c)** lipid molecules alone. The diffusion was calculated from the linear part of the curves *(dashed lines)*

be within the experimental range measured using the FRAP technique - 5-10 x 10^{-8} cm^2 s^{-1}. **(140–143)**

3.2.8 Ion distribution

We have evaluated the distribution of the Na^+ and Cl^- ions along the membrane normal, close to the interfacial region (for details see **2.3**). Dividing the tridimensional space in 0.1 Å-thick slabs, we computed the time-average percentual abundance of both Na^+ and Cl^- ions at an

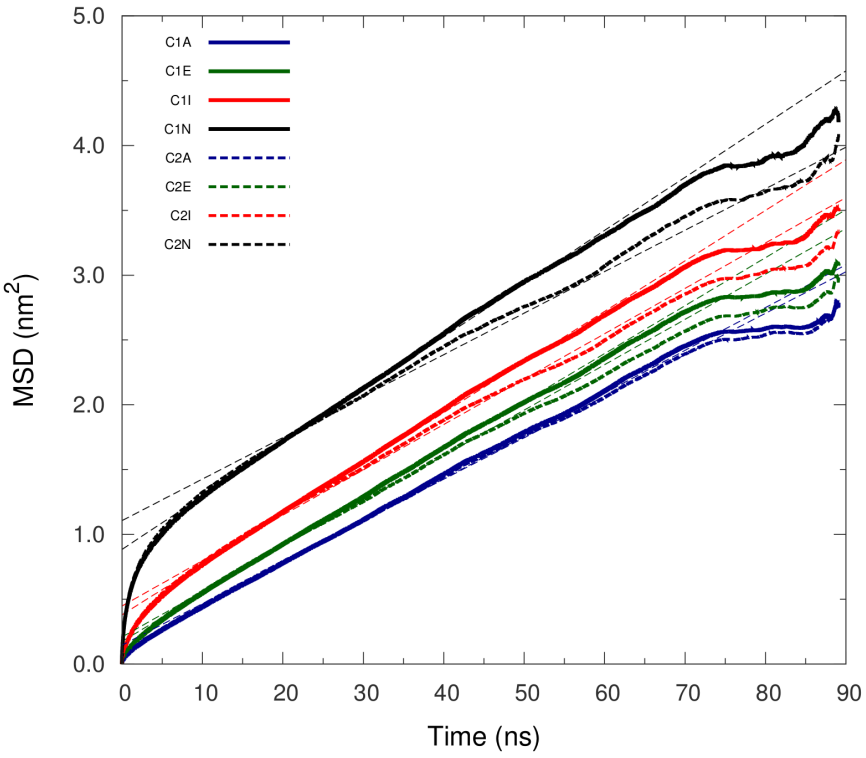

Figure 3.23: Mean square displacement as a function of time over three replicates at pH 07.0 for C1A, C2A, C1N and C2N atoms pertaining to both DMPA and DMPC lipids in a 25% PA/PC two-component membrane

increasing distance from the membrane (**Figure 3.24**).

As expected, **Figure 3.24a** shows that Cl^- ions tend to move away from an increasing negatively charged membrane surface. At pH 01.0, the membrane is only weakly charged and therefore we have a more uniform distribution of this ion. In this case, we can actually see a small accumulation of Cl^- ions interacting with the choline groups.

Figure 3.24b and **Figure 3.24c** show that Na^+ ions prefer to interact directly with the esther groups ($\sim$ 2.2 Å) below the phosphates, at $\sim$ 4.5 Å distance. These results are in very good agreement with the observations in DMPC by Böckmann *et al.* **(130)** The ion distribution around the phosphates show two high populated regions where Na^+ visits without major restrictions. At increasing pH values, and therefore increasing membrane ionization, Na^+ ions tend to be more attracted to the negatively charged phosphate headgroups, slightly moving away from the molecular electronegative "cage" formed between the surrounding esther groups and the lower region of the phosphates (**Figure 3.25**).

As soon as DMPA lipid molecules ionize, their charged polar groups will eventually disturb the electrostatic pattern of the superficial region of the membrane, relatively minimizing the depth of the electrostatic well, situated deep below the membrane, by creating a second favorable interaction spot near the phosphate headgroups. In our system, 25% of the lipid molecules do

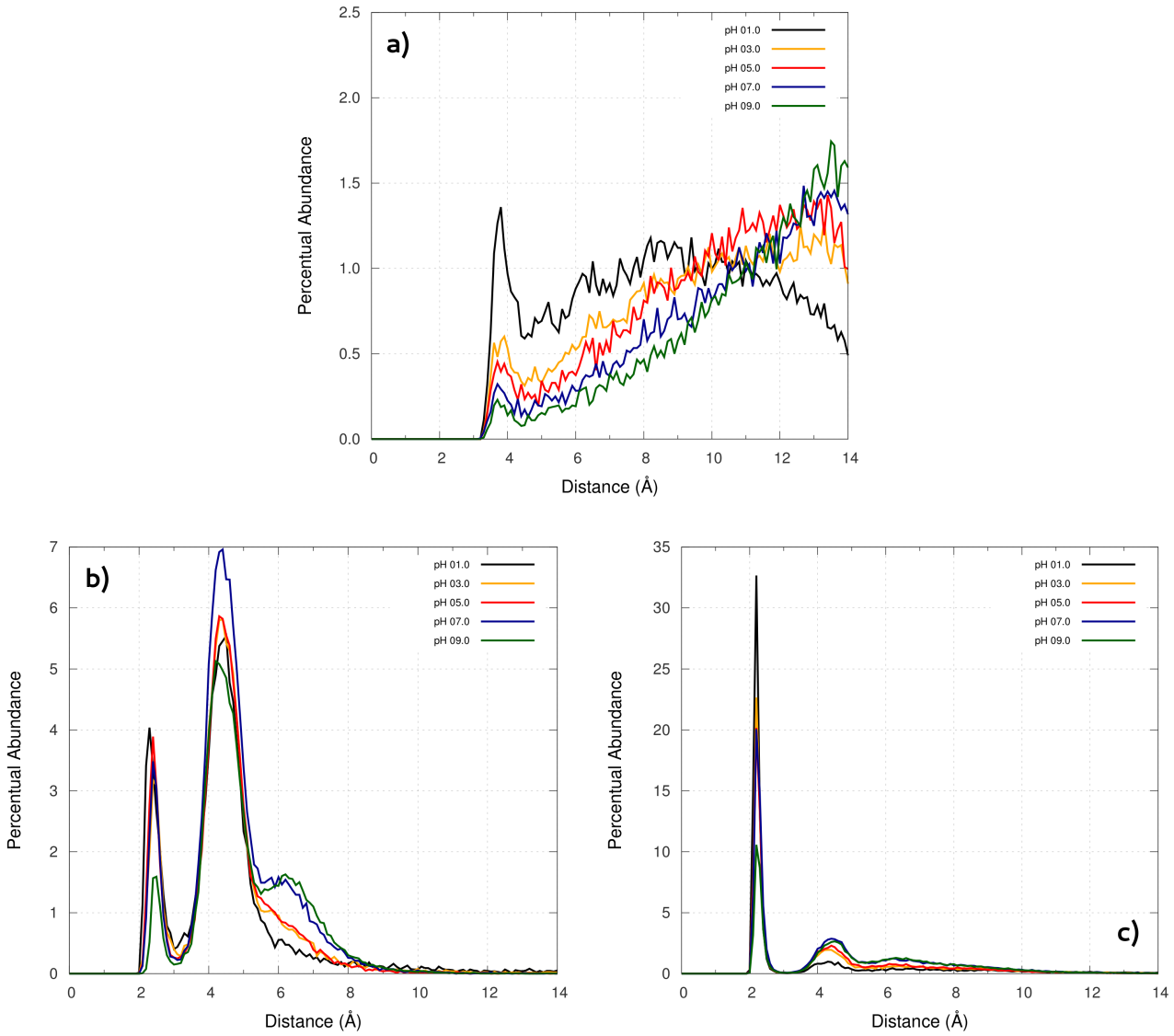

Figure 3.24: Time-average percentual abundance of Cl^- (a) and Na^+ (b,c) ions along the membrane normal. For Cl^- ion we used the choline methyl groups as reference, while for Na^+ ions we computed the distribution relative to the oxygens either in the phosphate groups (**b**) or in the esther groups (**c**).

not have the positive and rather bulky choline groups that form a barrier to the release of Na^+ ions (*data not shown*). Therefore, at higher ionizations we start to observe migrations of these ions towards the solvent, which can be seen at distances over 6 Å in **Figure 3.24b** and **Figure 3.24c**. The increase of Na^+ release at higher pH values is counterintuitive and can probably be explained by two effects. On one hand, higher negative charge should increase the Na^+ interactions with the phosphate groups, on the other hand, the membrane becomes more fluid and disordered, which may favor solvation and the consequent release of the ions.

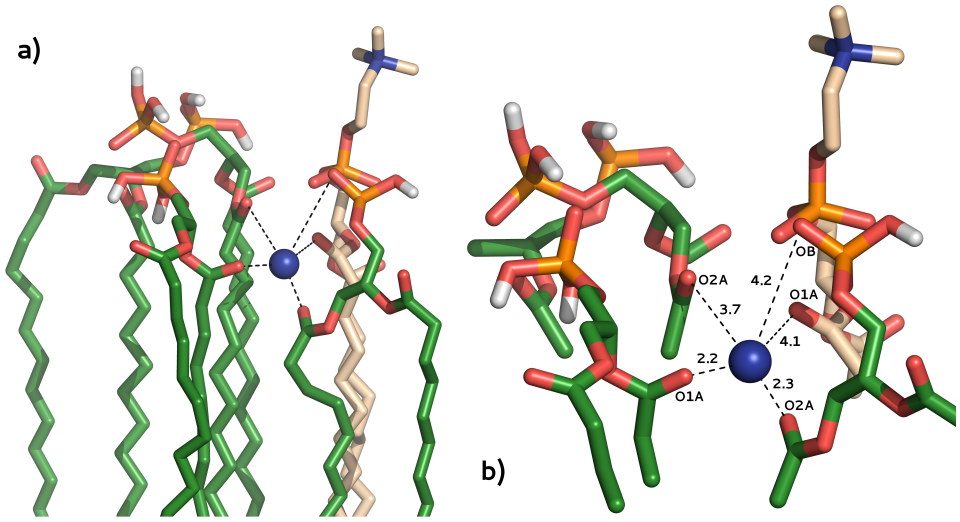

Figure 3.25: Typical snapshot of a Na^+ ion coordinating with lipid oxygen atoms. Na^+ ion is displayed by a blue sphere. Lipids are represented by sticks, either green or wheat for DMPA and DMPC lipids, respectively. The dashed lines indicate the coordination bond - **(a)** 3D structure of Na^+ ion coordinating with adjacent lipids. **(b)** Close view of the coordination pattern of Na^+ ion with four ester oxygen atoms and one phosphate oxygen atom

Chapter 4

Concluding Remarks

Phospholipid bilayers constitute the primary structural element of biological membranes. For many years, their lipid components have been considered passive bystanders with a merely structural function, but nowadays, this idea no longer seems to be appropriate. The comprehension of the molecular biophysical basis for the diversity seen in both membrane structure and function has been and still is one of the most appreciated and most common sought research topics when dealing with the study of biological membranes. Paradoxically, at the present time, experimental methodologies are still hindered from giving proper answers, suffering from insufficient spatial and temporal resolution, a problem that can be overcome by the correct use of MM/ MD methodologies. Many are the questions that remain unanswered, most of them associated with the intrinsic interplay between the physical phase behavior of lipids and the interactions that these establish with membrane or soluble proteins. Nowadays, computer simulations are gaining significant importance on the elucidation and forecast at the atomic/ molecular level of the detailed relations underlying biological and physical properties, the chemical structure of both lipids and proteins and the roles that these have when in a membranar environment.

In this thesis, we presented the first application of a modified version of the stochastic CpHMD method to the conformation-protonation coupling in a bilayer system composed of a 25% PA/PC binary mixture. By making use of a *"state of the art"* computational technique such as CpHMD, originally developed by Dr. António Baptista at ITQB, we were able to sample both conformation and protonation concomitantly and hence further extend the knowledge about their intrinsic relationship and postulate about the implication of pH effects, and hence electrostatics, on the structural and dynamical properties of the membrane. This problematic is of crucial importance to us since our phospholipid bilayer model containing an anionic lipid, PA, is subject to the acquisition of densely localized charges in its surface. Therefore, we aimed at probing the effect of a fixed amount of DMPA over DMPC (1:3) membranes at different pH

values. Our main focus was to study the protonation of PA in membrane systems, and as far as we know, we were the first group to quantitatively elucidate this phenomenon by producing a titration curve where two inflection points are visible, both associated with $PA^0 \rightarrow PA^{-1}$ and $PA^{-1} \rightarrow PA^{-2}$ conversions, at pH $\sim$ 2.5 and pH $\sim$ 7.0, respectively. This tool can be used to define accurately and precisely the pH ranges at which this system will be stable but also functional, and might be valuable at predicting such properties concerning other membrane compositions, distinct from the studied.

In addition, we analyzed various structural and dynamical parameters, from both area and volume per lipid reporting lower lipid packing densities at higher pH values; and order parameter and lateral diffusion coefficients linking a gain of disorder and fluidity with the increase of solution pH. This gave us strong insights on the characterization of our system, both structurally as dinamically and its dependence of the electrostatic interactions. Such a gain of knowledge will most certainly have a major impact on the study of protein-lipid interactions since it is well known that membrane structure and electrostatic pattern established at the interfacial membrane-solvent region can deeply influence the establishment of strong specific interactions between membranes and its ligands. Most precisely, at around physiological pH, when both PA^{-1} and PA^{-2} populations are the most abundant species, we conclude that the 25% PA/PC membrane presents itself with characteristics similar to those expected for a biological fully-functional membrane, which has fluidity and flexibility at the same time, being able to accomodate its structure framework to physical alterations behind many of the most essential biological processes. In fact, from comparison with experimental and theoretical MD studies we were able to validate our results. Therefore, we conclude that we are now able to broaden our study to other charged lipid species, subject to pH effects.

It is commonly accepted that the ion composition of the system can have major impact on the structural features of a charged membrane. By using a PB-based methodology to estimate the "correct" amount of Na^+ and Cl^- ions in the solution and by applying a proper electrostatic treatment through the use of GRF at 0.1 M ionic strength, we were able to obtain stable and reproductible lipid bilayers. In addition, we were also able to report that our PB-formalism based approach can fully and correctly predict the pH-dependent isothermal phase transition observed experimentally at 310 K and 0.1 M by Garidel and coworkers. **(50)** Hence, despite of possible force field related limitations **(126; 144)** this study is in our opinion one important step in the direction of minimizing the imprecisions that emerge through time.

Surprisingly, our results suggest that in most cases, especially on the order parameter profiles and thickness results, it is the DMPC lipids that do suffer major structural modulations with the pH variations. We hypothesise that there is an indirect effect of DMPA ionization on DMPC lipids. Also, when studying such properties concerning DMPC lipids either in a pure DMPC lipid bilayer or in a 25% PA/PC binary mixture (*e.g.* by plotting the titration curve of DMPC

lipids in both cases) we have come across effects that could be reasoned by electrostatics alone. Altogether, we are confident that, in a near future, we will be able to address in a quantitatively manner the existence and formation of microdomains at specific pH conditions.

Currently, there is work in progress concerning the pH titration of PA/PC bilayer systems at other molar fractions (*e.g.* 50% and 100%), in order to complement the present study, and help us bring some light on the effect of DMPA molar fraction in the titration and, hence, on the structural and dynamical parameters studied extensively in this work. Preliminary results suggest, to some extent, that such an influence on the molar fraction of PA/PC on the various properties studied do exist.

Chapter 5

Outlook

Within this work, we obtained promising results which we consider to be essential for further development of more correct and therefore realistic MD and CpHMD methodologies that can be applied either to lipid bilayer systems containing anionic lipids but also to other densily charged systems. As such, a methodology was developed on the system setup in order to improve the results obtained related to the ion-lipid and consequently lipid-lipid interactions. Through a PB formalism based on the Debye-Hückel theoretical framework, we were able to predict the "correct" distribution of ions near the membrane-solvent interfacial region based on the conformation of the charged lipidic components of our membrane and respective generated electrostatic potential at certain conditions (namely at different ionic strengths). Once these methods are completely and properly implemented and evaluated, we will be able to broaden our study to other anionic lipids. In fact, one of the numerous objectives that stems from this work concerns the study of the protonation behavior of polyphosphoinositodes (PIPs), namely PtdIns(4)P and PtdIns(4,5)P_2.

For many years, researchers have tried, in vain, to elucidate the fundamental biophysical principles governing most important molecular processes, among them protein-lipid interactions. Still, these remain largely misunderstood. With the current computational power, and by knowing that such interactions are electrostatically driven and hence inherently dependent on the solution pH, our methodology seems to be unique at being able to model and attest protein-lipid interactions at varying pH. Hence, at a long-term, the final application of this modified CpHMD methodogy would be to examine the interaction between membranes (containing these or other anionic lipids) with specific peptides or proteins target at various conditions (T, I and pH). Initially, we pretend to proceed to the study at the molecular detail of protein-lipid interactions of either PA or PIPs with some of their specific protein partners, *e.g.* Opi1 protein.

Finally, throughout the work developed in this thesis, we have come across apparent phe-

nomena such as lateral inhomogeneity and formation of microdomains which where preliminarly analyzed. The results obtained with this thesis lead us to think that the appearance of phase separation events is to be expected at low membrane ionization values and hence low pH, since at these conditions we have proven that DMPA and DMPC lipids seem to "sense" the pH solution in different ways, *i.e.* while DMPC lipids stay rather fluid, the DMPA lipids are expected to have increased ordering. Thermodinamically speaking, a system like the one studied at low pH, presenting itself as an inhomogeneous medium will eventually lead to the establishment of more favorable interactions between likewise partners and thus lead to the development of distinct regions if the kinetics of the system are permissive to such an event.

Appendix A

Auxiliary tables

Table A.1: Times of equilibration

PA/PC (%)	DMPA	Charge	Time Segment (*ns*)	
			Equilibration	Production
0.00	0	0	0-100	100-200
25.00	32	0	0-100	100-200
		8	0-100	100-200
		16	0-100	100-200
		24	0-100	100-200
		32	0-100	100-200
		40	0-100	100-200
		48	0-100	100-200
		56	0-100	100-200
		64	0-100	100-200
100.00	128	0	0-100	100-200
		32	0-100	100-200

Table A.2: Equilibration and production times in CpHMD simulations

Membrane	pH	Time Segment (*ns*)	
		Equilibration	Production
PC	0.0	0-10	10-100
	1.0	0-10	10-100
	2.0	0-10	10-100
PA/PC	0.0	0-80	80-150
	1.0	0-50	50-120
	1.5	0-40	40-110
	2.0	0-10	10-100
	3.0	0-10	10-100
	4.0	0-10	10-100
	5.0	0-10	10-100
	6.0	0-10	10-100
	7.0	0-10	10-100
	8.0	0-10	10-100
	9.0	0-10	10-100

Table A.3: Population percentage of each charge state of DMPC and DMPA at several pH values in CpHMD simulations

System	pH	Charge states				
		$DMPC^{+1}$	$DMPC^{0}$	$DMPA^{0}$	$DMPA^{-1}$	$DMPA^{-2}$
PC	0.0	7.98 ± 1.78	92.02 ± 1.78	-	-	-
	1.0	2.44 ± 1.06	97.56 ± 1.06	-	-	-
	2.0	0.22 ± 0.18	99.78 ± 0.18	-	-	-
PA/PC	0.0	15.75 ± 1.51	84.25 ± 1.51	92.12 ± 1.52	7.87 ± 1.53	0.01 ± 0.00
	1.0	7.72 ± 1.27	92.28 ± 1.27	80.16 ± 2.18	19.80 ± 2.22	0.04 ± 0.02
	1.5	5.10 ± 0.70	94.90 ± 0.70	68.81 ± 3.14	31.13 ± 3.13	0.05 ± 0.05
	2.0	2.74 ± 0.62	97.26 ± 0.62	56.42 ± 5.65	43.54 ± 5.65	0.04 ± 0.02
	3.0	1.22 ± 0.45	98.78 ± 0.45	37.03 ± 3.34	62.78 ± 3.33	0.19 ± 0.15
	4.0	0.41 ± 0.34	99.59 ± 0.34	11.00 ± 2.46	88.34 ± 2.60	0.66 ± 0.13
	5.0	0.12 ± 0.11	99.88 ± 0.11	4.36 ± 2.93	92.53 ± 3.03	3.11 ± 0.40
	6.0	0.02 ± 0.02	99.98 ± 0.02	1.59 ± 1.60	83.51 ± 2.14	14.90 ± 1.67
	7.0	0.02 ± 0.01	99.99 ± 0.01	0.14 ± 0.09	53.25 ± 2.08	46.62 ± 2.05
	8.0	0.00 ± 0.00	100.00 ± 0.00	0.03 ± 0.05	18.76 ± 1.56	81.21 ± 1.56
	9.0	0.00 ± 0.00	100.00 ± 0.00	0.00 ± 0.00	3.68 ± 0.85	96.32 ± 0.85

Table A.4: Fractions of *trans* and *gauche* isomers for both DMPA and DMPC lipids at several pH values for pure PC and 25% PA/PC lipid bilayer.

System	pH	DMPA		DMPC		Global	
		trans	***gauche***	***trans***	***gauche***	***trans***	***gauche***
100 % PC	0.0	-	-	77.52	22.48	77.52	22.48
	1.0	-	-	77.49	22.51	77.49	22.51
	2.0	-	-	77.54	22.46	77.54	22.46
25 % PA/PC	0.0	78.35	21.65	79.93	20.07	79.53	20.47
	1.0	78.37	21.63	80.24	19.76	78.77	20.23
	1.5	79.22	20.78	80.07	19.93	79.85	20.15
	2.0	77.58	22.42	78.62	21.38	78.36	21.64
	3.0	77.24	22.76	77.92	22.08	77.75	22.25
	4.0	77.27	22.73	77.35	22.65	77.33	22.67
	5.0	77.06	22.94	76.87	23.13	76.92	23.08
	6.0	76.89	23.11	76.54	23.46	76.63	23.37
	7.0	76.78	23.22	76.24	23.76	76.37	23.63
	8.0	76.67	23.33	75.74	24.26	75.97	24.03
	9.0	76.49	23.51	75.50	24.50	75.74	23.26

Appendix B

Auxiliary figures

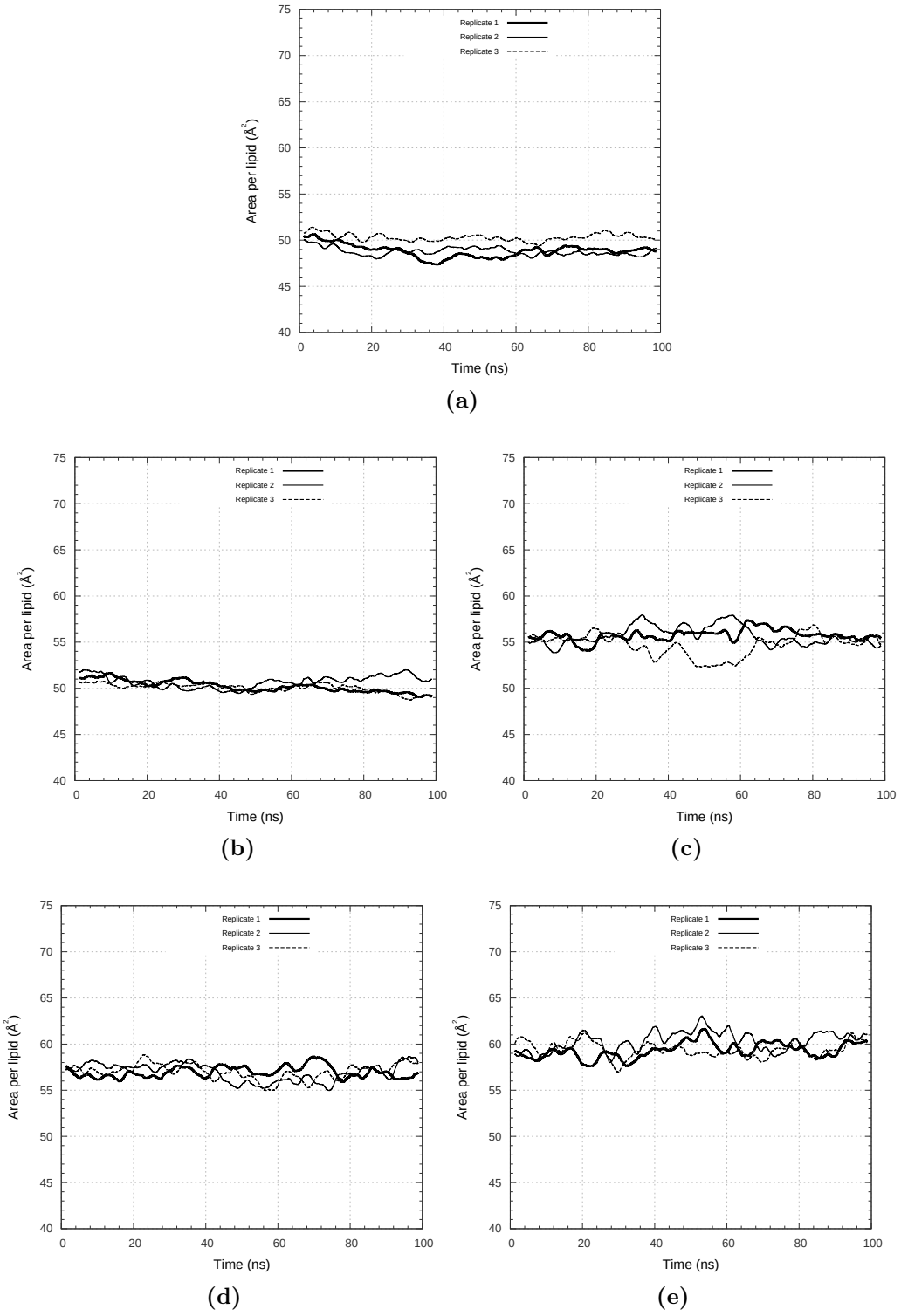

Figure B.1: Area per lipid time evolution, at different ionizations, for a 25% PA/PC lipid bilayer (Membrane charge equal to 0 **(a)**, 8 **(b)**, 16 **(c)**, 24 **(d)** and 32 **(e)**.)

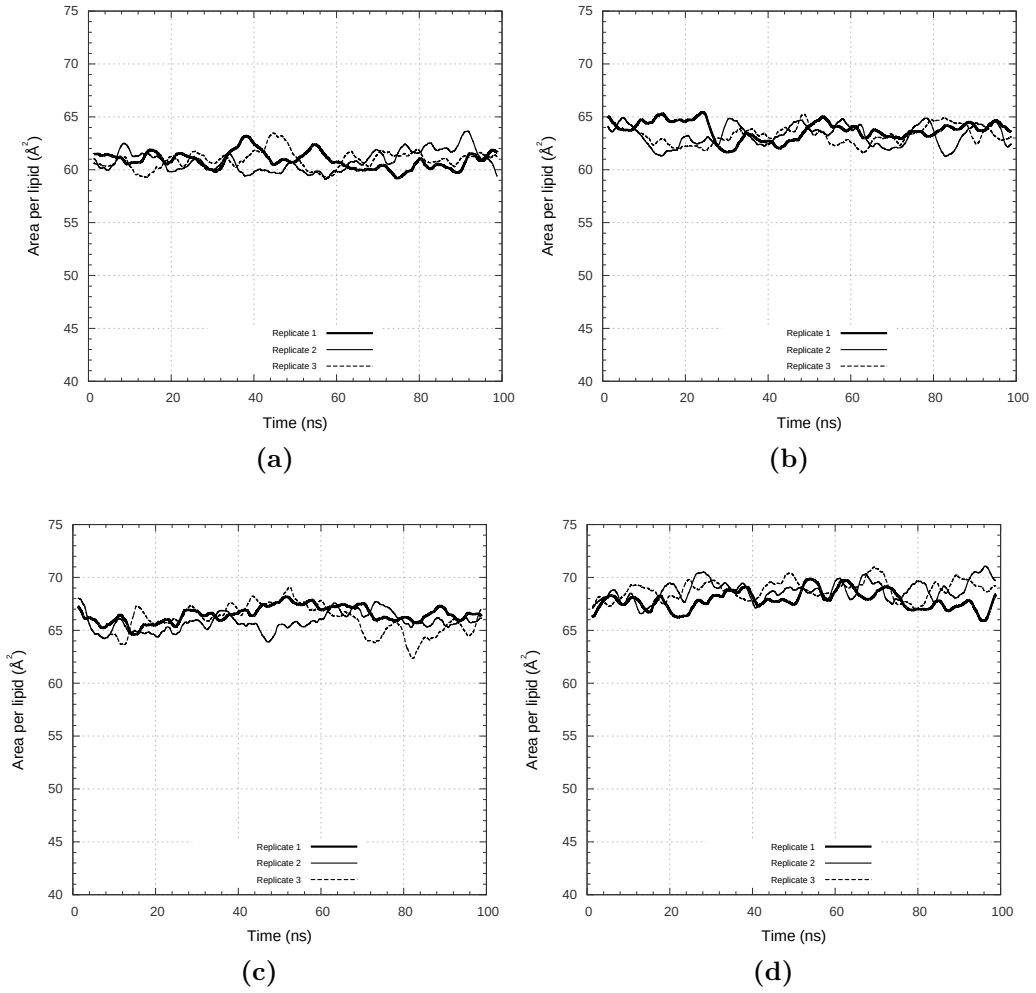

Figure B.2: Area per lipid time evolution, at different ionizations, for a 25% PA/PC lipid bilayer (Membrane charge equal to 40 **(a)**, 48 **(b)**, 56 **(c)** and 64 **(d)**.)

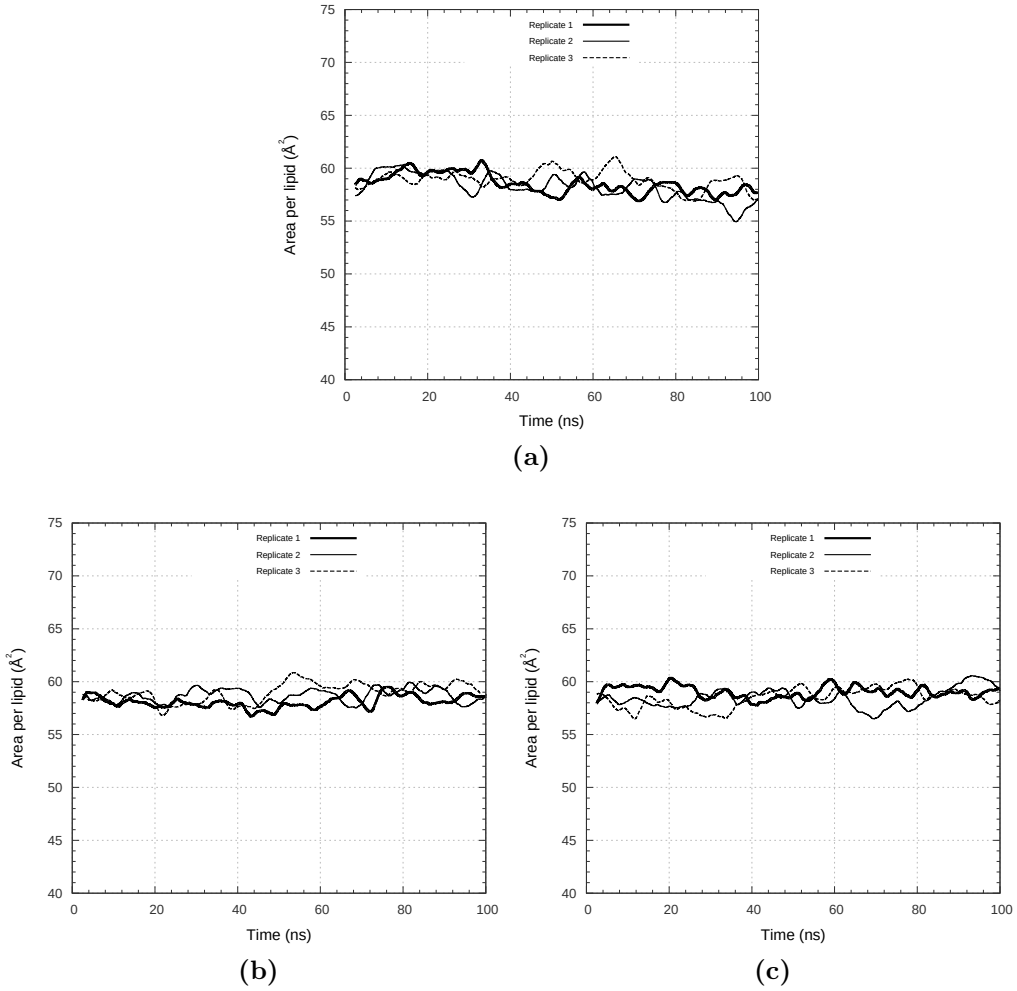

Figure B.3: Area per lipid time evolution, at different pH values, for a pure PC lipid bilayer (pH value equal to 0.0 **(a)**, 1.0 **(b)** and 1.5 **(c)**.)

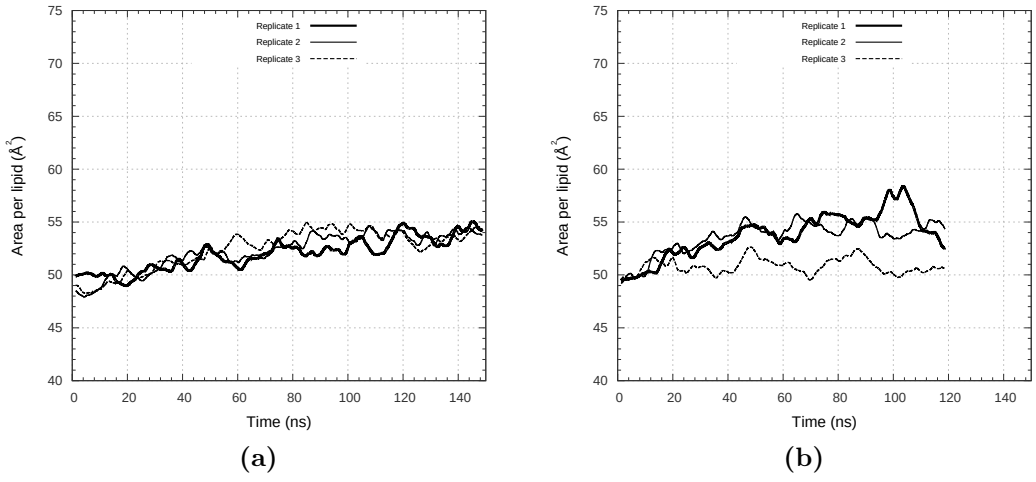

Figure B.4: Area per lipid time evolution, at different pH values, for a 25% PA/PC lipid bilayer (pH value equal to 0.0 **(a)**, 1.0 **(b)** and 1.5 **(c)**.)

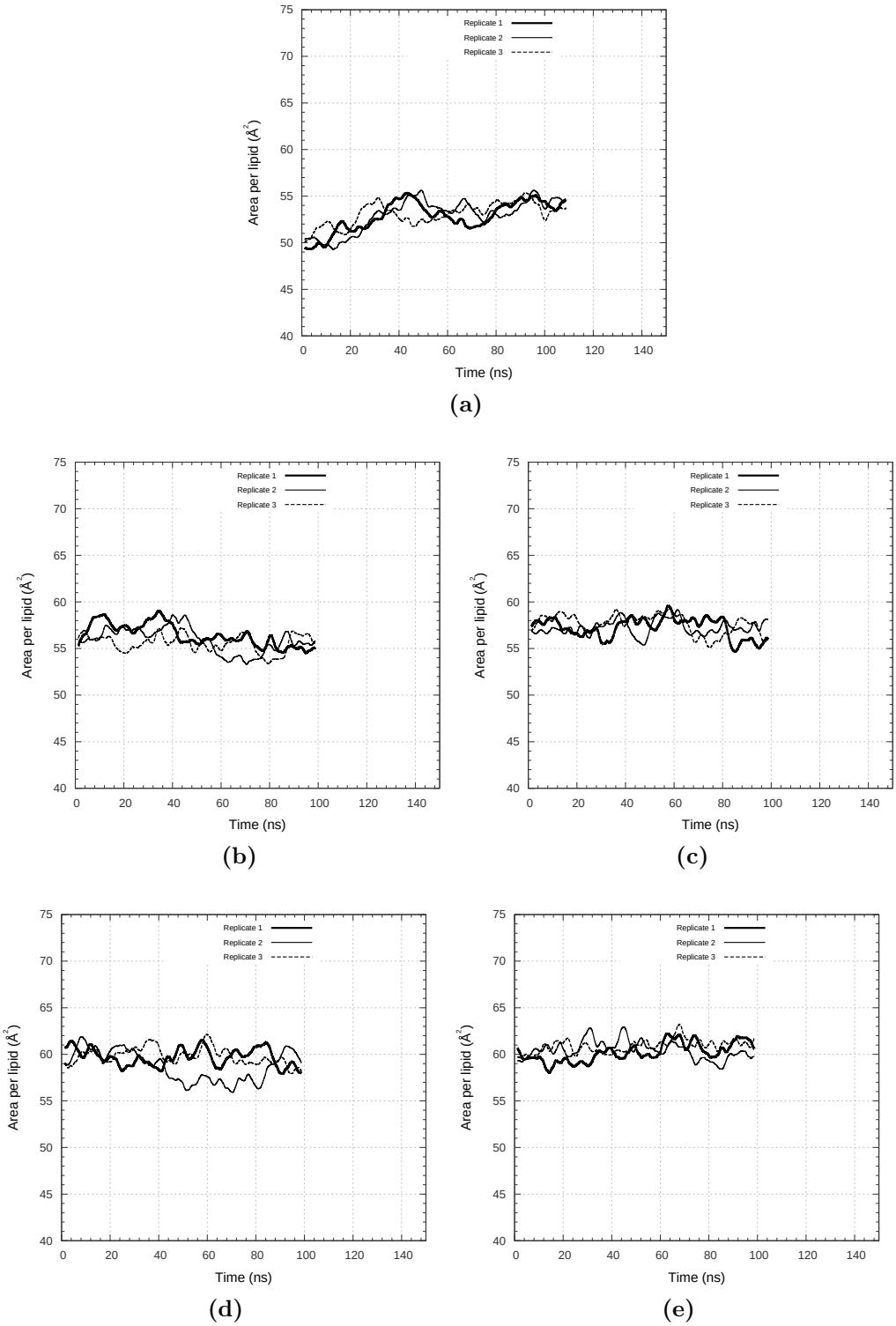

Figure B.5: Area per lipid time evolution, at different pH values, for a 25% PA/PC lipid bilayer (pH value equal to 2.0 **(a)**, 3.0 **(b)**, 4.0 **(c)** and 5.0 **(d)**.)

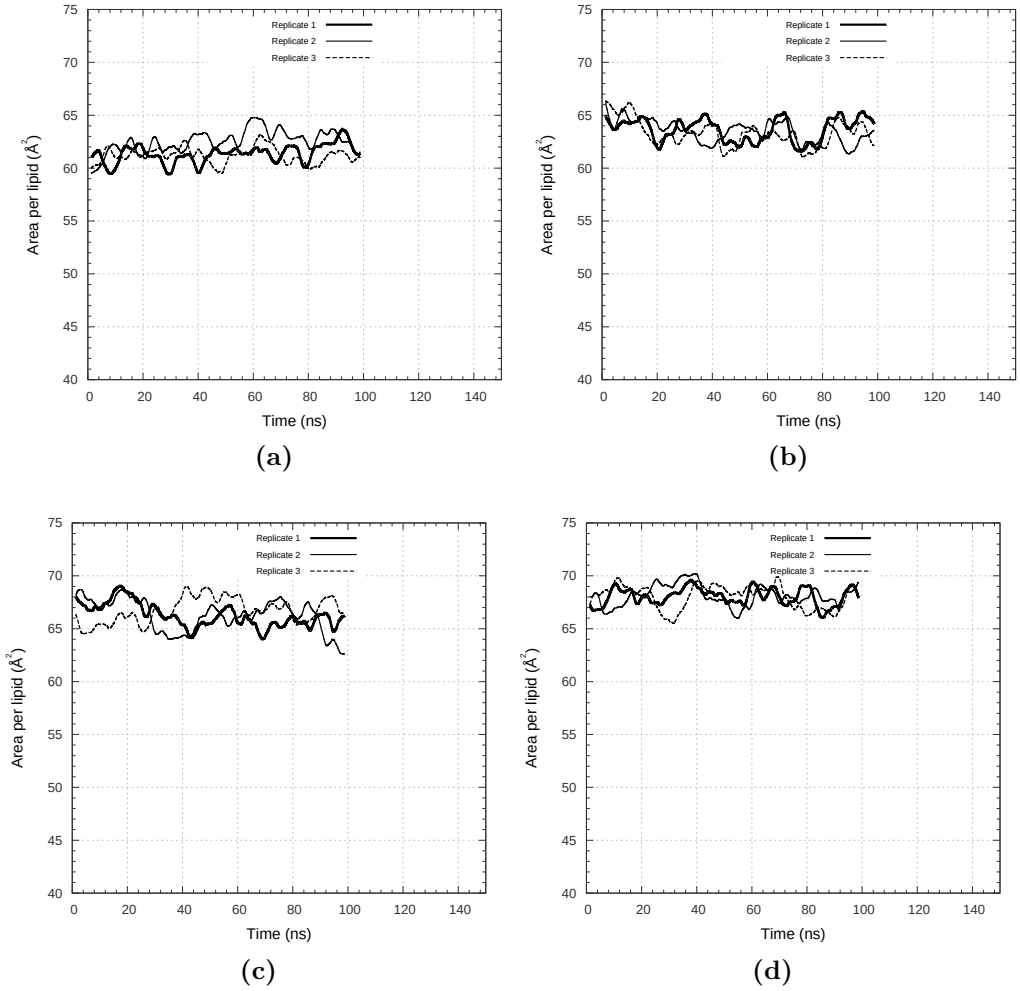

Figure B.6: Area per lipid time evolution, at different pH values, for a 25% PA/PC lipid bilayer (pH value equal to 6.0 **(a)**, 7.0 **(b)**, 8.0 **(c)** and 9.0 **(d)**.)

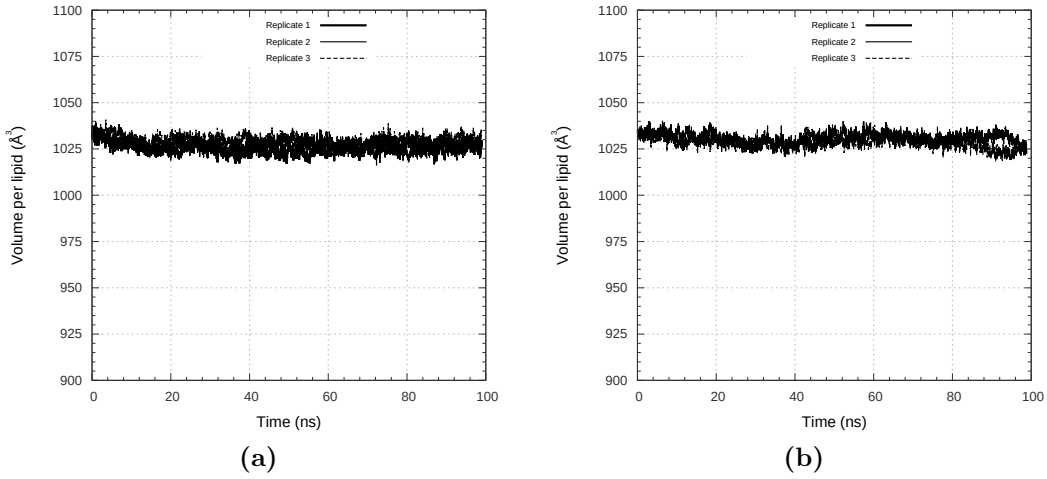

Figure B.7: Volume per lipid time evolution, at different ionizations, for a 25% PA/PC lipid bilayer (Membrane charge equal to 0 **(a)** and 8 **(b)**.)

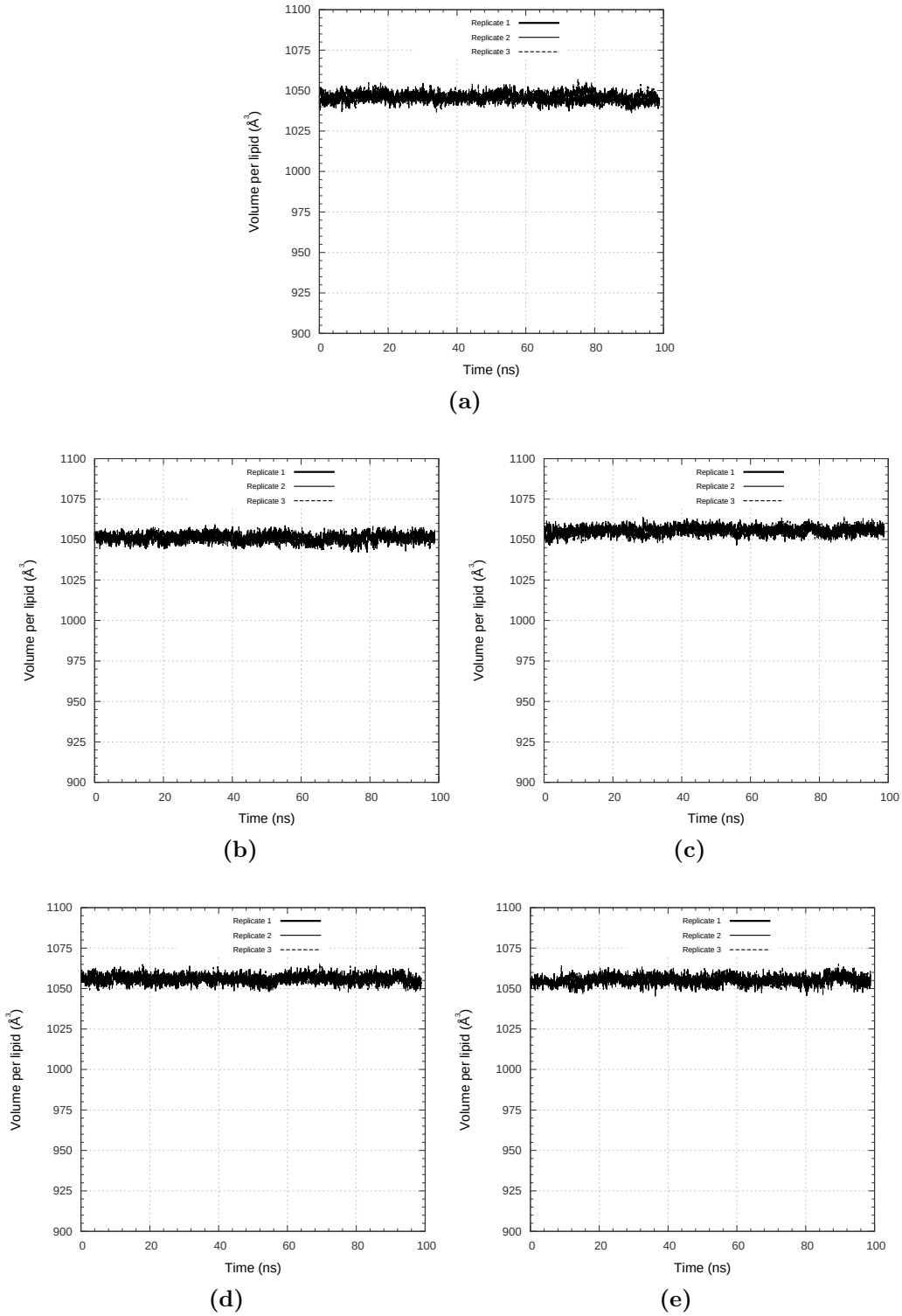

Figure B.8: Volume per lipid time evolution, at different ionizations, for a 25% PA/PC lipid bilayer (Membrane charge equal to 16 **(a)**, 24 **(b)**, 32 **(c)**, 40 **(d)** and 48 **(e)**.)

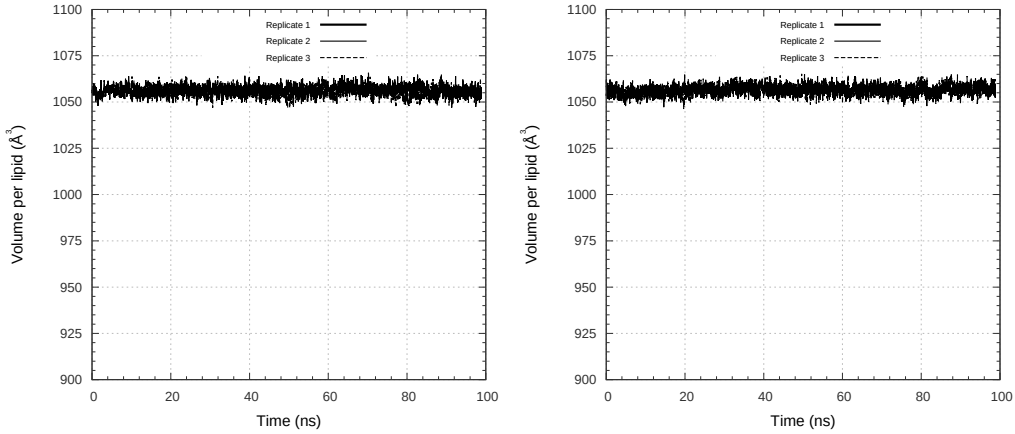

Figure B.9: Volume per lipid time evolution, at different ionizations, for a 25% PA/PC lipid bilayer (Membrane charge equal to 56 **(a)** and 64 **(b)**.)

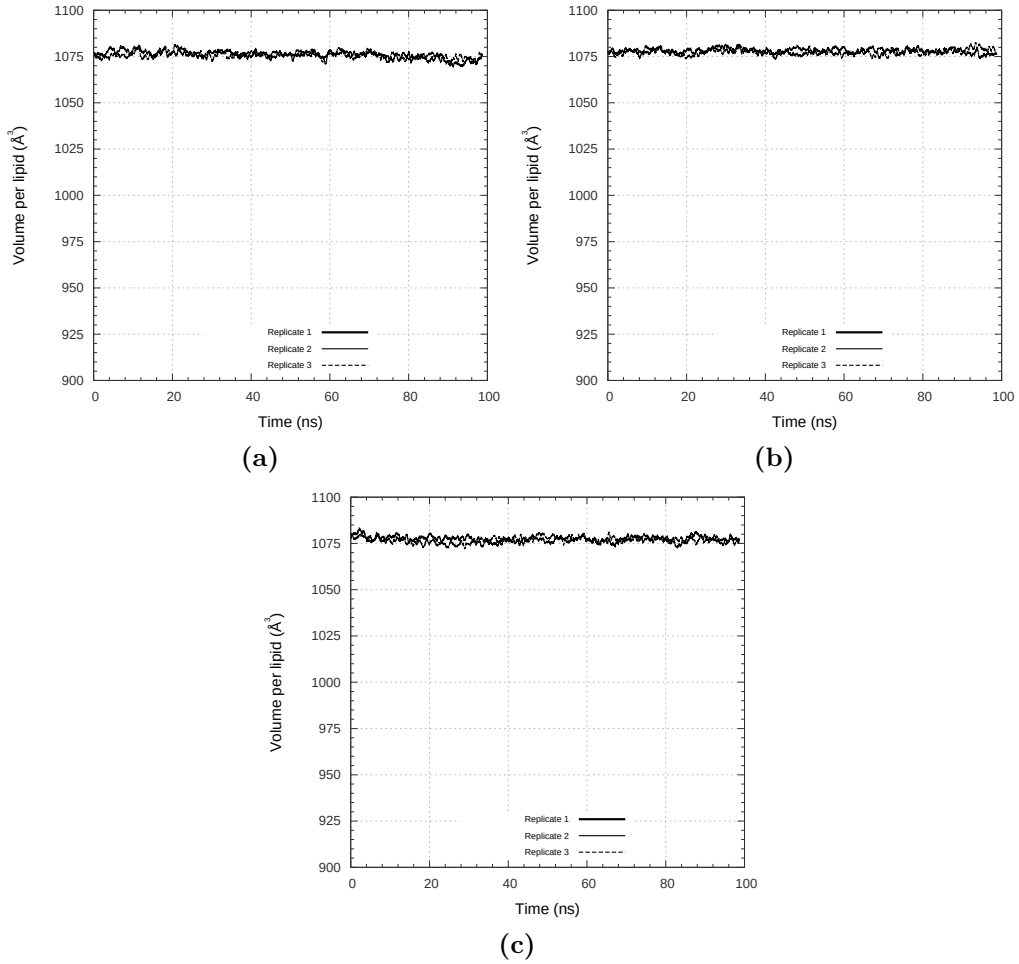

Figure B.10: Volume per lipid time evolution, at different pH values, for a pure PC lipid bilayer (pH value equal to 0.0 **(a)**, 1.0 **(b)** and 1.5 **(c)**.)

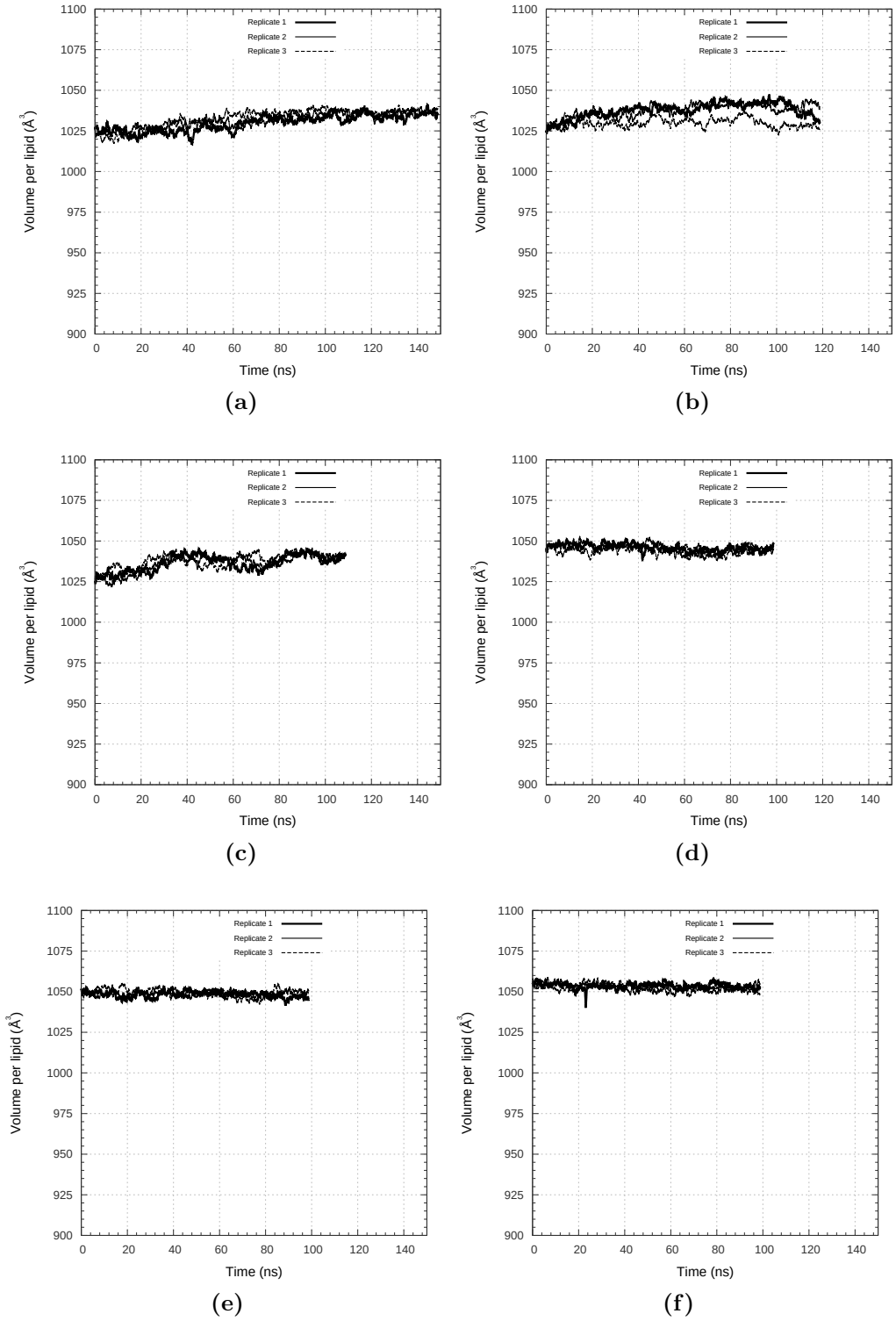

Figure B.11: Volume per lipid time evolution, at different pH values, for a 25% PA/PC lipid bilayer (pH value equal to 0.0 **(a)**, 1.0 **(b)**, 1.5 **(c)**, 2.0 **(d)**, 3.0 **(e)** and 4.0 **(f)**.)

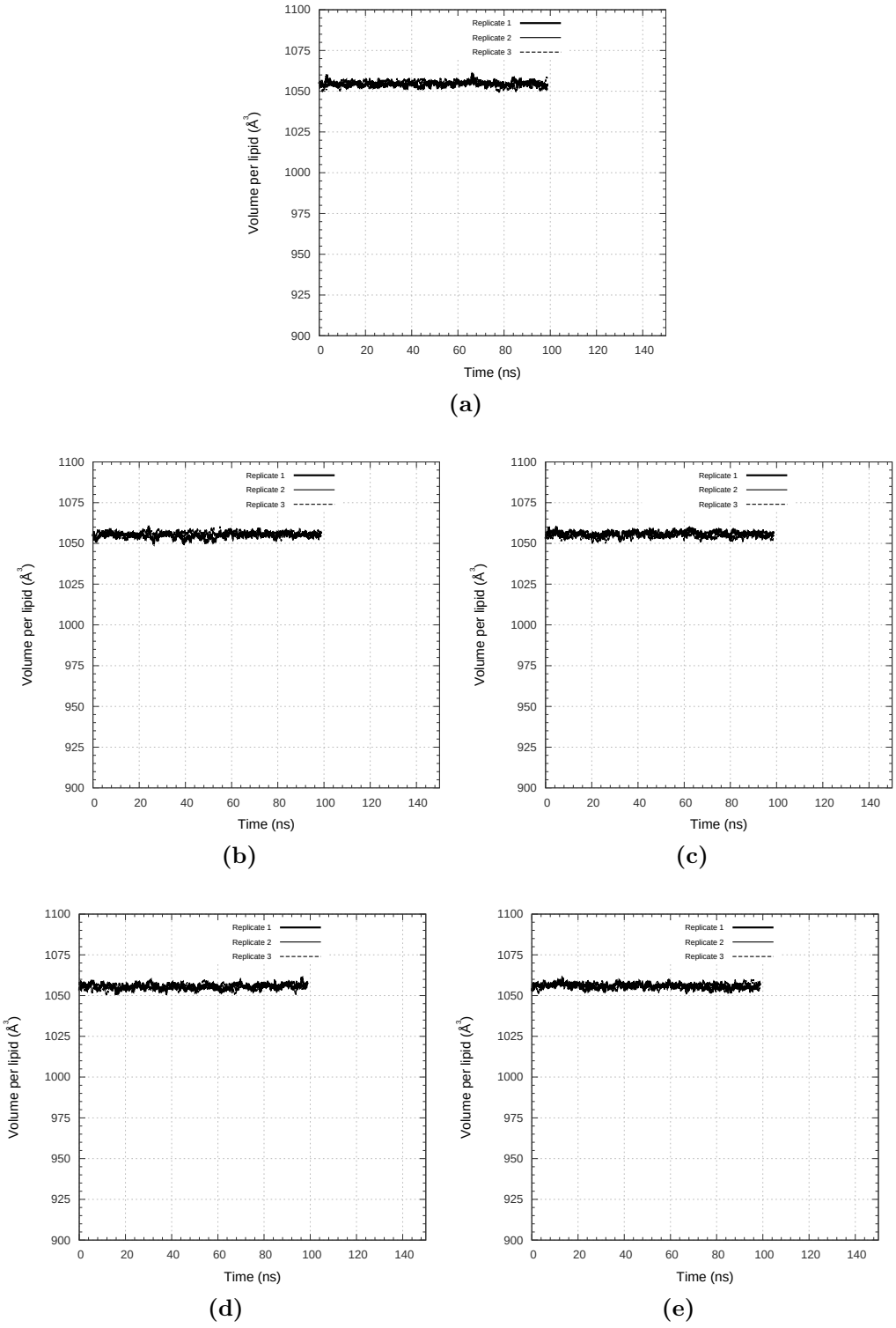

(a) **(b)** **(c)** **(d)** **(e)**

Figure B.12: Volume per lipid time evolution, at different pH values, for a 25% PA/PC lipid bilayer (pH value equal to 5.0 **(a)**, 6.0 **(b)**, 7.0 **(c)** and 8.0 **(d)** and 9.0 **(e)**.)

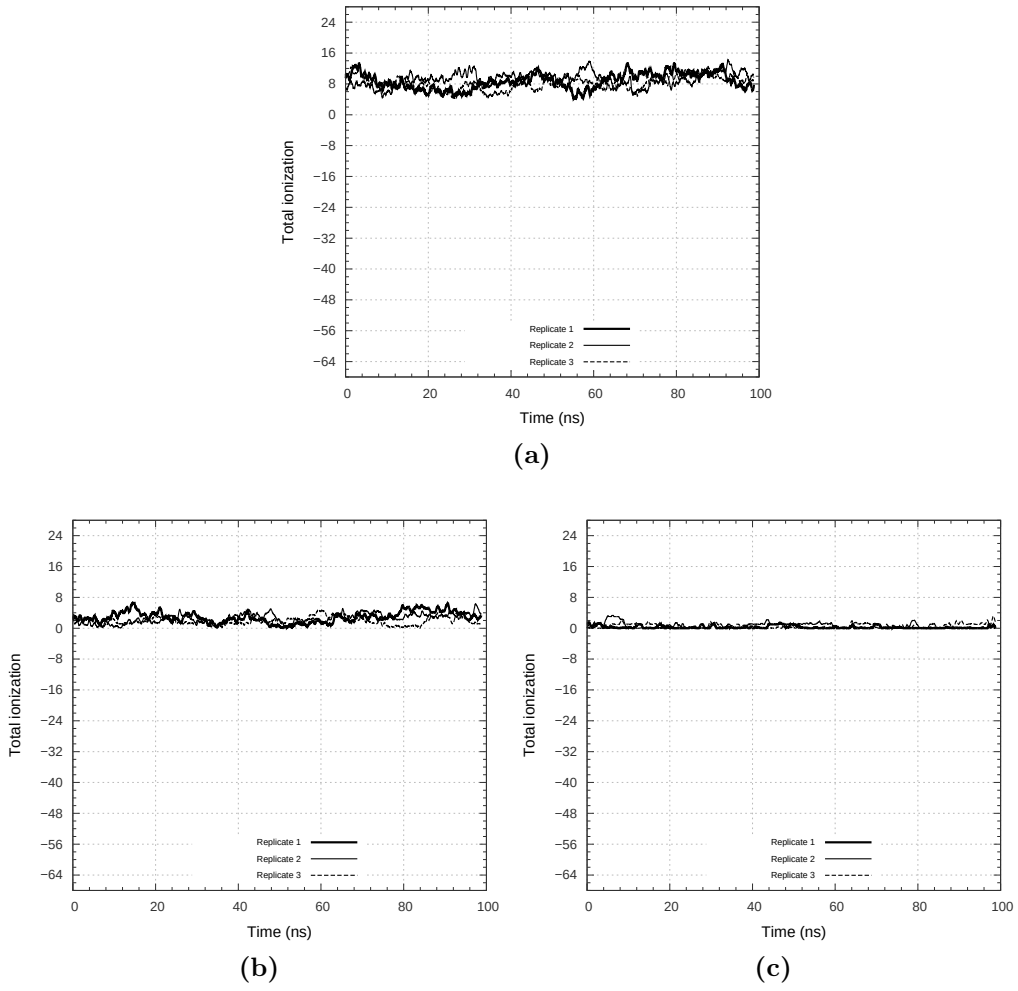

Figure B.13: Protonation time evolution, at different pH values, for a pure PC lipid bilayer (pH value equal to 0.0 **(a)**, 1.0 **(b)** and 1.5 **(c)**.)

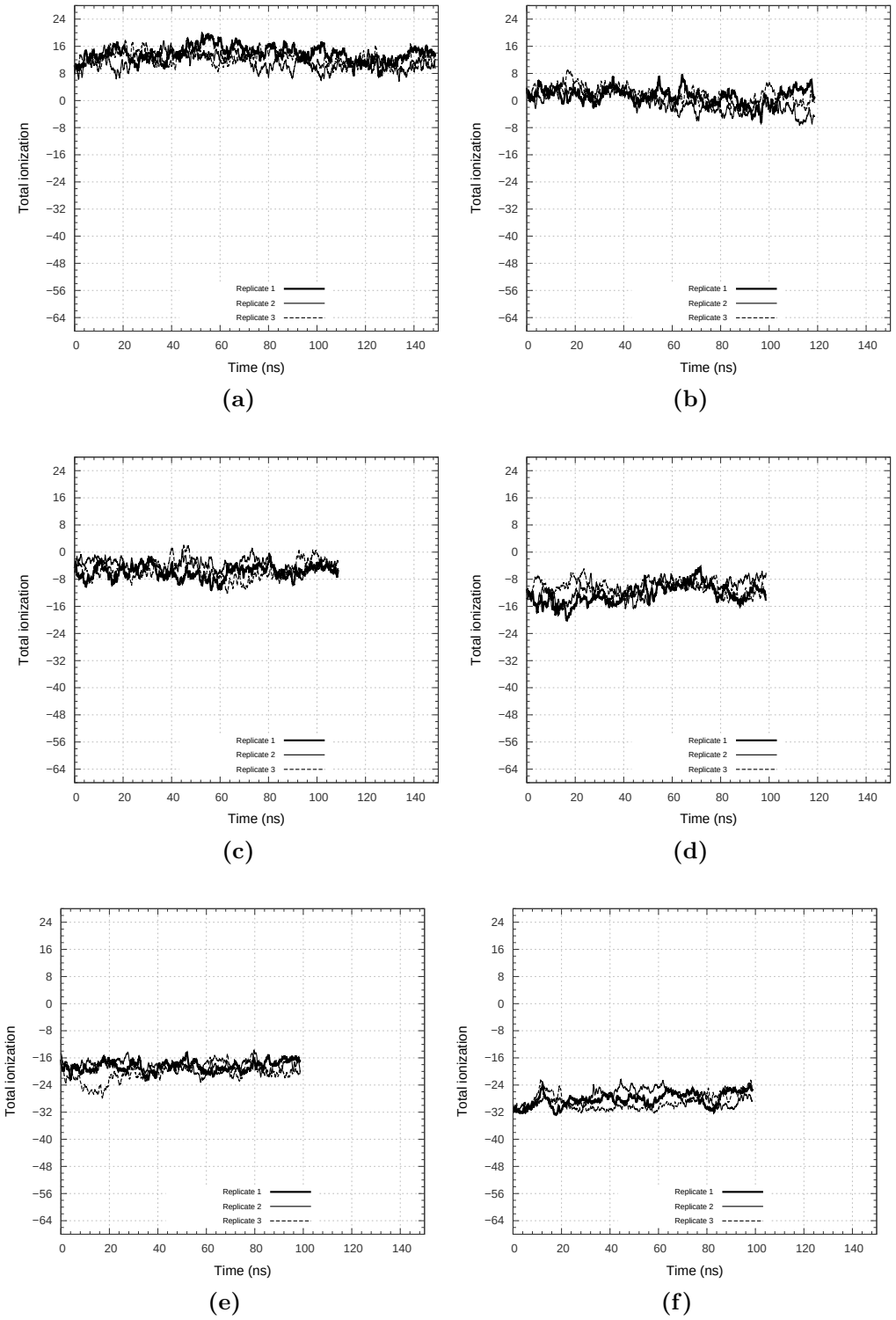

Figure B.14: Protonation time evolution, at different pH values, for a 25% PA/PC lipid bilayer (pH value equal to 0.0 **(a)**, 1.0 **(b)**, 1.5 **(c)**, 2.0 **(d)**, 3.0 **(e)**, 4.0 **(f)**.)

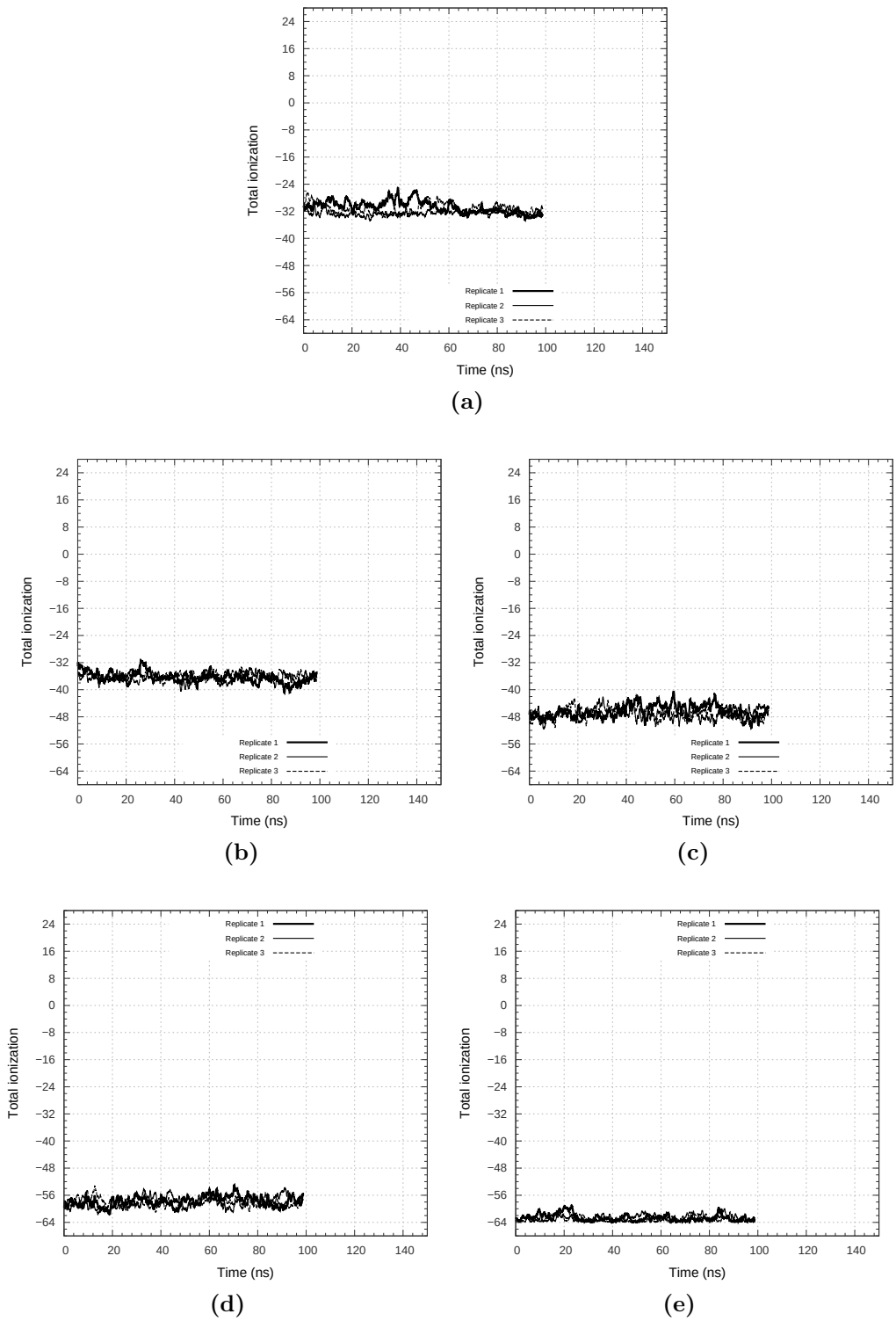

Figure B.15: Protonation time evolution, at different pH values, for a 25% PA/PC lipid bilayer (pH value equal to 5.0 **(a)**, 6.0 **(b)**, 7.0 **(c)** 8.0 **(d)** and 9.0 **(e)**.)

Acknowledgments

First and foremost, I find it righteous to start by acknowledging my supervisor Miguel Machuqueiro, who not only awakened my interest for the fascinating area of Molecular Modeling and Simulation , but did also fostered me through the process of turning this naive curiosity into a conscious personal endeavour - which hopefully will endure for many years to come. On a more personal note, I'm thankful towards you, Miguel for being a friend whose valuable lessons and opportunities presented throughtout the last pair of years did undoubtledly enriched my experience as a student and junior researcher. Without your patience and support this thesis would not have been possible. Your efforts will not be forgotten - aswell as the *"omoplata"* joke.

Thanks to all other staff at the Inorganic and Theoretical Chemistry group at CQB, for stimulating and enjoyable discussions inside and outside reunions/ seminars, and for the friendly environment - a constant -, where from times to times (*in fact, almost weekly!*) we are presented with delicious deserts - incluing the renowed "chocolate cake" from Prof. Helena Gaspar (thank you!).

In particular, I would like to thank Prof. Maria José Calhorda and Prof. Margarida Meireles for past opportunities and collaborations, and more recently, for being always available to aid me and share some of their experience and knowledge , which have certainly helped me throughtout this year.

Additionally, and returning to our lab, two individuals stand out, since they were more than mere colleagues, playing crucial roles as mentors for the past year, being responsible for many of my heartfelt, although "small", vitories. Hence, Diogo Vila-Viçosa, thank you for being present right on the other side of the room, always trying to make some time to answer my small and not-so-small questions. Your peculiar way of sharing knowledge and your "devil-advocate personna" made my work far more rigorous and thoughtful than it would be without your presence. In addition, for always being available to help me when I needed the most and for enduring my annoying way-too-many break-ins in his office, thank you Vitor Teixeira. Thanks to you, now I am proud to be part of that group of geeks who have written a program in C

language. For both of you, thank your for providing me with many helpful tips and suggestions along the way and by making your scripts available to be scrutinized and adapted to my needs.

To António Baptista, whose brilliant and helpful insights gave rise to an essential part of the methodological development needed to reveal part of the knowledge within this work. On a special side note, thank you for being my pool partner, even thought I turned out to be such a bad player. It was to be expected - either you were not able to predict it or you were too kind to take the risk. Either way, the competition was fierce!

My appreciation likewise extends to the friends with whom I had the opportunity, for the past years, to share my good and bad moments with, something I will treasure dearly. Thank you for the spontaneous laughs, hugs, toasts and eventually, when needed, a kind shoulder to lean on, or from time to time, to grip firmly - my former "apostles" will most certainly understand this last part! Hence, thank you especially to Catarina Fonseca, Joana "Pneuzão" Cruz, João Pereira and Neuza Silva, as well to Alena Khmensklaia, Joana "Carxa" Martins, Marta Gomes and Sara Carvalho.

For two of the best human beings I ever met, one of those hugs (*that tell so much*). I thank you, Catarina Fonseca and Neuza Silva, for being the living-proof that through kindness and perseverance we can conquer our place, without losing our identity and values. Thank you for your enduring friendship and for your guidance.

For being always ready to pull an *all-night*, with the proper (*and must deserved*) amount of "beverages", fun and companionship, I salute you "Maestra" Sara Carvalho. Thank you for being my friend, and for supporting me while we were writing-up - speaking about it, thanks for being the best victim of my pranks; it made it all much more enjoyable. By the way, that afternoon at the beach was a piece of heaven was is not?

To my ever supportive partner in life, thank you for always being there when I needed the most. I am really grateful to share my days with you, Tomás Machado - thank you for the undying love and support, for all the long walks that kept me sane, for all the good books and movies that we have shared, and for showing me how Lisbon can be so beautiful. I guess *"the company makes the feast"* afterall. For all this and so much more, thank you! Also, a big thank you to your Mother, for all the moral support she gave me while helping me to put my problems in perspective, and for sharing her vast knowledge so kindly - someday I will be able to speak proper French and *maybe* I will be able to be a contender winner of a Trivial Pursuit match with both of you.

Finally, I thank my family for their constant support, both economical and affective: to my parents, Maria e António, the most sincere thank you for their endless love and support, even during times when it has most certainly been undeserved. Without your help I would not be able to have come this far - thank you! For my sisters, for being there when we were younger

and for all the good memories that make my infancy to young adulthood a good one to revisit - thank you!

Last but not least, I would like to thank my dearest and lovely nephew Vitória, whose everlasting laughing and support accompanied me through this journey and made everything else worth it. Know that I am grateful to be the "goofy" uncle of the smartest and kindest seven-year old "toddler -girl" and I hope you will continue to look up to me in that way that only you seem to know how to, for many years to come, either for help or just to contemplate with curiosity what I am up to. You were a big part of the motivation I had, and hopefully I will be able to stay nearby and retribute.

On a private note, I would like to show the most sincere appreciation to my other three *friends*: Isaac Asimov, one of the most prolific writers of all time and one of the most influential biochemist in my young adult life, for presenting me with such a bright vision on Science and Life, I am in debt towards you; qit02 and qitMaximus, especially the latter, for coping with my many depreciative comments, thank you for being a hard (*and loud, especially loud!*) working "robot" - even thought you were not able to predict and prevent me from deleting one or two .xtc...

Bibliography

[1] Cooper, G. M. and Hausman, R. E. (2009). *The Cell: a Molecular Approach.* ASM Press and Sinauer Associates, 5th edn.

[2] Cantor, C. R. and Schimmel, P. R. (1980). *Biophysical Chemistry - Part I: the conformation of biological macromolecules.* W. H. Freeman and company, New York.

[3] Nossal, R. J. and Lecar, H. (1991). *Molecular and Cell Biophysics.* Addison-Wesley Publishing Company.

[4] Dowhan, W. (1997). Molecular basis for membrane phospholipid diversity: why are there so many lipids? *Annu. Rev. Biochem.* **66**: 199–232.

[5] Santos, A. X. S. and Riezman, H. (2012). Yeast as a model system for studying lipid homeostasis and function. *FEBS Letters* **586**: 2858–2867.

[6] Edidin, M. (2003). Lipids on the frontier: a century of cell-membrane bilayers. *Nature Rev. Mol. Cell Biol.* **4**: 414–418.

[7] Singer, S. J. and Nicolson, G. L. (1972). The fluid mosaic model of the structure of cell membranes. *Science* **175**: 720–731.

[8] Danielli, J. F. (1975). *The bilayer hypothesis of membrane structure.* G. Weissmann and R. Clairborne.

[9] Gennis, R. B. (1989). *Biomembranes - Molecular Structure and Function.* Springer.

[10] Langmuir, I. (1917). The constitution and fundamental properties of solids and liquids. II. Liquids. *J. Am. Chem. Soc.* **39**: 1848–1906.

[11] Gorter, E. and Grendel, F. (1925). On bimolecular layers of lipoids on the chromocytes of the blood. *J. Exp. Med.* **41**: 439–443.

[12] Danielli, J. F. and Davson, H. (1935). A contribution to the theory of permeability of thin films. *J. Cell. Comp. Physiol.* **5**: 495–508.

[13] Hendler, R. W. (1971). Biological membrane ultrastructure. *Physiol. Rev.* **51**: 66–97.

[14] Mouritsen, O. G. and Bloom, M. (1984). Mattress model of lipid-protein interactions in membranes. *Biophys. J.* **46**: 141–153.

[15] Jacobson, K., E., S., and Simson, R. (1995). Revisiting the fluid mosaic model of membranes. *Science* **268**: 1441–1442.

[16] Woodka, A. C., Butler, P. D., Porcar, L., Farago, B., and Nagao, M. (2012). Lipid bilayers and membrane dynamics: insight into thickness fluctuations. *Phys. Rev. Lett.* **109**: 58102–58106.

[17] van Meer, G., Voelker, D. R., and Feigenson, G. W. (2008). Membrane lipids: where they are and how they behave. *Nature* **9**: 112–124.

[18] Ochoa, J. A., Whitaker, S., and P., S. (1987). Determination of cell membrane permeability in concentrated cell ensembles. *Biophys. J.* **52**: 763–774.

[19] Stanfield, P. R. (1983). Tetraethylammonium ions and the potassium permeability of excitable cells. *Rev. Physiol. Biochem. Pharmacol.* **97**: 1–67.

[20] Bryant, D. M. and Mostov, K. E. (2008). From cells to organs: building polarized tissue. *Nature Rev. Mol. Cell Biol.* **9**: 887–901.

[21] Nelson, D. L. and Cox, M. M. (2008). *Lehninger Principles of Biochemistry.* W. H. Freeman & Company, 5th edn.

[22] Tanford, C. (1979). Interfacial free energy and the hydrophobic effect. *PNAS* **76**: 4175–4176.

[23] Haines, T. H. and Dencher, N. A. (2002). Cardiolipin: a proton trap for oxidative phosphorylation. *FEBS Letters* **528**: 35–39.

[24] Dimroth, P., Kaim, G., and Matthey, U. (2000). Crucial role of the membrane potential for ATP synthesis by F_1F_0 ATP synthases. *JEB* **203**: 51–59.

[25] Vojtiskova, A., Jesina, M., Kalous, M., Kaplanova, V., Houstek, J., Tesarova, M., Fornuskova, D., Zeman, J., Dubot, A., and Godinot, C. (2004). Mitochondrial membrane potential and ATP production in primary disorders of ATP synthase. *Toxicol. Mech. Methods* **14**: 7–11.

[26] Kahn, C. R. (1976). Membrane receptors for hormones and neurotransmitters. *JCB* **70**: 261–286.

[27] Peet, D. J., Turley, S. D., Ma, W., Janowski, B. A., Lobaccaro, J. M., Hammer, R. E., and Mangelsdorf, D. J. (1998). Cholesterol and bile acid metabolism are impaired in mice lacking the nuclear oxysterol receptor LXR alpha. *Cell* **93**: 693–704.

[28] Raetz, C. R. H. (1986). Molecular genetics of membrane phospholipid synthesis. *Annu. Rev. Genet.* **20**: 253–295.

[29] Dopico, A. M. and Tigyi, G. J. (2007). A glance at the structural and functional diversity of membrane lipids. *Method. Mol. Biol.* **400**: 1–13.

[30] Cohen, D. E. and Carey, M. C. (1991). Acyl chain unsaturation modulates distribution of lecithin molecular species between mixed micelles and vesicles in model bile. implications for particle structure and metastable cholesterol solubilities. *J. Lipid Res.* **32**: 1291–1302.

[31] Athenstaedt, K. and G., D. (1999). Phosphatidic acid, a key intermediate in lipid metabolism. *Eur J Biochem* **266**: 1–16.

[32] Wang, X., Devaiah, S. P., Zhang, W., and R., W. (2006). Signaling functions of phosphatidic acid. *Progress in Lipid Research* **45**: 250–278.

[33] de Kroon, A. I. P. M. (2007). Metabolism of phosphatidylcholine and its implications for lipid acyl chain composition in Saccharomyces cerevisiae. *Biochem. Biophys. Acta* **1771**: 343–353.

[34] Geiger, O., López-Lara, I. M., and Sohlenkamp, C. (2013). Phosphatidylcholine biosynthesis and function in bacteria. *Biochem. Biophys. Acta* **1831**: 503–513.

[35] Pavlovic, Z. and Bakovic, M. (2013). Regulation of phosphatidylethanolamine homeostasis — the critical role of CTP:phosphoethanolamine cytidylyltransferase (Pcyt2). *Int J Mol Sci* **14**: 2529–2550.

[36] Guillas, I., Vernay, A., Vitagliano, J., and Arkowitz, R. A. (2013). Phosphatidylinositol 4,5-bisphosphate is required for invasive growth in Saccharomyces cerevisiae. *J. Cell Sci.* **126**: 3602–3614.

[37] Vance, J. E. and Steenbergen, R. (2005). Metabolism and functions of phosphatidylserine. *Progress in Lipid Research* **44**: 207–234.

[38] Heimburg, T. (2007). *Thermal Biophysics of Membranes*. Wiley-VCH.

[39] Shinoda, W., Namiki, N., and Okazaki, S. (1997). Molecular dynamics study of a lipid bilayer: convergence, structure and long-time dynamics. *J Chem Phys* **106**: 5731–5743.

[40] McLaughlin, S. and Murray, D. (2005). Plasma membrane phosphoinositide organization. *Nature* **438**: 605–611.

[41] Cullis, P. R., Fenske, D. B., and Hope, M. J. (1996). *Biochemistry of Lipids, Lipoproteins and Membranes*. Elsevier Science.

[42] Trauble, H. and Eibl, H. (1974). Electrostatic effects on lipid phase transition: membrane structure and ionic environment. *Proc. Natl. Acad. Sci. USA* **71**: 214–219.

[43] Busa, W. B. (1986). Mechanisms and consequences of pH-mediated cell regulation. *Annu. Rev. Physiol.* **48**: 389–402.

[44] Kurkdjian, A. and Guern, J. (1989). Intracellular pH: measurement and importance in cell activity. *Annu. Rev. Plant Phys.* **40**: 271–303.

[45] Madshus, I. H. (1988). Regulation of intracellular pH in eukaryotic cells. *Biochem. J.* **250**: 1–8.

[46] Loewen, C., Gaspar, M., Jesch, S., Delon, C., Ktistakis, N., Henry, S., and Levine, T. (2004). Phospholipid metabolism regulated by a transcription factor sensing phosphatidic acid. *Science* **304**: 1644–1647.

[47] Loew, S., Kooijman, E. E., and May, S. (2013). Increased pH-sensitivity of protein binding to lipid membranes through the electrostatic-hydrogen bond switch. *Chem. Phys. Lipids* **169**: 9–18.

[48] Shin, J. J. H. and Loewen, C. J. R. (2011). Putting the pH into phosphatidic acid signaling. *BMC Biology* **9**: 1–10.

[49] Young, B. P., Shin, J. J. H., Orij, R., Chao, J. T., Li, S. C., Guan, X. L., Khong, A., Jan, E., Wenk, M. R., Prinz, W. A., Smits, G. J., and Loewen, C. J. R. (2010). Phosphatidic acid is a pH biosensor that links membrane biogenesis to metabolism. *Science* **329**: 1085–1088.

[50] Garidel, P., Johann, C., and Blume, A. (1997). Nonideal mixing and phase separation in phosphatidylcholine-phosphatidic acid mixtures as a function of acyl chain length and pH. *Biophys. J.* **72**: 2196–2210.

[51] Poger, D. and Mark, A. E. (2010). On the validation of molecular dynamics simulations of saturated and cis-monounsaturated phosphatidylcholine lipid bilayers: a comparison with experiment. *J. Chem. Theory Comput.* **6**: 325–336.

[52] Lyubartsev, A. P. and Rabinovich, A. L. (2011). Recent development in computer simulations of lipid bilayers. *Soft Matter* **7**: 25–39.

[53] Kinnunen, P. K. (2009). Amyloid formation on lipid membrane surfaces. *Open Biol. J.* **2**: 163–175.

[54] Tieleman, D., Marrink, S., and Berendsen, H. (1997). A computer perspective of membranes: molecular dynamics studies of lipid bilayer systems. *Biochem. Biophys. Acta* **1331**: 235–270.

[55] Allen, M. P. and Tildesley, D. J. (1987). *Computer Simulation of Liquids*. Oxford University Press, USA.

[56] Leach, A. R. (2001). *Molecular Modeling: principles and applications*. Pearson Education, Edinburgh, 2nd edn.

[57] Cisneros, G. A., Karttunen, M., Ren, P., and Sagui, C. (2013). Classical electrostatics for biomolecular simulations. *Chemical Reviews* **924**: 243–270.

[58] Scott, W. R. P., Hunenberger, P. H., Tironi, I. G., Mark, A. E., Billeter, S. R., Fennen, J., Torda, A. E., Huber, T., Kruger, P., and van Gunsteren, W. F. (1999). The GROMOS biomolecular simulation program package. *J. Phys. Chem.* **103**: 3596–3607.

[59] van Gunsteren, W. F., Billeter, S. R., Eising, A. A., Hunenberger, P. H., Kruger, P., Mark, A. E., Scott, W. R. P., and Tironi, I. G. (1996). *Biomolecular simulation: The GROMOS96 manual and user guide.*

[60] Darden, T., York, D., and Pedersen, L. (1993). Particle mesh ewald: An n·log(n) method for ewald sums in large systems **98**: 10089–10092.

[61] Barker, J. A. and Watts, R. O. (1973). Monte carlo studies of the dielectric properties of water-like models. *Molecular Physics* **26**: 789–792.

[62] Tironi, I. G., Sperb, R., Smith, P. E., and van Gunsteren, W. F. (1995). A generalized reaction field method for molecular dynamics simulations. *J. Chem. Phys.* **102**: 5451–5459.

[63] Machuqueiro, M. and Baptista, A. M. (2006). Constant-pH molecular dynamics with ionic strength effects: protonation-conformation coupling in decalysine. *J. Phys. Chem. B* **110**: 2927–2933.

[64] Brooks, B. R., Bruccoleri, R. E., Olafson, B. D., States, D. J., Swaminathanand, S., and Karplus, M. (1983). Charmm: A program for macromolecular energy, minimization, and dynamics calculations. *J. Comput. Chem.* **4**: 187–217.

[65] Wang, J., Wolf, R. M., Caldwell, J. W., Kollman, P. A., and Case, D. A. (2004). Development and testing of a general Amber force field. *J. Comput. Chem.* **25**: 1157–1174.

[66] Rizzo, R. C. and Jorgensen, W. L. (1999). Opls all-atom model for amines: resolution of the amine hydration problem. *JACS* **121**: 4827–4836.

[67] Kukol, A. (2009). Lipid models for united-atom molecular dynamics simulations of proteins. *JCTC* **5**: 615–626.

[68] Schmid, N., Eichenberger, A. P., Choutko, A., Riniker, S., Winger, M., Mark, A. E., and van Gunsteren, W. F. (2011). Definition and testing of the GROMOS force-field versions 54A7 and 54B7. *Eur. Biophys. J.* **40**: 843–856.

[69] Chiu, S., Clark, M., Balaji, V., Subramaniam, S., Scott, H., and Jakobsson, E. (1995). Incorporation of Surface Tension into Molecular Dynamics Simulation of an Interface: A Fluid Phase Lipid Bilayer Membrane. *Biophys. J.* **69**: 1230–1245.

[70] Ash, W. L., Zlomislic, M. R., O. E. O., and Tieleman, D. P. (2004). Computer simulations of membrane proteins. *Biochem. Biophys. Acta* **1666**: 158–189.

[71] Scott, H. L. (2002). Modeling the lipid component of membranes. *Curr. Opin. Struct. Biol.* **12**: 495–502.

[72] Feller, S. E. (2000). Molecular dynamics simulations of lipid bilayers. *Curr. Opin. Colloid In.* **5**: 217–223.

[73] Merz, K. M. (1997). Molecular dynamics simulations of lipid bilayers. *Curr. Opin. Struct. Biol.* **7**: 511–517.

[74] Lindahl, E., Hess, B., and van der Spoel, D. (2001). GROMACS 3.0: A package for molecular simulation and trajectory analysis. *J. Mol. Model.* **7**: 306–317.

[75] Bashford, D. and Karplus, M. (1990). pK_a's of ionizable groups in proteins: Atomic detail from a continuum electrostatic model. *Biochemistry* **29**: 10219–10225.

[76] Feig, M., Im, W., and Brooks III, C. L. (2004). Implicit solvation based on generalized born theory in different dielectric environments. *J. Chem. Phys.* **120**: 903.

[77] Warshel, A. (1979). Calculations of chemical processes in solutions. *Journ Phys Chem* **83**: 1640–1652.

[78] Warshel, A., Sussman, F., and King, G. (1986). Free energy of charges in solvated proteins: microscopic calculations using a reversible charging process. *Biochemistry* **25**: 8368–8372.

[79] Sharp, K. A. and Honig, B. (1990). Electrostatic interaction in macromolecules: theory and applications. *Annu. Rev. Biophys. Biophys. Chem.* **19**: 301–332.

[80] Gilson, M. K. (1995). Theory of electrostatic interactions in macromolecules. *Current Biology* **5**: 216–223.

[81] Bashford, D. (2004). Macroscopic electrostatic models for protonation states in proteins. *Front. Biosci.* **9**: 1082–1099.

[82] Baptista, A. M., Martel, P. J., and Soares, C. M. (1999). Simulation of electron-proton coupling with a Monte Carlo method: Application to cytochrome c_3 using continuum electrostatics. *BJ* **76**: 1–21.

[83] Martel, P. J., Baptista, A., and Petersen, S. B. (1996). Protein electrostatics. *Biotechnology Annual Review* **2**: 315–372.

[84] Metropolis, N., Rosenbluth, A., Rosenbluth, M., Teller, A., and Teller, E. (1953). Equation of state calculations by fast computing machines. *J. Chem. Phys.* **21**: 1087–1092.

[85] Becker, T., Ullmann, R. T., and Ullmann, G. M. (2007). *Simulation of the Electron Transfer between the Tetraheme Subunit and the Special Pair of the Photosynthetic Reaction Center Using a Microstate Description.*

[86] Li, Z., Venable, R. M., Rogers, L. A., Murray, D., and Pastor, R. W. (2009). Molecular dynamics simulations of pip_2 and pip_3 in lipid bilayers: Determination of ring orientation, and the effects of surface roughness on a poisson-boltzmann description. *Biophys. J.* **97**: 155–163.

[87] da Silva, F. L. B., Bogren, D., Söderman, O., Åkesson, T., and Jönsson, B. (2002). Titration of fatty acids solubilized in cationic, nonionic, and anionic micelles. theory and experiment. *J. Phys. Chem. B* **106**: 3515–3522.

[88] Morrow, B. H., Wang, Y., Wallace, J. A., Koenig, P. H., and Shen, J. K. (2011). Simulating pH titration of a single surfactant in ionic and nonionic surfactant micelles. *J. Phys. Chem. B* **115**: 14980–14990.

[89] Morrow, B. H., Koenig, P. H., and Shen, J. K. (2012). Atomistic simulations of pH-dependent self-assembly of micelle and bilayer from fatty acids. *J. Chem. Phys.* **137**: 194902–194902.

[90] Oostenbrink, C., Villa, A., Mark, A. E., and Van Gunsteren, W. F. (2004). A biomolecular force field based on the free enthalpy of hydration and solvation: The GROMOS force-field parameter sets 53A5 and 53A6. *J. Comput. Chem.* **25**: 1656–1676.

[91] Baptista, A. M., Teixeira, V. H., and Soares, C. M. (2002). Constant-pH molecular dynamics using stochastic titration. *J. Chem. Phys.* **117**: 4184–4200.

[92] Hermans, J., Berendsen, H., van Gunsteren, W., and Postma, J. (1984). A consistent empirical potential for water-protein interactions. *Biopolymers* **23**: 1513–1518.

[93] Berendsen, H., Postma, J., van Gunsteren, W., DiNola, A., and Haak, J. (1984). Molecular dynamics with coupling to an external bath. *J. Chem. Phys.* **81**: 3684–3690.

[94] van der Ploeg P., B. H. (1982). Molecular dynamics simulation of a bilayer membrane **76**: 3271–3275.

[95] Hess, B. (2008). P-LINCS: A Parallel Linear Constraint Solver for Molecular Simulation. *J. Chem. Theory Comput.* **4**: 116–122.

[96] Li, L., Li, C., Sarkar, S., Zhang, J., Witham, S., Zhang, Z., Wang, L., Smith, N., Petukh, M., and Alexov, E. (2012). DelPhi: a comprehensive suite for DelPhi software and associated resources. *BMC Biophys.* **5**: 9.

[97] Baptista, A. M. and Soares, C. M. (2001). Some theoretical and computational aspects of the inclusion of proton isomerism in the protonation equilibrium of proteins. *JPCB* **105**: 293–309.

[98] Teixeira, V. H., Cunha, C. C., Machuqueiro, M., Oliveira, A. S. F., Victor, B. L., Soares, C. M., and Baptista, A. M. (2005). On the use of different dielectric constants for computing individual and pairwise terms in Poisson-Boltzmann studies of protein ionization equilibrium. *J. Phys. Chem. B* **109**: 14691–14706.

[99] Schutz, C. N. and Warshel, A. (2001). What are the dielectrict "constants" of proteins and how to validate electrostatic models? *Proteins* **44**: 400–417.

[100] Kumler, W. D. and Eiler, J. J. (1943). The acid strength of mono and diesters of phosphoric acid. the n-alkyl esters from methyl to butyl, the esters of biological importance, and the natural guanidine phosphoric acids. *J. Am. Chem. Soc.* **65**: 2355–2361.

[101] Frisch, M. J., Trucks, G. W., Schlegel, H. B., Scuseria, G. E., Robb, M. A., Cheeseman, J. R., Montgomery, Jr., J. A., Vreven, T., Kudin, K. N., Burant, J. C., Millam, J. M., Iyengar,

S. S., Tomasi, J., Barone, V., Mennucci, B., Cossi, M., Scalmani, G., Rega, N., Petersson, G. A., Nakatsuji, H., Hada, M., Ehara, M., Toyota, K., Fukuda, R., Hasegawa, J., Ishida, M., Nakajima, T., Honda, Y., Kitao, O., Nakai, H., Klene, M., Li, X., Knox, J. E., Hratchian, H. P., Cross, J. B., Bakken, V., Adamo, C., Jaramillo, J., Gomperts, R., Stratmann, R. E., Yazyev, O., Austin, A. J., Cammi, R., Pomelli, C., Ochterski, J. W., Ayala, P. Y., Morokuma, K., Voth, G. A., Salvador, P., Dannenberg, J. J., Zakrzewski, V. G., Dapprich, S., Daniels, A. D., Strain, M. C., Farkas, O., Malick, D. K., Rabuck, A. D., Raghavachari, K., Foresman, J. B., Ortiz, J. V., Cui, Q., Baboul, A. G., Clifford, S., Cioslowski, J., Stefanov, B. B., Liu, G., Liashenko, A., Piskorz, P., Komaromi, I., Martin, R. L., Fox, D. J., Keith, T., Al-Laham, M. A., Peng, C. Y., Nanayakkara, A., Challacombe, M., Gill, P. M. W., Johnson, B., Chen, W., Wong, M. W., Gonzalez, C., and Pople, J. A. (2004). Gaussian 03, Revision C.02.

[102] Becke, A. D. (1993). Density-functional thermochemistry. iii. the role of exact exchange. *J. Chem. Phys.* **98**: 5648.

[103] Stephens, P., Devlin, F., Chabalowski, C., and Frisch, M. J. (1994). Ab initio calculation of vibrational absorption and circular dichroism spectra using density functional force fields. *J. Chem. Phys.* **98**: 11623–11627.

[104] Lee, C., Yang, W., and Parr, R. G. (1988). Development of the colle-salvetti correlation-energy formula into a functional of the electron density. *Phys. Rev. B* **37**: 785.

[105] McLean, A. D. and Chandler, G. S. (1980). Contracted gaussian basis sets for molecular calculations. i. second row atoms, z= 11–18. *J. Chem. Phys.* **72**: 5639.

[106] Krishnan, R. B. J. S., Binkley, J. S., Seeger, R., and Pople, J. A. (1980). Self-consistent molecular orbital methods. xx. a basis set for correlated wave functions. *J. Chem. Phys.* **72**: 650.

[107] Wachters, A. J. (1970). Gaussian basis set for molecular wavefunctions containing third-row atoms. *J. Chem. Phys.* **52**: 1033.

[108] Hay, P. J. (1977). Gaussian basis sets for molecular calculations. the representation of 3d orbitals in transition-metal atoms. *J. Chem. Phys.* **66**: 4377.

[109] Raghavachari, K. and Trucks, G. W. (1989). Highly correlated systems. excitation energies of first row transition metals sc–cu. *J. Chem. Phys.* **91**: 1062.

[110] Curtiss, L. A., McGrath, M. P., Blaudeau, J., Davis, N. E., Binning Jr, R. C., and Radom, L. (1995). Extension of gaussian-2 theory to molecules containing third-row atoms ga–kr. *J. Chem. Phys.* **103**: 6104.

[111] McGrath, M. P. and Radom, L. (1991). Extension of gaussian-1 (g1) theory to bromine-containing molecules. *J. Chem. Phys.* **94**: 511.

[112] Case, D. A., Cheatham III, T. E., Darden, T., Gohlke, H., Luo, R., Merz Jr, K. M., Onufriev, A., Simmerling, C., Wang, B., and Woods, R. J. J. (2005). The Amber biomolecular simulation programs. *Comput. Chem.* **26**: 1668–1688.

[113] Dupradeau, F. Y., Pigache, A., Zaffran, T., Savineau, C., Lelong, R., Grivel, N., Lelong, D., Rosanski, W., and Cieplak, P. (2010). The R.E.D. tools: advances in RESP and ESP charge derivation and force field library building. *Phys. Chem. Chem. Phys.* **12**: 7821–7839.

[114] Bayly, C., Cieplak, P., Cornell, W., and Kollman, P. (1993). A well behaved electrostatic based method using charge restraints for deriving atomic charges: The RESP model. *J. Phys. Chem.* **97**: 10269–10280.

[115] Edholm, O. and Nagle, J. F. (2005). Areas of molecules in membranes consisting of mixtures. *Biophys. J.* **89**: 1827–1832.

[116] Greenwood, A. I., Tristram-Nagle, S., and Nagle, J. F. (2006). Partial molecular volumes of lipids and cholesterol. *Chemistry and Physics of Lipids* **143**: 1–10.

[117] Machuqueiro, M., Campos, S. R., Soares, C. M., and Baptista, A. M. (2010). Membrane-induced conformational changes of kyotorphin revealed by molecular dynamics simulations. *J. Phys. Chem. B* **114**: 11659–11667.

[118] Vermeer, L. S., de Groot, B. L., Reat, V., Milon, A., and Czaplicki, J. (2007). Acyl chain order parameter profiles in phospholipid bilayers: computation from molecular dynamics simulations and comparison with ^{2}H NMR experiments. *Eur. Biophys. J.* **36**: 919–931.

[119] Hauser, H. I., Pascher, R. H., Pearson, and Sundell, S. (1981). Preferred conformation and molecular packing of phosphatidylethanolamine and phosphatidylcholine. *BBA* **650**: 21–51.

[120] Daura, X., Mark, A. E., and Van Gunsteren, W. F. (1998). Parametrization of aliphatic CHn united atoms of GROMOS96 force field. *J. Comput. Chem.* **19**: 535–547.

[121] Kucerka, N., Nieh, M., Pencer, J., Sachs, J. N., and Katsaras, J. (2009). What determines the thickness of a biological membrane. *Gen Physiol Biophys* **28**: 117–125.

[122] Pearson, R. H. and Pascher, I. (1979). The molecular structure of lecithin dihydrate. *Nature* **281**: 499–501.

[123] Sackmann, E. (1995). *Handbook of Biological Physics*. Elsevier Science B. V.

[124] Wohlert, J. and Edholm, O. (2006). Dynamics in atomistic simulations of phospholipid membranes: nuclear magnetic resonance relaxation rates and lateral diffusion. *J. Chem. Phys.* **125**: 204703.

[125] Qian, H., Sheetz, M. P., and Elson, E. L. (1991). Single particle tracking. analysis of diffusion and flow in two-dimensional systems. *Biophys. J.* **60**: 910–921.

[126] Knecht, V. and Klasczyk, B. (2013). Specific binding of chloride ions to lipid vesicles and implications at molecular scale. *Biophys. J.* **104**: 818–824.

[127] Woolf, T. B. (2013). A tale of two ions and their membrane interactions: Clearly the same or clearly different? *Biophys. J.* **104**: 746–747.

[128] T., B. and Reuter, N. (2010). Molecular dynamics simulations of mixed acidic/zwitterionic phospholipid bilayers. *Biophys. J.* **99**: 825–833.

[129] Lee R Cambrea, Farzin Haque, J. L. S. J.-C. R. and Hovis, J. S. (2007). Effect of ions on the organization of phosphatidylcholine/phosphatidic acid bilayers. *Biophys. J.* **93**: 1630–1638.

[130] Bockmann, R. A., H. A. H. T. and Grubmuller, H. (2003). Effect of sodium chloride on a lipid bilayer. *Biophys. J.* **85**: 1647–1655.

[131] H., Y., Y., X., Z., G., Y., M., Y., D., and H., J. (). Effects of Na^+, K^+ and Ca^{2+} on the structures of anionic lipid bilayers and biological implication .

[132] Bockmann, R. A. and Grubmuller, H. (2004). Multistep binding of divalent cations to phospholipid bilayers: a molecular dynamics study. *Angew. Chem. Int. Edit.* **43**: 1021–1024.

[133] Anézo, C., de Vries, A. H., Höltje, H., Tieleman, D. P., and Marrink, S. (2003). Methodological issues in lipid bilayer simulations. *JPCB* **107**: 9424–9433.

[134] Cevc, G. (1991). Isothermal lipid phase transitions. *Chem. Phys. Lipids* **57**: 293–307.

[135] Janiak, M. J., Small, D. M., and Shipley, G. G. (1979). Temperature and compositional dependence of the structure of hydrated dimyristoyl lecithin. *J. Biol. Chem.* **254**: 6068–6078.

[136] Rosso, L. and Gould, I. R. (2008). Structure and dynamics of phospholipid bilayers using recently developed general all-atom force fields. *J. Comput. Chem.* **29**: 24–37.

[137] Pasenkiewicz-Gierula, M., Murzyn, K., Rog, T., and Czaplewski, C. (2000). Molecular dynamics simulation studies of lipid bilayer systems. *Acta Biochim. Pol.* **47**: 601–611.

[138] Petrache, H. I., Dodd, S. W., and Brown, M. F. (2000). Area per lipid and acyl length distributions in fluid phosphatidylcholines determined by ^{2}h nmr spectroscopy. *Biophys. J.* **79**: 3172–3192.

[139] Kucerka, N., Nieh, M., and Katsaras, J. (2011). Fluid phase lipid areas and bilayer thicknesses of commonly used phosphatidylcholines as a function of temperature. *Biochem. Biophys. Acta* **1808**: 2761–2771.

[140] Almeida, P. F. F. and Vaz, W. L. C. (1995). *Handbook of Biological Physics*. Elsevier Science B. V.

[141] Rubenstein, J. L. R., S. B. A. and McConnell, H. M. (1979). Lateral diffusion in binary mixtures of cholesterol and phosphatidylcholines. *Proc. Natl. Acad. Sci. USA* **76**: 15–18.

[142] Alecio, M. R., G. D. E. V. W. R. and Rando, R. R. (1982). Use of a fluorescent cholesterol derivative to measure lateral mobility of cholesterol in membranes. *Proc. Natl. Acad. Sci. USA* **79**: 5171–5174.

[143] title=Lateral diffusion in binary mixtures of cholesterol and phosphatidylcholines, journal=PNAS, y. v. p. () .

[144] Venable, R. M., Luo, Y., Gawrisch, K., Roux, B., and Pastor, R. W. (2013). Simulations of anionic lipid membranes: development of interaction-specific ion parameters and validation using NMR data. *J. Phys. Chem. B* **117**: 10183–10192.